

**The Immunologic Basis of Xenograft Heart Valve Deterioration**

by

Sabin J. Bozso

A thesis submitted in partial fulfillment of the requirements for the degree of

Doctor of Philosophy

Department of Surgery

University of Alberta

© Sabin J. Bozso, 2021

## Abstract

Valvular heart disease (VHD) is a common diagnosis with an approximate prevalence of 2.5% of the total population having moderate to severe VHD [1, 2]. The most common treatment for end-stage VHD is surgical valve replacement with constructs categorized into three classes: mechanical valves, homografts and xenografts. Given the need for lifelong anticoagulation with mechanical valves and the significant lack of availability of homografts, xenografts have become the most common valve type implanted clinically. The main issue facing xenograft tissue heart valve (XTHV) prostheses is their rate of structural valve deterioration (SVD) over time, leading to hemodynamic dysfunction and clinical symptoms of valve obstruction [3]. Emerging evidence from laboratory and clinical investigations suggests that XTHVs generate an immune response that has been implicated in the failure of these grafts [4-9]. To address these shortcomings, several attempts have been made to create functional heart valve replacements, using decellularized xenograft matrices with autologous cell recellularization to mask the xenograft scaffold from host immune recognition. However, to date, it remains unclear what effect an autologous recellularized xenograft has on the immune response in the host. Therefore, the objectives of this thesis are to establish the role of the immune system in prosthesis failure by analyzing explanted XTHVs developing SVD, to attenuate the immune response with autologous recellularized xenograft heart valves in a human, *in-vitro* and small animal, *in-vivo* model, and finally to assess the effect of immunomodulatory medication on clinical rates of SVD amongst patients receiving a XTHV. This work will lead to a better understanding of the immune mechanisms elicited by XTHVs and autologous recellularized xenografts, allowing us to ascertain if this approach may be a viable option for future valve constructs.

## Preface

This thesis is an original work by Sabin J. Bozso. The research project, of which this thesis is a part, received research ethics approval from the University of Alberta Research Ethics Board for the following project names: “Extracellular Environment Influences Human Mesenchymal Stem Cell Differentiation”, Pro52175, June 30, 2015; “Longevity of Bioprosthetic Valves after Transplant”, Pro88802, February 8, 2019; “Characterization of Cellular Infiltrate in Bioprosthetic Aortic and Mitral Valves”, Pro69274, November 25, 2016; “Tissue Engineered Heart Valves Using a Decellularized Xenogeneic Matrix”, AUP2414, May 23, 2018.

**Chapter 2** of this thesis has been accepted for publication as S.J. Bozso, R. EL-Andari, D. Al-Adra, M.C. Moon, D.H. Freed, J. Nagendran, J. Nagendran, “A Review of the Immune Response Stimulated by Xenogenic Tissue Heart Valves” by the journal, *Scandinavian Journal of Immunology*. Sabin J. Bozso performed the literature search and wrote the manuscript. Ryaan EL-Andari performed the literature search. David Al-Adra, Michael C. Moon, Darren H. Freed, Jayan Nagendran and Jeevan Nagendran edited the manuscript.

**Chapter 3** of this thesis has been accepted for publication as S.J. Bozso, J.J.H. Kang, A. Mathew, M.C. Moon, D.H. Freed, J. Nagendran, J. Nagendran, “Comparing Scaffold Design and Recellularization Technique for Development of Tissue Engineered Heart Valves” by the journal, *Regenerative Engineering and Translational Medicine*. Sabin J. Bozso performed the literature search and wrote the manuscript. Jimmy J.H. Kang performed the literature search. Anoop Mathew, Michael C. Moon, Darren H. Freed, Jayan Nagendran and Jeevan Nagendran edited the manuscript.

**Chapter 4** of this thesis has been submitted for publication to the journal *Current Protocols in Stem Cell Biology*. Jimmy J.H. Kang and Sabin J. Bozso contributed equally to this work, performing the experimental design, data collection, laboratory analysis, data analysis, data synthesis, manuscript preparation, manuscript submission and manuscript revisions. Ryaan EL-Andari performed data collection and data analysis. Michael C. Moon, Darren H. Freed, Jayan Nagendran and Jeevan Nagendran performed data synthesis, manuscript preparation, manuscript submission and manuscript revisions.

**Chapter 5** of this thesis has been accepted for publication as S.J. Bozso, J.J.H. Kang, R. Basu, B. Adam, J.R.B. Dyck, G.Y. Oudit, M.C. Moon, D.H. Freed, J. Nagendran, J. Nagendran, “Structural Valve Deterioration is Linked to Increased Immune Infiltrate and Chemokine Expression” by the *Journal of Cardiovascular Translational Research*. Sabin J. Bozso performed the experimental design, data collection, laboratory analysis, data analysis, data synthesis, abstract preparation, abstract presentation, manuscript preparation, manuscript submission and manuscript revisions. Jimmy J.H. Kang and Ratnadeep Basu performed data collection and laboratory analysis. Benjamin Adam, Jason R.B. Dyck, Gavin Y. Oudit, Michael C. Moon, Darren H. Freed, Jayan Nagendran and Jeevan Nagendran performed data analysis, data synthesis and manuscript revisions.

For **Chapter 6** of this thesis, Sabin J. Bozso performed the experimental design, data collection, laboratory analysis, data analysis, data synthesis, abstract preparation, abstract presentation, manuscript preparation, manuscript submission and manuscript revisions. Jimmy J.H. Kang, Ryaan EL-Andari, Dana Boe and Hannah Hedtke participated in research design and the performance of experiments. Michael C. Moon, Darren H. Freed and Jayan Nagendran

participated in manuscript preparation and revisions. Jeevan Nagendran participated in research design, data analysis, manuscript preparation and revisions.

For **Chapter 7** of this thesis Sabin J. Bozso performed the experimental design, data collection, laboratory analysis, data analysis, data synthesis, abstract preparation, abstract presentation, manuscript preparation, manuscript submission and manuscript revisions. Jimmy J.H. Kang, Ryaan EL-Andari, Nicholas Fialka and Lin Fu Zhu participated in research design and the performance of experiments. Steven R. Meyer, Darren H. Freed and Jayan Nagendran participated in manuscript preparation and revisions. Jeevan Nagendran participated in research design, data analysis, manuscript preparation and revisions.

**Chapter 8** of this thesis has been accepted for publication as S.J. Bozso, J.J.H. Kang, D. Al-Adra, Y. Hong, M.C. Moon, D.H. Freed, J. Nagendran, J. Nagendran, “Outcomes Following Bioprosthetic Valve Replacement in Prior Non-Cardiac Transplant Recipients” by the journal, *Clinical Transplantation*. Sabin J. Bozso performed the experimental design, data collection, data analysis, data synthesis, abstract preparation, abstract presentation, manuscript preparation, manuscript submission and manuscript revisions. Jimmy J.H. Kang performed data collection and laboratory analysis. David Al-Adra assisted with manuscript preparation and revisions. Yongzhe Hong performed statistical analysis. Michael C. Moon, Darren H. Freed, Jayan Nagendran and Jeevan Nagendran performed data analysis, data synthesis and manuscript revisions.

## **Acknowledgements**

I would like to thank my supervisor, Jeevan Nagendran, for his unrelenting support, encouragement, guidance and mentorship throughout the course of this research endeavour. Your enthusiasm for innovation and the betterment of surgery for valvular heart disease created an unprecedented learning environment rich with opportunity. I am truly grateful for the time and effort you have invested in the development of my career as a scientist and cardiac surgeon. I would also like to thank the other members of my committee, Jayan Nagendran and Darren Freed, for the time and energy you have invested over the course of my research. The mentorship and guidance you have all provided me has been invaluable and I will be forever grateful.

A significant amount of appreciation is owed to all the individuals who provided the guidance and technical support required to complete these studies: Xiuhua Wang, Jimmy Kang, Ryaan EL-Andari, Dana Boe, Hannah Hedtke, and Nicholas Fialka. I am also grateful to Benjamin Adam, Shalawny Miller and all the staff at the Pathology Core Lab for their collaboration and support. I must also express my gratitude to Lin Fu Zhu and all of the staff at the Ray Rajotte Surgical Medical Research Institute. I would like to thank the staff and veterinarians at the HSLAS Facility for their ongoing support.

I am extremely grateful to Canadian Institutes of Health Research, the University Hospital Foundation, the Edmonton Civic Employees Research Award and the University of Alberta Clinician Investigator Program for their financial support that allowed me to undertake this work.

## Table of Contents

<b>Abstract</b>	<b>ii</b>
<b>Preface</b>	<b>iii</b>
<b>Acknowledgements</b>	<b>vi</b>
<b>List of Tables</b>	<b>xi</b>
<b>List of Figures</b>	<b>xiii</b>
<b>List of Abbreviations</b>	<b>xvi</b>
<b>Chapter 1: Thesis Overview</b>	<b>1</b>
<b>Background</b>	<b>1</b>
<b>Hypothesis</b>	<b>3</b>
<b>Objectives</b>	<b>3</b>
<b>Chapter 2: A Review of the Immune Response Stimulated by Xenogenic Tissue Heart Valves</b>	<b>5</b>
<b>Abstract</b>	<b>6</b>
<b>Introduction</b>	<b>7</b>
<b>Immune Response to Xenogenic Tissue Heart Valves</b>	<b>8</b>
<b>Role of Antigens</b>	<b>12</b>
<b>Antigen Modification</b>	<b>15</b>
<b>Conclusion</b>	<b>17</b>
<b>Chapter 3. Comparing Scaffold Design and Recellularization Techniques for Development of Tissue Engineered Heart Valves</b>	<b>18</b>
<b>Abstract</b>	<b>19</b>
<b>Introduction</b>	<b>20</b>
<b>Decellularization and Scaffold Type</b>	<b>21</b>
<b>Xenogenic and Allogenic Scaffolds</b>	<b>22</b>
<b>Synthetic Scaffolds</b>	<b>27</b>
<b>Refinement of Recellularization</b>	<b>29</b>
<b>Conclusions</b>	<b>31</b>
<b>Chapter 4. Sternal Bone Marrow Harvesting and Culturing Techniques from Patients Undergoing Cardiac Surgery</b>	<b>33</b>

<b>Abstract</b>	<b>34</b>
<b>Introduction</b>	<b>35</b>
<b>Basic Protocol 1: Sternal Bone Marrow Collection and MSC Isolation and Culturing Protocol</b>	<b>36</b>
Materials List	37
Bone Marrow Collection	37
MSC Isolation and Culturing	39
MSC Expansion	40
<b>Basic Protocol 2: Protocol for MSC Surface Phenotyping</b>	<b>40</b>
Materials List	41
Surface Phenotyping	41
<b>Basic Protocol 3: Differentiation of MSCs into Adipogenic, Osteogenic and Chondrogenic Lineages</b>	<b>42</b>
Materials List	43
Adipogenesis Differentiation	44
Osteogenesis Differentiation	44
Chondrogenesis Differentiation	45
<b>Reagents and Solutions</b>	<b>46</b>
<b>Discussion</b>	<b>48</b>
<b>Chapter 5. Structural Valve Deterioration is Linked to Increased Immune Infiltrate and Chemokine Expression</b>	<b>57</b>
<b>Abstract</b>	<b>58</b>
<b>Introduction</b>	<b>59</b>
<b>Methods</b>	<b>60</b>
Patients and Explanted Valves	60
Immunohistochemical Analysis	61
Tissue Analysis	61
Gene Expression Analysis	61
Statistical Analysis	66
<b>Results</b>	<b>66</b>
Xenogenic tissue heart valves deteriorate in non-immune suppressed patients	66
Non-structural valve deteriorated controls are not infiltrated by cells of adaptive immunity	67
Structural valve deterioration of xenogenic tissue heart valves is associated with increased immune cellular infiltrate	69
Increased chemokine gradient accompanies infiltration by the cells of adaptive immunity	71
<b>Discussion</b>	<b>74</b>
Study Limitations	78
<b>Conclusion</b>	<b>79</b>

<b>Chapter 6. Recellularization of Bovine Pericardium with Autologous Mesenchymal Stem Cells Attenuates Initial Immune Activation</b>	<b>80</b>
<b>Abstract</b>	<b>81</b>
<b>Introduction</b>	<b>82</b>
<b>Methods</b>	<b>83</b>
Patient Population	83
MSC Isolation and Culturing	85
MSC Surface Phenotyping and Differentiation	85
Decellularization and Recellularization	86
Tissue Exposure to Whole Blood	87
Qualitative Analysis	87
Quantitative Analysis	88
Statistical Analysis	88
<b>Results</b>	<b>89</b>
Bovine pericardium is immunogenic, stimulating an immune response similar to PMA/ionomycin stimulation	89
Bovine pericardium can be decellularized and recellularized successfully without damaging the extracellular matrix	92
Decellularization alone does not significantly reduce initial cytokine production	93
Autologous human MSC recellularization reduces initial cytokine production equivalent to that elicited by autologous human pericardium	97
Autologous human MSC recellularization reduces initial cytokine production equivalent to that elicited by autologous human pericardium	101
<b>Discussion</b>	<b>105</b>
Study Limitations	110
<b>Conclusion</b>	<b>110</b>
<b>Chapter 7. Recellularization of Xenograft Heart Valves Reduces the Xenoreactive Immune Response in an <i>in vivo</i> Rat Model</b>	<b>112</b>
<b>Abstract</b>	<b>113</b>
<b>Introduction</b>	<b>115</b>
<b>Methods</b>	<b>116</b>
Experimental Animals	116
Surgical Technique	116
MSC Isolation and Culturing	118
Decellularization and Recellularization	118
Immunohistochemistry	121
Tissue Analysis	121
Rat IgG ELISAs	121
Statistical Analysis	122
<b>Results</b>	<b>123</b>

Guinea pig aortic valve constructs can be successfully decellularized and recellularized with rat MSCs	123
Recellularization of xenograft heart valves reduces the cellular immune response similar to syngeneic tissue	130
Recellularization of xenograft heart valves reduces the humoral immune response similar to syngeneic tissue	135
Recellularization of xenograft heart valves improves graft patency and recipient survival compared to non-decellularized and decellularized xenograft	138
<b>Discussion</b>	<b>139</b>
Study Limitations	142
<b>Conclusion</b>	<b>144</b>
<b>Chapter 8. Outcomes Following Bioprosthetic Valve Replacement in Prior Non-Cardiac Transplant Recipients</b>	<b>145</b>
<b>Abstract</b>	<b>146</b>
<b>Introduction</b>	<b>147</b>
<b>Methods</b>	<b>148</b>
Data Source	148
Study Cohort	148
Outcomes	149
Statistical Analysis	149
<b>Results</b>	<b>150</b>
Study Population	150
Primary and Secondary Outcomes	152
<b>Discussion</b>	<b>154</b>
Study Limitations	156
<b>Conclusion</b>	<b>157</b>
<b>Chapter 9: Thesis Summary</b>	<b>158</b>
<b>References</b>	<b>161</b>

## List of Tables

### **Chapter 3. Comparing Scaffold Design and Recellularization Techniques for Development of Tissue Engineered Heart Valves**

Table 3.1. Comparison of various scaffold types

### **Chapter 4. Sternal Bone Marrow Harvesting and Culturing Techniques from Patients Undergoing Cardiac Surgery**

Table 4.1. Solutions and Reagents Used in Basic Protocol 1

Table 4.2. Special Equipment Used in Basic Protocol 1

Table 4.3. Solutions and Reagents Used in Basic Protocol 2

Table 4.4. Solutions and Reagents Used in Basic Protocol 3

Table 4.5. Media and Solutions Used in Basic Protocols 1, 2, and 3

Table 4.6. Troubleshooting

Table 4.7. Cell Count and Time Took to P2 Split of MSCs since Harvest

### **Chapter 5. Structural Valve Deterioration is Linked to Increased Immune Infiltrate and Chemokine Expression**

Table 5.1. Raw gene expression counts for all SVD samples used.

Table 5.2. Raw gene expression counts for all normal human heart valve samples used.

Table 5.3. Patient characteristics

### **Chapter 6. Recellularization of Bovine Pericardium with Autologous Mesenchymal Stem Cells Attenuates Initial Immune Activation**

Table 6.1. Patient characteristics

Table 6.2. Raw data for TNF- $\alpha$  presented as concentrations in pg/mL for each sample.

Table 6.3. Raw data for IL-1 $\beta$  presented as concentrations in pg/mL for each sample.

Table 6.4. Raw data for DNA presented as concentration in ng/ $\mu$ L for each sample.

Table 6.5. Raw data for hydroxyproline presented as quantity in  $\mu$ g for each sample.

Table 6.6. Raw data for glycosaminoglycan presented as concentration in ng/mL for each sample.

Table 6.7. Raw data for TNF-a presented as concentrations in pg/mL for each sample at T1D, T3D and T5D.

Table 6.8. Raw data for IL-1b presented as concentrations in pg/mL for each sample at T1D, T3D and T5D.

Table 6.9. Raw data for TNF-a presented as concentrations in pg/mL for each sample at T1D, T3D and T5D.

Table 6.10. Raw data for IL-1b presented as concentrations in pg/mL for each sample at T1D, T3D and T5D.

## **Chapter 7. Recellularization of Xenograft Heart Valves Reduces the Xenoreactive Immune Response in an *in vivo* Rat Model**

Table 7.1. Raw data for DNA presented as concentrations in ng/uL for each sample.

Table 7.2. Raw granulocyte infiltration cell counts at 7-days and 21-days. Cell counts are presented as average per HPF for each sample examined.

Table 7.3. Raw T-cell infiltration cell counts at 7-days and 21-days. Cell counts are presented as average per HPF for each sample examined.

Table 7.4. Raw serum immunoglobulin concentration at 7-days and 21-days. Concentrations are presented as mg/mL for each sample examined.

## **Chapter 8. Outcomes Following Bioprosthetic Valve Replacement in Prior Non-Cardiac Transplant Recipients**

Table 8.1. Preoperative characteristics

Table 8.2. Intraoperative characteristics

Table 8.3. Clinical outcomes

## List of Figures

### Chapter 1. Thesis Overview

Figure 1.1 Thesis Overview

### Chapter 2. A Review of the Immune Response Stimulated by Xenogenic Tissue Heart Valves

Figure 2.1. Proposed interaction between innate and adaptive immunity resulting in xenogenic tissue heart valve deterioration

### Chapter 3. Comparing Scaffold Design and Recellularization Techniques for Development of Tissue Engineered Heart Valves

Figure 3.1. Schematic of recellularization protocol

### Chapter 4. Sternal Bone Marrow Harvesting and Culturing Techniques from Patients Undergoing Cardiac Surgery

Figure 4.1. Sternal bone marrow harvest with a 5mL blunted tip syringe following a sternotomy

Figure 4.2. Surface phenotyping under flow cytometry for positive cell surface antigen CD 90 (A), CD105 (B), CD 73 (C) expression and absence of negative cell surface antigen in a negative cocktail of CD 34, CD 11b, CD19, CD45, and HLA-DR (D) expression in bone marrow-derived MSCs

Figure 4.3. (A) Micrograph representing bone marrow derived MSCs. (B) Adipocyte differentiation of MSCs with LipidTOX™ Stain. (C) Osteocyte differentiation of MSCs with Alizarin Red S stain. (D) Chondrocyte differentiation of MSCs with Alcian Blue stain

Figure 4.4. (A) Time took for MSCs to reach 80% confluency since the date of collection stratified based on age groups (50-60, N=9; 61-70, N=19; 71-80, N=19; 81+, N=3). (B) Cell count at the time of P2 and time took to P2 split of MSCs

### Chapter 5. Structural Valve Deterioration is Linked to Increased Immune Infiltrate and Chemokine Expression

Figure 5.1. Representative histology of normal human heart valves with hematoxylin and eosin stain for neutrophil and plasma cell identification (A), CD3 stain for T-cell identification (B), CD20 stain for B-cell identification (C), and CD68 stain for macrophage identification (D)

Figure 5.2. Representative histology of explanted xenogenic tissue heart valves for structural valve deterioration with hematoxylin and eosin stain for neutrophil and plasma cell identification (A), CD3 stain for T-cell identification (B), CD20 stain for B-cell identification (C), and CD68 stain for macrophage identification (D)

Figure 5.3. Quantification of immunohistochemical analysis for neutrophils (A), plasma cells (B), T-cells (C), B-cells (D) and macrophages (E). All cell counts are presented as number of cells counted per high powered field

Figure 5.4. Quantification of mRNA transcripts using Nanostring technology for a screening panel of nine gene products including, BTLA (A), CTLA4 (B), CXCL1 (C), CXCL10 (D), CXCL13 (E), CXCL16 (F), CXCL9 (G), CXCR3 (H) and IFNG (I). All gene expression is presented as log<sub>2</sub> normalized counts and corrected for GAPDH expression

## **Chapter 6. Recellularization of Bovine Pericardium with Autologous Mesenchymal Stem Cells Attenuates Initial Immune Activation**

Figure 6.1. Production of pro-inflammatory cytokines TNF- $\alpha$  and IL-1 $\beta$ . Native bovine pericardium (NBP) produces a similar production of TNF- $\alpha$  and IL-1 $\beta$  as forced stimulation with PMA/ionomycin (Stimulated), while unstimulated whole blood does not result in any cytokine production.

Figure 6.2. DAPI nuclei staining, SEM and TEM images assessing decellularization and recellularization procedure and impact on the ultrastructure of the extracellular matrix.

Figure 6.3. H&E, elastic van Gieson and Gomori's assessment on the distribution of elastin or collagen, respectively.

Figure 6.4. Biochemical quantification of DNA and ECM components hydroxyproline and glycosaminoglycans in NBP, after decellularization (DBP), and after recellularization (RBP).

Figure 6.5. Decellularization alone does not significantly reduce initial pro-inflammatory cytokine production. Initial TNF- $\alpha$  cytokine production tapers off after 3 and 5-days of exposure to NBP and DBP, with significantly less production in the DBP group at 3-days. Initial IL-1 $\beta$  cytokine production is sustained and remains robust through 5-days, with no significant difference between NBP and DBP.

Figure 6.6. Immunofluorescent staining assessing presence of the alpha-gal epitope (red) on the NBP (A), DBP (B) and RBP (C). *Blue- DAPI nuclear stain; green- collagen, red- alpha-gal.*

Figure 6.7. Autologous MSC recellularization (RBP) of native bovine pericardium reduces initial pro-inflammatory cytokine production equivalent to that generated by autologous human pericardium (HP). At 1, 3 and 5-days, there is no significant difference in TNF- $\alpha$  or IL-1 $\beta$  cytokine production between HP and RBP.

## **Chapter 7. Recellularization of Xenograft Heart Valves Reduces the Xenoreactive Immune Response in an *in vivo* Rat Model**

Figure 7.1. Schematic of aortic valve graft harvest and infrarenal implantation model.

Figure 7.2. DAPI nuclear staining on non-decellularized guinea pig (NGP, A&D), decellularized guinea pig (DGP, B&E) and recellularized guinea pig (RGP, C&F) aortic valve constructs.

Figure 7.3. Gross histology was performed with H&E and vimentin staining. Syngeneic rat aortic valves are shown in A and B confirming presence of cellular material and an intact ECM. Presence of cellular material and an intact ECM structure was observed in the NGP tissue prior to decellularization (C and D). Following decellularization there is complete absence of cellular material, however the ECM structure is grossly preserved (E and F). Recellularization with rat MSCs was performed and resulted in restoration of a confluent layer of MSCs lining the valvular tissue (G and H).

Figure 7.4. Biochemical quantification of DNA in NGP, after decellularization (DGP), and after recellularization (RGP).

Figure 7.5. Panel A summarizes the granulocyte cell infiltration observed in the explanted grafts at 7-days and 21-days. Panel B summarizes the CD3<sup>+</sup> T-cell infiltration observed in the explanted grafts at 7-days and 21-days.

Figure 7.6. Representative gross histology for granulocytes with H&E staining and T-cells with anti-CD3 staining in syngeneic (A and B), NGP (C and D), DGP (E and F) and RGP (G and H) explanted tissues.

Figure 7.7. Panel A summarizes the total serum immunoglobulin results observed after 7-days of implantation. Panel B summarizes the total serum immunoglobulin results observed after 21-days of implantation, revealing similar overall trends as seen after 7-days.

Figure 7.8. Overall survival and graft thrombosis at the 21-day endpoint.

Supplementary Figure 7.1. Gross histology demonstrating negative staining for CD34 of MSCs used in recellularization protocol.

Supplementary Figure 7.2. Gross histology was performed with H&E and vimentin staining. Presence of cellular material and an intact ECM structure was observed in the NGP tissue prior to decellularization (A and B). Following decellularization there is complete absence of cellular material, however the ECM structure is grossly preserved (C and D). Recellularization with rat MSCs was performed and resulted in restoration of a confluent layer of MSCs lining the valvular tissue (E and F).

## **Chapter 8. Outcomes Following Bioprosthetic Valve Replacement in Prior Non-Cardiac Transplant Recipients**

Figure 8.1. Kaplan-Meier curve for long-term survival

## List of Abbreviations

Alpha-gal,  $\alpha(1,3)$ -galactose  
APC, antigen presenting cell  
BM, bone marrow  
BMC, bone marrow derived mononuclear cells  
CD, cluster of differentiation  
CXCL, chemokine ligand  
CXCR, chemokine receptor  
DAG, diacyl glycerol  
DAPI, 4',6-diamidino-2-phenylindole  
DBP, decellularized bovine pericardium  
DDH<sub>2</sub>O, double distilled water  
DGP, decellularized guinea pig  
DMEM, Dulbecco's modified eagle medium  
DNA, deoxyribonucleic acid  
ECM, extracellular matrix  
EDTA, ethylenediaminetetraacetic acid  
ELISA, enzyme linked immunosorbent assay  
eVG, elastic Verhoeff's van Gieson  
FBS, fetal bovine serum  
FFPE, formalin-fixed paraffin-embedded  
GAG, glycosaminoglycan  
H&E, hematoxylin and eosin  
HPF, high-powered field  
HYP, hydroxyproline

IFC, ice-free cryopreservation  
IFN, interferon  
IL, interleukin  
MHC, major histocompatibility complex  
MMP, matrix metalloprotease  
MSC, mesenchymal stem cell  
NGP, native guinea pig  
NBP, native bovine pericardium  
PBS, phosphate-buffered saline  
PCL, polycaprolactone  
PGA, polyglycolic acid  
PLA, polylactic acid  
PMA, phorbol 12-myristate 13-acetate  
RBP, recellularized bovine pericardium  
RGD, arginylglycylaspartic acid  
RGP, recellularized guinea pig  
RNA, ribonucleic acid  
RT-PCR, real-time polymerase chain reaction  
SDS, sodium dodecyl sulfate  
SEM, scanning electron microscopy  
SVD, structural valve deterioration  
TAVI, transcatheter aortic valve insertion  
TEHV, tissue engineered heart valve  
TEM, transmission electron microscopy  
TNF, tumour necrosis factor

TrypLE, trypsin-like enzyme

VIC, valvular interstitial cell

VHD, valvular heart disease

XTHV, xenogenic tissue heart valve

## Chapter 1: Thesis Overview

### Background

Valvular heart disease (VHD) is a common diagnosis with an approximate prevalence of 2.5% of the total population having moderate to severe VHD [1, 2]. Furthermore, the prevalence of valvular disease increases with age, as VHD is < 2% before the age of 65 years and is increased to 13.2% after the age of 75 years [1, 2, 10, 11]. Therefore, as the population of the developed world continues to age, the burden of VHD on health care will continue to expand as is emphasized by the five million Americans diagnosed with VHD each year [1, 10]. The most common treatment for end-stage valvular diseases is surgical intervention. Whereas valve replacement surgery has evolved since the early 1950's, major clinical advances in valve replacement constructs have lagged. There still exist only two basic alternatives, mechanical and biological prostheses, both of which have significant limitations [11]. Mechanical valves display good structural durability but are associated with the risk of prosthetic valve endocarditis, and thromboembolic complications caused by their non-physiological surfaces and flow abnormalities [12, 13]. Life-long anticoagulation therapy is necessary for these patients, associated with substantial risks of spontaneous bleeding and embolism, particularly in patients over 70 years old [14]. Bioprosthetic heart valve replacements are either of animal origin (xenografts), such as porcine aortic valves and bovine pericardial valves, or taken from human donors (homografts and autografts). Xenografts are chemically cross-linked. This inhibits autolysis, enhances the mechanical stability, and creates the possibility of having valves of different sizes stored and available off-the-shelf [15-17]. Unfortunately, these valves differ in many respects from native valves, for example in their opening and closing behavior due to the above-mentioned chemical pretreatment [12, 16]. The risk of thromboembolic complications is

much lower when compared with mechanical prostheses, but their durability is limited [8, 18]. Structural failure is strongly age dependent, making them suitable primarily for the elderly and less for children and young adults.

Several attempts have been made to create functional heart valve replacements, with the ability to grow, repair and to remodel, using the concept of tissue engineering. A decellularized tissue engineered heart valve (TEHV) has potential to provide excellent initial performance [19-22]. That said, despite early reports showing that decellularized TEHVs mitigate issues with valve prosthesis and have thus shown early success, more recent reports have suggested that nonviable tissue valves are prone to degradation, thrombus formation and calcification [23]. One concept in heart-valve tissue engineering is to use decellularized biologic matrices with autologous cell reseeded [24-28]. These matrices consist of allogeneic or xenogeneic materials that are decellularized either enzymatically or by detergent methods [29, 30]. As the availability of autologous heart valves is limited in the context of worldwide organ scarcity, current research focuses on xenogeneic tissue [31].

There is emerging evidence suggesting that current xenograft constructs used in cardiac surgery provoke an intense cell-mediated and humoral immune response that is largely believed to be the cause of time-dependent structural valve deterioration [4-6, 32]. The mechanism surrounding the immune response elicited by this tissue remains largely unknown. Furthermore, it remains unclear what effect an autologous recellularized xenograft has on the immune response in the host. As such, there is a significant gap in knowledge regarding the role of the immune system in the development of xenograft heart valve deterioration. By addressing these gaps and improving our understanding of the immune mechanisms elicited by XTHVs and

autologous recellularized xenografts, we can ascertain if this approach may be a viable option for future valve constructs.

## **Hypothesis**

We hypothesize that xenograft heart valve deterioration and subsequent prosthesis failure is due to a chronic, xenoreactive immune response. We further hypothesize that this xenoreactive immune response can be attenuated with the creation of an autologous recellularized acellular matrix or administration of immunomodulatory therapeutics, leading to improved valvular durability.

## **Objectives**

The objectives of this thesis are displayed in **Figure 1.1**.

1. Provide an overview of the immune system, the immune response to xenografts and how this immune response impacts valvular function (Chapter 2)
2. Describe the various scaffold design and recellularization techniques for the development of tissue engineered heart valves (Chapter 3)
3. Develop a protocol for isolation and culturing techniques of mesenchymal stem cells (MSCs) from sternal bone marrow from patients undergoing cardiac surgery (Chapter 4)
4. Establish the role of immunity in development of xenograft heart valve deterioration by analyzing explanted xenograft heart valves (Chapter 5)
5. Demonstrate the ability to attenuate the xenoreactive immune response using autologous recellularized tissue in a human, *in-vitro* model (Chapter 6)
6. Demonstrate the ability to attenuate the xenoreactive immune response using autologous recellularized tissue in a small animal, *in-vivo* model (Chapter 7)

7. Analyze the effect of immunomodulatory therapeutics on clinical rates of xenograft heart valve deterioration amongst patients undergoing valve replacement (Chapter 8)

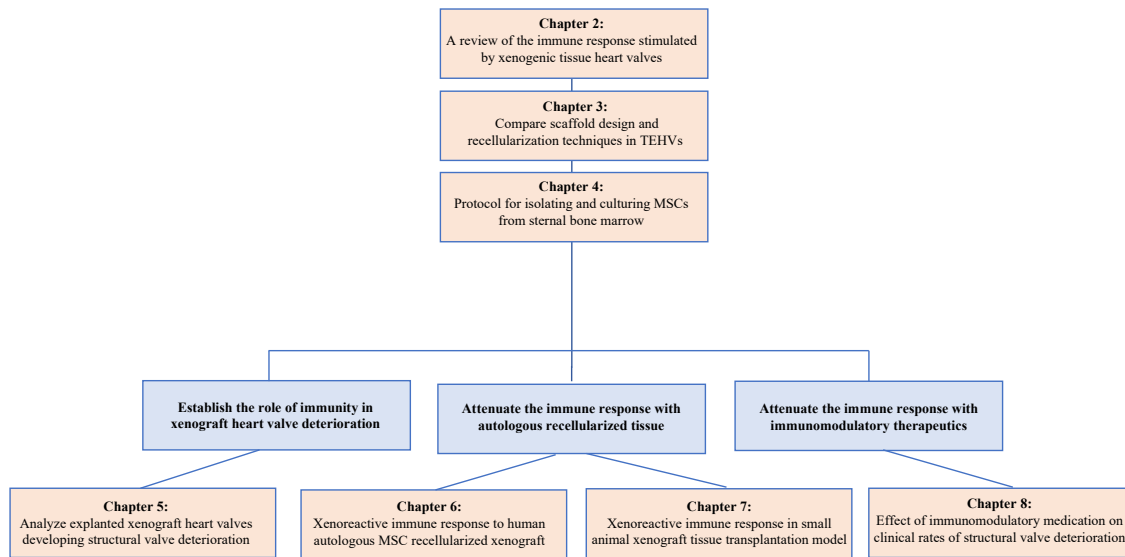


**Figure 1.1.** Thesis Overview

**Chapter 2: A Review of the Immune Response Stimulated by Xenogenic  
Tissue Heart Valves**

*Scandinavian Journal of Immunology*

2020

DOI: 10.1111/sji.13018

## **Abstract**

Valvular heart disease continues to afflict millions of people around the world. In many cases, the only corrective treatment for valvular heart disease is valve replacement. Valve replacement options are currently limited, and the most common construct utilized are xenogenic tissue heart valves. The main limitation with the use of this valve type is the development of valvular deterioration. Valve deterioration results in intrinsic permanent changes in the valve structure, often leading to hemodynamic compromise and clinical symptoms of valve re-stenosis. A significant amount of research has been performed regarding the incidence of valve deterioration and determination of significant risk factors for its development. As a result, many believe that the underlying driver of valve deterioration is a chronic immune-mediated rejection process of the foreign xenogenic-derived tissue. The underlying mechanisms of how this occurs is an area of ongoing research and active debate. In this review, we provide an overview of the important components of the immune system and how they respond to xenografts. A review of the proposed mechanisms of xenogenic heart valve deterioration is provided including the immune response to xenografts. Finally, we discuss the role of strategies to combat valve degeneration such as preservation protocols, epitope-modification, and decellularization.

## Introduction

The immune system is a complex network of diverse cell types, signalling pathways and effector molecules that has evolved to provide defense against foreign pathogens. The immune system can be divided into 2 broad categories: innate and adaptive immunity, each able to recognize and respond to a multitude of antigens. Adaptive immunity is primarily conferred by T- and B-lymphocytes, plasma cells and antibody generation. Adaptive immunity is capable of specifically recognizing and eliminating foreign pathogens, including foreign antigen on transplanted tissue/organs. The ability of the immune system to distinguish self from non-self and respond only to non-self is essential for immune homeostasis. Recognizing foreign antigen is the key mechanism to xenograft structural valve deterioration after xenotransplantation[4, 5, 33].

The primary basis of hyperacute rejection in xenotransplantation is the post-translational modification  $\alpha(1,3)$ -galactose (alpha-gal) that is found in all non-primate mammals and new world primates[34, 35]. From exposure to natural gut bacteria all humans develop anti-alpha-gal antibodies. These anti-alpha-gal antibodies constitute 1-8% of IgM and 1-2.5% of IgG's found in human circulation[36]. Therefore, the alpha-gal antigen is the dominant mediator of hyperacute rejection in discordant xenotransplants. Acute rejection involves recipient T cell activation by recognition of intact donor Major Histocompatibility Complex (MHC) on donor antigen presenting cells (APC), contained within the transplanted organ, and is manifested in days to weeks[37]. Chronic rejection, occurring over months, is thought to be due to continual recipient T cell activation by recipient APCs presenting foreign peptides as they are shed by the donor organ.

As the availability of autologous heart valves is limited due to organ scarcity, current research focuses on xenogenic tissue[31]. There is a growing body of evidence demonstrating

that xenograft constructs used in cardiac surgery provoke a cell-mediated and humoral immune response that is believed to be the cause of their valve deterioration[4, 5].

## **Immune Response to Xenogenic Tissue Heart Valves**

The mechanisms by which the immune system recognizes and responds to xenogenic tissue heart valves likely involve the initial activation of the innate immune system, with subsequent adaptive immune activation (Figure 2.1). Two of the dominant effector cells of innate immunity are macrophages and neutrophils. The process of crosslinking preserves collagen in its intact fibrillar formation, which is susceptible to degradation by matrix metalloprotease (MMP)-1 and MMP-8, secreted primarily by macrophages and neutrophils, respectively. This front-line inflammatory response is enhanced by neutrophil binding of complement components including iC3b, and preformed IgM[38]. Class I MHC molecules can be cross-linked; therefore 3 main mechanisms of immune responses are possible: pre-formed antibodies, macrophage interaction, and IgG response via MHC Class II on macrophages. Macrophages adhere to low-flow areas of the valve, primarily in the fibrosa, and interaction must result in degraded molecules presentable on MHC Class II molecules. Macrophages also play a pivotal role in myointimal proliferation, with a reaction to even the Dacron sewing ring with upregulation of basic fibroblast growth factor, a chemoattractant for fibroblasts. In fact, specific antibodies are detected in recipients of xenogenic bioprosthetic heart valves (IgG against HLA Class I antigens)[38]. Furthermore, extracellular matrix (ECM) proteins are capable of inducing a strong and specific antibody response, and Class II, rather than Class I, antigens may be contributing to valve failure with 3-fold higher calcification in aortic wall tissue pre-incubated in serum containing high levels of graft-specific antibodies[38]. Others suggest that macrophage activation through IgM and IgG and neutrophil activation via IgM and iC3b appear to be crucial in the degeneration process

observed in damaged xenogenic tissue heart valves[39]. Alpha-gal has been identified even in decellularized scaffolds with an elicited anti-alpha-gal IgG antibody response. In-vitro studies have shown a strong iC3b deposition on decellularized porcine heart valves incubated with human plasma, leading to increased adhesion of polymorphonuclear (PMN) leucocytes[39]. Finally, another important carbohydrate residue involved in the humoral anti-xenograft response is the N-glycolylneuraminic acid (Neu5Gc), the hydroxylated form of Neu5Ac. Humans do not possess the functional enzyme CMP-Neu5Ac-hydroxylase (CMAH) that catalyzes conversion of Neu5Ac to Neu5Gc, therefore it is recognized as foreign [40].

The role of circulating graft-specific antibody in the development of valve deterioration has also been studied[41]. Immune-calcification studies were performed in rabbit and correlated with analysis of specific antibodies. Porcine aortic wall buttons were implanted into 2 groups of rabbits; one group that was immune serum-treated and the other naïve. Tissue calcium was increased in all immune serum-treated samples compared with the controls, suggesting a role of circulating graft-specific antibody in the development of valve deterioration. The impact of T-cells was further examined by assessing the T cell subsets of peripheral blood from recipients of long-term functioning xenogenic tissue and mechanical heart valve prostheses[42]. Several T-cell types were examined for including naïve, central memory, effector memory and terminally differentiated T-cells. The numbers of central memory and naïve cells was decreased, while the number of terminally differentiated effector cells was increased, with an altered composition of T-cell subsets in the mechanical valve group. This points to the development of a unique and specific inflammatory tissue reaction against both mechanical and xenogenic tissue heart valve prostheses. The timing of this inflammatory reaction has been elucidated by studying wild-type porcine hearts before and after heterotopic transplantation into baboons[43]. Alpha-gal was not

detected on the endothelium of porcine valves, and neither was IgM, on either aortic or pulmonary valves, suggesting that xenograft heart valve leaflets are protected from hyperacute rejection. Crosslinking clearly prevents hyperacute and acute rejection of xenogeneic tissue, however glutaraldehyde-fixed xenogenic heart valves possess considerable residual chronic immunogenicity. This residual immunogenicity may be related to xenoepitope exposure secondary to the repetitive biomechanical stress endured by these bioprostheses, resulting in cracking of the glutaraldehyde chemical shield. Furthermore, it is important to note that decellularized, glutaraldehyde-fixed porcine heart valves are not considered xenotransplants. This is conferred by IgG-class antibodies towards both non-alpha-gal antigens and alpha-gal epitopes and directed specifically towards two porcine proteins, albumin and collagen alpha-1 (VI) [44]. Furthermore, a vegetarian diet may reduce pre-formed a-Gal antibodies, with reduced anti-alpha-gal antibodies in vegetarian subjects[44].

While the humoral immune response has been implicated with a clear role for IgG antibodies directed towards foreign antigen such as alpha-gal, the role of cell infiltration has been less studied. Another method of analyzing the immune response to xenogenic tissue heart valves is by studying clinically utilized valves that have degenerated requiring re-operation. Studies aimed at analyzing explanted normal human valves compared to explanted xenograft constructs have been performed to further elucidate mechanisms and cell types involved in the immune response. Normal and abnormal human valves were examined for the presence of stem cells in human heart valves[45]. Interestingly, clusters of CD 117-positive cells, later identified as mast cells, were found in all groups along with a small number of CD 117-positive cells and toluidine blue-negative stem cells in diseased adult human heart mitral valves. This suggests progenitor cells play a role in the maintenance and propagation of a chronic immune response to

abnormally functioning valves. The clinical feasibility of using immunologically untreated xenogeneic valves was studied using a porcine-to-goat pulmonary valved conduit[46]. The valves were explanted at 12-months and host cells had gradually replaced xenograft cells with removal of donor cells by pyknosis and karyolysis, suggesting a self-healing potential for xenografts. It is important to note that both porcine and goat species possess the alpha-gal and Neu5Gc antigens and are therefore not discordant for these epitopes. Thus, the results this study should be interpreted with caution in regard to the context of immune responses to xenotransplanted tissues. Optimism should be tempered, however, since midterm results of xenograft valved conduits found that up to 20% required reoperation due to conduit failure with the main reason being conduit stenosis[47].

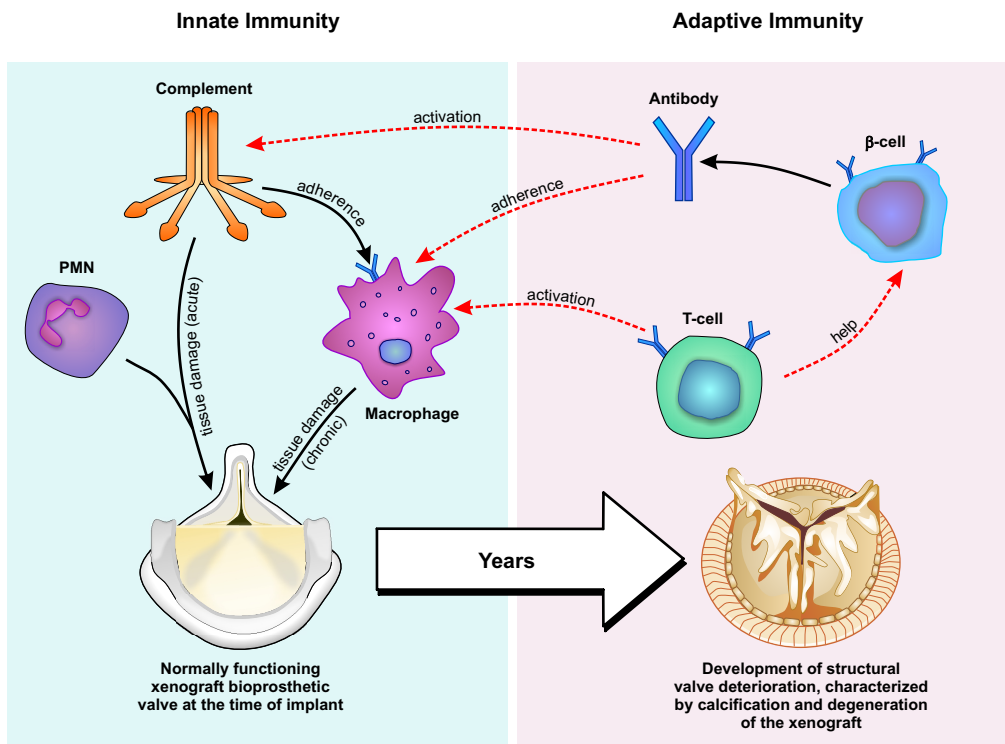


**Figure 2.1.** Proposed interaction between innate and adaptive immunity resulting in xenogenic tissue heart valve deterioration

## Role of Antigens

The antigenicity of xenograft constructs, primarily porcine and bovine, has been extensively investigated. Most notable is the alpha-gal epitope, consisting of the Gal-alpha (1,3) Gal dimer linked to N-acetylglucosamine, similar to the structure of blood group B antigens in humans. It is expressed in non-primate mammals and synthesized by the alpha 1,3-galactosyltransferase (GGTA1) and is silent in human and old-world primates [48, 49]. It is possible to create GGTA1-KO animal models in an attempt to decrease alpha-gal expression. However, in the absence of GGTA1, another enzyme (iGb3 synthase) leads to production of low-levels of alpha-gal epitope, undermining the immunological benefit derived from the use of GGTA1-KO animals[50]. Alpha-gal expression using Western blot was assessed on porcine valve endothelium, aortic endothelium and human vein endothelium and was detectable only on porcine valve endothelium[51]. The presence of alpha-gal epitope on porcine valves was examined using ELISA to quantify anti-alpha-gal IgM antibodies and compared to patients undergoing isolated coronary artery bypass grafting and isolated mechanical valve replacement. Implantation of a porcine bioprosthesis induced a xenograft-specific immune response, that can selectively exert cytotoxic effects on alpha-gal bearing cells[52]. The presence of the alpha-gal epitope on commercially available porcine bioprosthesis has also been described[53]. The same authors also demonstrated that it is possible to remove this epitope with a decellularization protocol. They determined that alpha-gal interacts with natural preformed IgG antibodies, activating the classic complement pathway in humans. Analysis for alpha-gal has been performed in commercially available glutaraldehyde-fixed xenogenic tissue heart valves [54]. Valves were divided into bovine and porcine valves, with all commercially available valves having less alpha-gal than native bovine or porcine tissue. The Epic <sup>TM</sup> valve was the only one

tested that was completely shielded from alpha-gal. All others express alpha-gal not significantly different from that exhibited by porcine tissue.

Several other antigenic epitopes exist on xenogenic tissue, in addition to alpha-gal. Porcine valve tissue from 20 animals was used to isolate and structurally characterize both non-acid and acid glycosphingolipids other than alpha-gal[55]. The components were structurally characterized by thin-layer chromatography, liquid chromatography-mass spectrometry and binding of monoclonal antibodies and lectins. Several non-acid glycosphingolipids including globotetraosylceramide, H-type 2 pentaosylceramide, fucosyl-gangliotetraosylceramide and Gal-alpha-3-neolactotetraosylceramide were identified. The acid glycosphingolipids had both sulfatide and gangliosides, all containing the important antigen, N-acetyl neuraminic acid. An elegant immunoproteomic identification of bovine pericardial xenoantigens in rabbits has also been performed[56]. These investigators identified 31- putative protein antigens, including a variety of structural and functional protein types with both cellular and matrix proteins. It is clear that both humoral and cell-mediated immune responses occur to glutaraldehyde-fixed xenografts. Furthermore, the apparent elimination of intact cells by light microscopy does not assure adequate removal of xenoantigens, thus the emphasis has shifted from simply decellularization to more complex antigen removal.

One potential reason decellularization alone does not completely eliminate the xenoreactive immune response may be secondary to a variety of foreign ECM protein, resulting in a robust host immune response [57-59]. Therefore, antigen removal or masking treatments must account for both cellular and ECM antigens. Our understanding of antigenicity of bovine pericardium can be improved by application of a combined affinity chromatography shotgun immunoproteomic approach to identify novel antigens. This especially focused on the

antigenicity of bovine ECM, since decellularization has proven to be a poor predictor of *in-vivo* recipient graft-specific immune response. This approach identified 133 antigens, importantly, from all subcellular locations, including 18 integral membrane protein antigens[60]. It's important to note that previous methods have underrepresented highly lipophilic proteins. Interestingly, the immune response, coagulation and inflammation accounted for 10.5%, 6%, and 3.8% of total antigen identifications. Compared to the percentage of proteins associated with these processes in the total bovine proteome of 4.3%, 0.2% and 1.5%, these are clearly overrepresented. This suggests that the xenogenic immune response is intimately related and intricately coordinated to the coagulation and inflammatory cascades.

Similar to alpha-gal, the role of Neu5Gc has been extensively investigated as an important xenogenic antigenic epitope, capable of stimulating a robust, specific immune response [61]. The expression of both alpha-gal and NeuGc on heart valves and pericardium of pigs in wild-type (WT), GGTA1-KO and CMAH-KO was compared to commercially available xenogenic tissue heart valves to determine human antibody binding to those tissues[62]. High levels of alpha-gal and Neu5Gc expression on all xenogenic tissue heart valves, fresh or fixed, was identified. Interestingly, glutaraldehyde fixation did not alter expression of alpha-gal or Neu5Gc. After incubation with human serum, human IgM and IgG bound to all xenogenic tissue heart valves and WT pig valves. However, valves from GGTA1-KO and GGTA1-KO/CMAH-KO pigs showed significantly less IgM and IgG binding. Neu5Gc immunogenicity on xenogenic tissue heart valves has also been assessed through recognition by human anti-Neu5Gc IgG[63]. Neu5Gc levels differ depending on tissue type, with porcine and bovine pericardium expressing 4-fold higher levels compared to porcine aortic or pulmonary valves. This is of significant interest, given that the far majority of commercially available xenogenic tissue heart valves are

composed of xenogenic derived pericardium. Furthermore, affinity-purified human anti-Neu5Gc IgG showed high specificity toward Neu5Gc-glycans and strongly bound to all tested commercial xenogenic tissue heart valves, supporting the Neu5Gc antigen as immunogenic. Although presence of Neu5Gc on xenogenic valve tissue is still being debated, immunofluorescence analysis provides evidence of Neu5Gc on collagen of pig aortic and pulmonary valves, as well as on pig pericardium[64]. Furthermore, anti-Neu5Gc antibodies can form and may contribute to delayed xenograft rejection[65].

### **Antigen Modification**

Given the demonstrated immune response to xenografts, several attempts at mitigating the immune response have been undertaken. These include preservation protocols, epitope-modification, and decellularization. The effect xenogeneic immune responses on the histopathological changes in aortic valve grafts and the influence of preservation techniques has been investigated. Compared to immediate implantation, both cryopreserved and fresh-preserved xenografts showed more prominent disruption of the elastic fibers, more microthrombi and earlier disappearance of the leaflet[66]. This is due to failure of retention of cellular components during preservation, exposing extracellular antigens. Comparing cryopreserved and fresh xenografts, cryopreserved grafts maintained more fibroblasts than fresh grafts at 1-month, providing an improvement in durability[67]. Cryopreserved xenografts had increased T-cell infiltration; however, the fresh xenografts had lost cellularity, implying cryopreservation might influence the morphological changes in valve xenotransplantation[68]. In contrast, others have found preserved cellular viability and fewer degenerative changes using a fresh-storage protocol, compared to frozen-stored xenografts[69]. The modulatory effects of ice-free cryopreservation (IFC) of xenogeneic heart valve leaflet matrices, without decellularization, on the adaptive

human immune response in vitro has been assessed. IFC-preserved valves demonstrated reduced proliferation of T-cells, reduced IFN- $\gamma$ , TNF- $\alpha$  and IL-10 expression[32]. Therefore, IFC may be an appropriate treatment method or processing step to mitigate activation of the adaptive immune system.

Modification of antigenic epitopes has been undertaken with enzymatic cleavage of epitopes and generation of genetically modified animals. One of the first targets, given the demonstrated immunogenicity, is alpha-gal. Recombinant human alpha galactosidase A removes the alpha-gal epitope from porcine aortic valve and pericardial tissue, and can therefore remove the alpha-gal epitope effectively[70]. The effectiveness of alpha-galactosidase treatment to degrade the major xenoreactive antigens on porcine heart valves using a mass spectrometer found alpha-gal in 6-8% of tissue surface area. After treatment, the alpha-gal epitope was not detected. No difference in mechanical properties was observed using TEM. This suggests that alpha-galactosidase can effectively remove the alpha-gal epitope and does not affect biomechanical properties[71]. The generation of engineered pigs lacking both GGTA1 and CMAH has been reported [72]. This has had beneficial effects in decreasing, but not eliminating, the binding and cytotoxicity of human antibodies directed to porcine cells. However, unintended consequences from deletion of GGTA1 and CMAH may shift sugar metabolism toward expression of de novo, previously non-existing, glycoconjugates. Recently, a novel beta-1,4-N-acetylgalactosaminyltransferase responsible for the synthesis of the rare SD<sup>a</sup> blood group antigen has been implicated in the rejection of porcine cardiac xenografts, with significant induction of non-alpha-gal antibody[73]. Many believe that an IgG and granulocyte activating immune response with secondary dystrophic calcification may be the reason that xenogenic tissue heart valves fail; meanwhile others believe it is due to chemical processes (free aldehyde groups with

phospholipids as a nidus for calcification). In an attempt to differentiate between these theories, authors treated glutaraldehyde-fixed bovine pericardium with 3 different treatments: 10% citric acid, 10% citric acid, aldehyde-dehydrogenase and physical plasma treatment, and titanium nanocoating. Only nanocoating with titanium reduced the immunologic response to glutaraldehyde-fixed bovine pericardium, significantly reducing iC3b deposits and PMN leucocyte activation, suggesting crosslinking with glutaraldehyde does not completely render the xenograft immune privileged [74].

## **Conclusion**

There is an ongoing focus on the development of an immunologically acceptable, unfixed xenogeneic scaffold for future heart valve constructs. Both decellularization and antigen modification have emerged as early methods of attenuating the immune response. However, this relies on the flawed fundamental assumption of relying on scaffold acellularity as a sole outcome measure, since this ignores the importance of ECM components in stimulating an immune response. It is crucial to understand that the absence of cellularity does not imply the absence of antigenicity. Therefore, there is a critical need to remove, or mask, antigenic components. This recognizes that cellular and non-cellular antigens within a tissue both represent immunological barriers, and we must strive to eliminate these sources of antigenicity. We must also appreciate the need to assess residual antigenicity and determine how this outcome measure translates to the ultimate goal of generating immunologically acceptable, unfixed tissue-derived scaffold.

**Chapter 3. Comparing Scaffold Design and Recellularization Techniques for  
Development of Tissue Engineered Heart Valves**

*Regenerative Engineering and Translational Medicine*

2020

DOI: 10.1007/s40883-020-00167-x

## **Abstract**

Valvular heart disease continues to afflict millions of people around the world. In many cases, the only corrective treatment for valvular heart disease is valve replacement. Valve replacement options are currently limited, and the most common constructs utilized are xenogenic tissue heart valves. The main limitation with the use of this valve type is the development of valve deterioration. Emerging evidence suggests that the underlying driver of valve deterioration is a chronic immune-mediated rejection process of the foreign xenogenic-derived tissue. There is an ongoing focus on the development of an immunologically acceptable, unfixed xenogeneic scaffold for future heart valve constructs. Tissue engineering heart valves are a promising method of developing a durable, non-immunogenic, non-thrombotic, easily implantable and readily available implant. In this review we summarize the various decellularization protocols and scaffold designs for tissue engineered heart valve use and highlight the different cell types and methods for recellularization of tissue engineered heart valves.

## Introduction

The immune response to xenograft tissue has been clearly elucidated, with several critical antigenic epitopes identified [55, 56, 60]. Modification of those epitopes by enzymatic cleavage or decellularization lessens, but does not eliminate, the xenogenic-induced immune response. This immune response, when directed to xenogenic tissue heart valves (XTHVs), is an integral component of the development of valvular calcification [75]. This calcification occurs independent of glutaraldehyde-fixation that stabilizes the xenograft tissue. The cross-linking of major surface proteins achieved by glutaraldehyde-fixation does not eliminate the formation of calcification [76]. Predictably, explanted XTHVs developing clinical manifestations of valvular deterioration contain evidence of a protracted, chronic, immune-mediated rejection [6]. The impact of valvular deterioration on patients receiving XTHVs is significant, with considerable rates of re-operation required.

All of these factors have been the impetus for the development of tissue engineered heart valves (TEHV); valves designed to be durable, non-immunogenic, non-thrombotic, easily implantable and readily available. Several different scaffold types exist that have each been used in a variety of methods experimentally and clinically. Similarly, there has been significant investigation to determine the optimal cell type to be used to repopulate acellular TEHVs while synthesizing an immuno-privileged tissue. Tissue-engineering relevant to heart valves is defined as the manipulation of biological molecules and cells for the purpose of creating new structures capable of metabolic activity [77]. In this review we summarize the various decellularization protocols and scaffold designs for TEHV use and highlight the different cell types and methods for recellularization of TEHVs.

## Decellularization and Scaffold Type

Initial attempts at TEHVs were very basic, exploring the effects of dynamic vs static glutaraldehyde-fixation of porcine aortic valve xenografts. The dynamic glutaraldehyde-fixed valves had a stress-relaxation more closely mimicking fresh valves, and a greater degree of intra vs intercellular cross-linking. This was one of the earliest attempts at a TEHV, focused on improving long-term biomechanical performance and durability [78]. In order to utilize a scaffold with cellular structures present (i.e. xenogenic tissue) to create a TEHV, the cells must be removed with a decellularization protocol. The impact of different decellularization protocols on extracellular membrane (ECM) integrity of xenogenic tissue using multiphoton laser scanning microscopy was assessed. Utilizing trypsin-EDTA solution incubated for varying time periods, it was found that at 5 and 8-h, there was incomplete cell removal by histology compared to 24-h. However, there is also a time-dependent decrease in glycosaminoglycan content and mechanical strength related to the efficiency of insoluble collagen extraction increasing proportionally with decellularization time. This suggests ECM-integrity may be compromised with prolonged incubation and that 24-h is the optimal time for enzymatic decellularization [79]. Another method of decellularization is to use a detergent based approach. The effects of enzymatic (trypsin) and detergent (Triton) based decellularization of ECM were compared [30]. Enzymatic based led to fragmentation and distortion of elastic fibers, while changes in collagen distribution were observed in both groups, including loss of adhesion molecules laminin and fibronectin. Consequently, detergent-based methods for decellularization should be utilized since they best preserve the ECM. Novel storage methods for decellularized xenografts have been investigated, including freeze-drying. However, after implantation, a high number of immune cells (CD45+ and CD11b+) are present in the freeze-dried grafts, despite good mechanical function [80].

Nonetheless, this may represent a promising method to extend the shelf-life of future valvular grafts. Other materials have been proposed as potential biomaterials for cardiac application. Tuna cornea is composed of only collagen fibers and no cells. Mitral valves have been fabricated from tuna corneal leaflets with stable valve performance after implantation in sheep [81].

As discussed, xenogenic valvular grafts stimulate a variety of immune responses in the host. A consistent set of data has been amassed establishing that these immunologic responses are the foundation of the valve deterioration seen in xenogenic implants. A modality to render xenogeneic matrices immunoprivileged and amenable to further autologous-like regeneration has been offered by decellularization technology. This extraction process aims to achieve removal of all endogenous cell elements including cell membranes, organelles, and nucleic acids, which can adversely prompt inflammatory, immune, and calcific events. This cell removal will decrease the effects of acute and chronic rejection via an elimination of MHC I mediated immune responses. While the decellularization of xenogenic tissue will significantly reduce the immune response of the host to the graft, it does not significantly decrease it in the way that has been seen with allograft tissue. Unlike decellularized allograft tissue, the antigenic ECM composed of xenoantigens still poses a significant barrier to xenograft implants. It is clear that the decellularized xenografts represent a promising TEHV scaffold for implantation, but the overall goal is to create an immunoprivileged xenograft.

## **Xenogenic and Allogenic Scaffolds**

The ECM of native tissues has the potential to be an ideal scaffold for use in tissue engineering and regenerative medicine applications. For a given tissue type, the inherent ECM composition and architecture confers the appropriate mechanical properties necessary for immediate physiological function of the resultant scaffold. This is in contrast to synthetic

scaffolds, which require extended periods of time to undergo tissue morphogenesis and remodeling under optimal environmental conditions in order to gain acceptable mechanical properties. The advantage of having an inherently mechanically appropriate scaffold is particularly important for grafts that are required to function immediately upon implantation, such as heart valves, which must maintain unidirectional blood flow in the heart. Moreover, the complex compositional and architectural elements that constitute ECM, organized at the levels of molecules, macromolecules, and complexes of macromolecules provide both molecular and topographical cues which are capable of directing cellular phenotype and organization. Recipient immune response to the antigenic components of xenogeneic tissues, including xenogenic ECM, represents the critical barrier to the use of xenogeneic scaffolds in translational applications.

<b>Scaffold Type</b>	<b>Advantages</b>	<b>Disadvantages</b>
Xenogenic	<ul style="list-style-type: none"> <li>• Inherent extracellular matrix allows for immediate physiologic function</li> <li>• Widely available</li> <li>• Shelf-stable</li> </ul>	<ul style="list-style-type: none"> <li>• Immunogenic</li> <li>• Decellularization generally required</li> <li>• Inability to remodel and repair</li> </ul>
Allogenic	<ul style="list-style-type: none"> <li>• Less immunogenic</li> <li>• May not require decellularization</li> </ul>	<ul style="list-style-type: none"> <li>• Limited availability</li> </ul>
Synthetic	<ul style="list-style-type: none"> <li>• Less immunogenic</li> <li>• Able to remodel and repair</li> </ul>	<ul style="list-style-type: none"> <li>• Labor intensive</li> <li>• Prohibitively expensive</li> </ul>

**Table 3.1.** Comparison of various scaffold types

XTHVs are not composed of viable structures with the potential to remodel and repair, leading to premature degeneration of the valve and the need for earlier reoperation. A TEHV, made of autologous cells and a biocompatible scaffold, with the potential to remodel, repair and grow, would be a favorable option. Allogenic or xenogeneic pulmonary valve constructs were recellularized with autologous myofibroblasts and endothelial cells, then implanted in sheep

[82]. The grafts were explanted at 9-months and complete cellular reconstitution of endothelial cells was identified, however 50% of valves degenerated and developed regurgitation. The first attempt at creation of a xenogenic-derived matrix seeded with human autologous cells was performed in 1998 [83] using a decellularized porcine aortic valve and human endothelial cells. The porcine matrix was successfully re-seeded with cells and maintained in culture for 3-days, demonstrating the feasibility of this very preliminary approach. Other cell types have also been investigated for use in various recellularization protocols, including aortic valve interstitial cells (VICs), bone marrow (BM) derived mononuclear cells, and mesenchymal stem cells (MSCs) [84, 85]. VICs can successfully repopulate detergent-treated matrices and can give rise to a heterogenous mesenchymal stromal cell population while gradients are lower in the MSC valves.

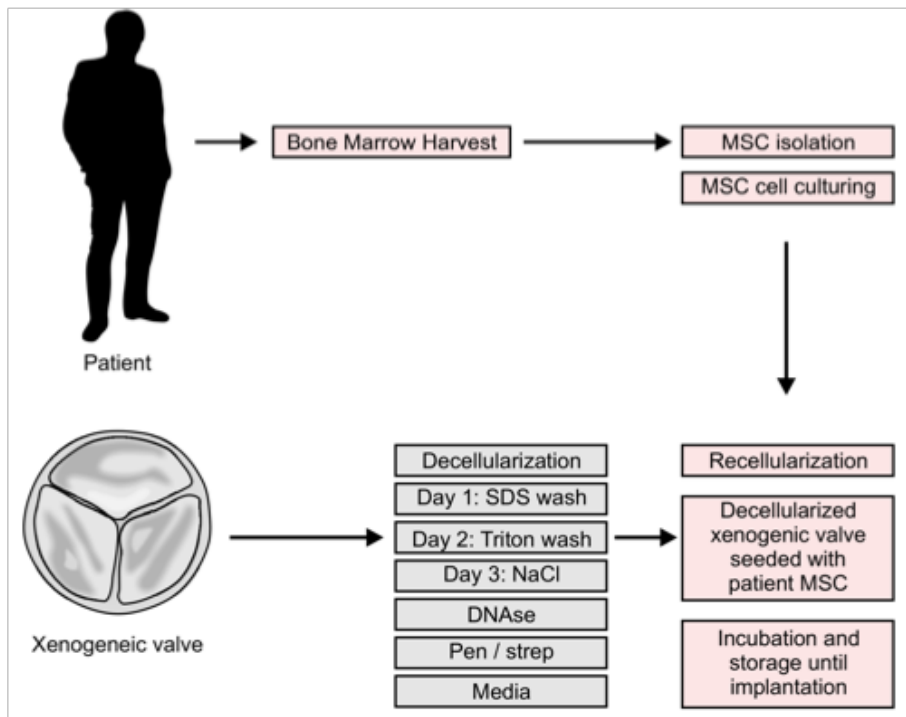


**Figure 3.1.** Schematic of recellularization protocol

Given the early success of xenogenic matrices, the first clinical implantation of the SynerGraft (Cryolife Inc) [86], a novel, decellularized porcine aortic valve construct, was attempted. These valves were implanted in sheep for up to 1-year, compared to cryopreserved allografts, and as aortic valve replacements in 9 human subjects. At explant in the sheep, a small amount of calcium was present and no thrombus, however, compared to the allografts, SynerGraft had more cellular elements. The human implants were functioning well up to 9-months post-operatively with no neo-endothelialization of the grafts. Unfortunately, there was no analysis concerning the presence of immune cells or any attempt at analyzing the immune response to this scaffold. Subsequently the SynerGraft was assessed for evidence of *in-vivo* recellularization implanted in a sheep model [87]. Limited lymphocytic infiltrate and as much as 80% repopulation of leaflet tissue with smooth muscle cells and an intact ECM was observed. This provides evidence for the feasibility of decellularization of xenogenic tissue as a scaffold, but again did not assess for any immune markers. Enthusiasm for the use of decellularized xenografts without repopulation was significantly tempered after the technology failed in a group of pediatric patients, leading to death in 75% of children implanted [88]. All explanted grafts showed severe inflammation macroscopically leading to structural failure and severe degeneration of the leaflets. Of significance, neutrophil and macrophage infiltration and interestingly incomplete decellularization by the SynerGraft protocol was observed, providing pause in using decellularized xenografts clinically. Nonetheless, after the failure of the SynerGraft, another decellularized porcine construct was manufactured [89]. The novel Matrix P, a decellularized porcine pulmonary valve, is similar to the SynerGraft, but utilized a different proprietary decellularization process. This valve construct was implanted clinically in the PV position in 61 patients with acceptable intermediate-term outcomes in terms of reoperation (4/61)

and mortality (8.2%). However, similar to other clinical studies, there is no definitive immunologic analysis.

Allograft scaffolds represent an alternative to xenogenic derived scaffolds and have been investigated as a potential starting point for TEHVs. The first attempt at an allograft derived TEHV came in 2002 [90]. A TEHV using a decellularized human allograft matrix reseeded with autologous cells was created utilizing primary human venous endothelial cells for recellularization. Recellularization occurred under shear stress conditions, finding the formation of a viable confluent endothelial cell layer. After the early failure of the decellularized xenogenic SynerGraft in pediatric patients, attention was turned to using decellularized allografts for clinical use in humans. The first described use of human decellularized pulmonary valve allografts, recellularized with peripheral mononuclear cells, was implanted in 2 pediatric patients [91]. The valves were reseeded in a bioreactor system for 21-days. Promisingly, the annulus diameter enlarged according to the body surface area of the growing child, followed over 3.5 years, without evidence of valve degeneration, demonstrating the safety and feasibility of using autologous seeded human allografts for pulmonary valve replacement. More recently, transcatheter technology has been tested in the implantation of allogenic-derived, autologous cell repopulated TEHVs. A decellularized homograft scaffold was seeded with fibroblasts and endothelial cells cultured for 5 days under low flow conditions [92]. The TEHVs then underwent TAVI-simulation with crimping and re-perfusion at high flow conditions with successful cell seeding. Unfortunately, the crimping procedure led to a significant number of lethal cells, implying that damage is inflicted during the crimping process, suggesting further refinement of this technique is required.

## Synthetic Scaffolds

As an alternative to xenogenic and allogenic scaffolds, synthetic based matrices have been created. Several different matrices exist, many relying on polymer-based structures such as polyglycolic acid (PGA), polycaprolactone (PCL) and polylactic acid (PLA). In general, two types of scaffold exist: biodegradable and hybrid. Synthetic biodegradable scaffolds rely on the introduction of autologous cells to remodel and create an ECM *in-vivo*. The remodelling required in these grafts is a by-product of a robust immune response and requires a balance of immune-led degradation and tissue formation, which can be challenging to predict clinically. Hybrid scaffolds are created by recellularizing a biodegradable scaffold, producing a living ECM. The scaffolds are then decellularized and can be stored long-term with off-the-shelf availability. In contrast to biodegradable scaffolds, hybrid scaffolds have improved biocompatibility and reduced immunogenicity but are time-consuming and prohibitively expensive to manufacture.

A novel PGA biodegradable scaffold was created seeded with MSCs from sheep marrow then implanted in sheep for up to 8-months [93]. Functionally, the valves performed very well, with acceptable gradients and only trivial regurgitation. Histological assessment found a similar phenotype between the TEHV and native valve. Interestingly, they also found a confluent layer of host endothelial cells on the blood contacting layer of the grafts; significant for anti-thrombogenic properties. This demonstrates the *in-vivo* remodelling of biodegradable grafts seeded with MSCs. A transcatheter, non-woven, biodegradable synthetic composite scaffold integrated onto a self-expanding nitinol stent has also been designed [94]. Bone marrow derived mononuclear cells (BMCs) were isolated in a one-step implantation method without culture in a primate model. Valve function was maintained throughout the 4-week study period and confluent endothelial coverage was seen, however, so was evidence of leucocyte attraction. An

advantage compared to MSCs, the use of BMCs does not need cell expansion, allowing for one-step creation and implantation of TEHVs. Others have developed a novel decellularized, hybrid scaffold TEHV, seeded with neonatal human dermal fibroblasts to create a mature, fibrin-based ECM, then removed those cells with a detergent-based decellularization [24]. These decellularized TEHV scaffolds demonstrated significantly better MSC infiltration compared to a decellularized xenograft.

Synthetic scaffold design has been a significant limiting factor in clinical application of this technology so far. As a result, several modifications have been made to their design in an attempt to improve valve function and longevity. Transcatheter deployment of a decellularized TEHV where the novel PGA scaffold was recellularized with autologous fibroblasts for several weeks, allowing ECM deposition, then decellularized and then implanted in the pulmonary valve position of sheep was performed [95]. This particular valve design was novel, including proper sinus of Valsalva, mimicking a more physiologic leaflet curvature, potentially contributing to long-term functionality.

The application of TEHV and other tissue-engineered grafts is limited to adolescent and adult patients, where an appropriate stock of repopulating cells can be obtained. However, investigation into cell types that can be obtained in-utero represents one potential solution to that problem [96, 97]. Human prenatal progenitor cells can be isolated from prenatal chorionic villus sampling. These cells can also be seeded onto a synthetic biodegradable leaflet scaffold and then recellularized with the umbilical cord blood-derived endothelial progenitor cells. The neo-tissues exhibited organization, cell phenotypes, ECM production and DNA content comparable to the native valves. In contrast to chorionic villus sampling, amniotic fluid derived cells can be utilized as well. Isolated fetal human amniotic progenitor cells (CD-133+) can be cultured and seeded

into the same biodegradable scaffold. Interestingly, the CD-133+ cells had features consist with mesenchymal progenitors, including CD44 and CD105 expression. These cells also expressed eNOS and CD141, similar to endothelial cells. This represents an interesting approach that may be enable autologous replacements to be ready at the time of birth.

## **Refinement of Recellularization**

Several advances and refinements have been made to the recellularization process used to generate TEHVs. These include unique scaffold modifications, protocol adjuncts and cell-type modifications. Chemical and mechanical conditioning constitute two ways in which the scaffolds are modified for improved *in vitro* cell seeding. These conditioning processes confer the benefits of bolstering valve mechanics, driving cell differentiation and proliferation, encouraging ECM remodelling, and supporting cellular attachments [98]. Decellularized BP has been treated with acetic acid and arginylglycylaspartic acid (RGD) polypeptides adhered to the BP scaffolds. RGD sequence is a cell adhesion recognition motif found in collagen, fibronectin and tenascin C and is the ligand for integrin-mediated cell adhesion. These modified scaffolds then underwent recellularization with MSCs and found that cell adhesion was the strongest and cell proliferation the fastest on the RGD-modified scaffolds, supporting the modification of these scaffolds[99, 100]. Another method to improve *in-vitro* VIC repopulation of decellularized xenograft scaffolds using a novel 3D heart valve model is the use of cyclical strain, femto second laser, trypsin and a transwell system. Trypsinization increased the susceptibility of the scaffold to VIC penetration and the transwell system increased the total number of cells and mean migration distance [101]. These findings provide some novel approaches to improve the *in-vitro* results of TEHV. Additionally, few groups have explored chemical modification of decellularized BP using polyelectrolyte multilayers (PEMs) with heparin and SDF-1alpha or vascular endothelial growth

factor [102-104] and others have proposed the overexpression of fibroblast inducible factor 14 (Fn14) to induce differentiation of BM-MSCs into VICs [105]. MSCs appear to be a source of VIC, which are responsible for maintaining normal valve integrity through ECM signalling. This may potentially provide a novel approach to recellularization with MSCs. Mechanical conditioning and its impact on endothelialisation were explored by several groups using a dynamic bioreactor with pulsatile flow [106-108] mimicking pulmonic conditions. While others have explored non physiologic conditions in decellularizing decellularized valve tissue using positive and negative cyclic pressures [109]. The studies demonstrated adequate coverage of leaflet surface under physiological pulsatile flow and variable pressure conditions, but incomplete endothelial and interstitial cellular coverage of leaflets noted in animal studies warrant further studies to determine strategies to maintain optimal coverage of leaflets from *in vitro* to animal studies [110, 111].

Other advancements and refinements in recellularization and TEHV are being made in the storage of valve, guided recellularization, and scaffold construction and delivery. A novel method of developing an off-the-shelf decellularized TEHV based on a biodegradable scaffold is by storing the decellularized TEHV for up to 18-mo in medium at 4-degrees. Despite that, it is still possible to successfully recellularize with MSCs [100]. This demonstrates that decellularized valve constructs can be preserved for a prolonged period of time, without damaging the ability to seed cells. Magnetic guidance recellularization of porcine pericardium with mesenchymal cord blood cells magnetically labelled with antibody has recently been developed [112]. This demonstrates that *in-vitro* recellularization of detergent-decellularized valves with human cord blood stem cells is feasible in a short period of time using magnetic guidance after a recellularization period of 4 to 7 days. Further refinements include a proof-of-concept *in-situ*

heart valve tissue engineered using a novel, supramolecular elastomer based on bis-urea-modified polycarbonate. This valve construct has been implanted in sheep and found to undergo extensive colonization by VICs and progressive endothelialization. However, an abundance of inflammatory cells including macrophages and neutrophils were found in the TEHV, likely related to a foreign body reaction. This demonstrates feasibility of a bioresorbable synthetic heart valve that can maintain long-term functionality as a pulmonary valve in sheep, recruit host cells, and support the in-situ formation of neo-tissue by these cells to match scaffold resorption [113]. Finally, another transcatheter decellularized TEHV has been developed, however, with the addition of a polyether-ether ketone insert. This leads to improved functionality of the TEHV by helping to improve the geometry of the transcatheter decellularized TEHV. Similar to the TEHV developed with sinus of Valsalva [95], the valve hemodynamics should be improved with this technique. Importantly, this is the first transcatheter, *in-situ* TEHV [114]. These advancements extend beyond the traditionally described recellularization refinement techniques such as chemical and mechanical processing and highlights the potential of TEHV to develop in many innovative ways.

## **Conclusions**

There is certainly ample evidence to suggest that XTHVs in use clinically result in rapid and robust immune activation, leading to eventual valvular deterioration. One of the proposed solutions to the development of valvular deterioration is the creation of TEHVs. An incredible amount of work has been done to date in conceptualizing and creating TEHVs. These TEHVs are made with a variety of techniques, including decellularized xenografts, decellularized allografts, synthetic recellularized scaffolds and xenogenic recellularized scaffolds. Recellularization of valve scaffolds has been proposed to provide an immunoprivileged tissue; one that does not

generate an immune response. Nonetheless, significant strides have been made in the design and long-term function of TEHVs. Ongoing studies will serve to establish the immune response to xenograft tissue *in-vivo* and autologous recellularized tissue both *in-vitro* and *in-vivo*. This work will help lead to the optimal scaffold design and cell type to generate a TEHV that is durable, non-immunogenic, non-thrombotic, easily implantable and readily available.

**Chapter 4. Sternal Bone Marrow Harvesting and Culturing Techniques from  
Patients Undergoing Cardiac Surgery**

Submitted

*Current Protocols in Stem Cell Biology*

2021

## **Abstract**

Mesenchymal stromal cells (MSCs) are the most prominent cell type used in clinical regenerative medicine and stem cell research. MSCs are commonly harvested from bone marrow that has been aspirated from patients' iliac crest. However, the ethical challenges of consenting patients and obtaining fresh autologous cells via invasive extraction methods remain barriers to MSC research. Herein, we describe a technique of harvesting sternal bone marrow from patients who are already undergoing open-chest cardiac surgery to reduce the invasiveness of bone marrow harvesting. The protocols listed in this manuscript will demonstrate sternal bone marrow harvesting, isolating and culturing MSCs, MSC surface phenotyping, and MSC differentiation. By being able to bypass the ethical challenges for MSC collection as well as the ability to culture and expand cells to demonstrate that MSC derived from sternal bone marrow meets the characterization criteria by the International Society of Cellular Therapy (ISCT) opens doors to further clinical application of MSC research and such as constructing autologous MSC derived biomaterials.

**Basic Protocol 1:** Sternal Bone Marrow Collection and MSC Isolation and Culturing Protocol

**Basic Protocol 2:** Protocol for MSC Surface Phenotyping

**Basic Protocol 3:** Differentiation of MSC Into Adipogenic, Osteogenic, and Chondrogenic Lineages

## Introduction

Mesenchymal stromal cells (MSCs) also described as mesenchymal stem cells, or multipotent mesenchymal stromal cells [115] are the most prominent cell type used in clinical regenerative medicine and stem cell research today. Over 200 active MSC clinical trials [116] have been performed and continue to rise exponentially since 2004 [117]. Despite being at early stages of development with limited clinical applications, MSC's descriptions of its multipotency, immunomodulatory and trophic effects [118, 119] have garnered interest among researchers and clinicians to explore MSC therapy in treating a wide variety of conditions. These conditions include immune-mediated diseases like the graft versus host disease [120] and regenerating damaged tissues of mesodermal origin such as the heart [121, 122], bones[123], and cartilages [124, 125], as well as tissue-engineering of patient-specific biomaterials [116, 126, 127].

MSCs were originally described by Freidenstein et al. in the early 1970s through a series of papers describing the isolation of clonal fibroblastic cells from bone marrow using its ability to adhere to plastic culture vessels [128-130]. Their capability to differentiate into osteogenic cells was later developed by Pittinger et al. in 1999 where they successfully differentiated the colony of cells into adipocytic, chondrocytic, osteocytic lineages [131]. Since then, scientists were able to successfully isolate MSC from bone marrow [132], the dental pulp [133], adipose tissue [134] and umbilical cord [135] Protocols have also been developed for proper cultivation and multilineage differentiation [135-137]. In 2006, the International Society of Cellular Therapy (ISCT) further established 3 minimal criteria for defining MSCs [115]. First, MSCs must be plastic adherent under standard culturing conditions (Basic Protocol 1). Second, they must be positive for CD105, CD73 and CD90, and negative for CD45, CD34, CD14 or CD11b,

CD79alpha or CD19 and HLA-DR surface molecules (Basic Protocol 2). Lastly, they must differentiate into adipocytes, osteoblasts, and chondroblasts in vitro (Basic Protocol 3).

Despite the structured guidelines in place, the ethical challenges of consenting patients and obtaining fresh autologous cells via invasive extraction methods remain as barriers to MSC research. Recent developments in perivascular MSC extraction using adipose tissues attempts to remedy this dilemma, but the invasive nature of the procurement of bone marrow presents as a significant challenge for human MSC study [138]. Herein, we describe a method of harvesting bone marrow from the sternum of patients who are undergoing open-chest cardiac surgery. This is ironically the least invasive method of collecting bone marrow for research as the sample collection is done from patients already scheduled to undergo a sternotomy and as the process of collecting marrow takes less than 30 seconds with the collection occurring from a split sternum that is already actively secreting marrow. The only other reported methods of obtaining autologous bone marrow are from iliac crest aspirations [139], sternum aspirations [140] and femur rasping during hip replacements [141]. Further, our protocol and results on MSC culturing, phenotyping, and differentiation using sternal bone marrow are described in this review.

## **Basic Protocol 1: Sternal Bone Marrow Collection and MSC Isolation and Culturing Protocol**

In this protocol, the process of harvesting sternal bone marrow and the principles of isolating and expanding MSC from the extracted sternal bone marrow are described. This is the initial step of harvesting the MSC for additional phenotyping and differentiating into its lineages

as outlined in the MSC characterization criteria by the International Society of Cellular Therapy (ISCT).

## Materials List

**Table 4.1.** Solutions and Reagents Used in Basic Protocol 1.

Article	Cat. No.	Final Conc.	Company
Dulbecco's Modified Eagle Medium Nutrient Mixture DMEM F12	11330-032	-	ThermoFisher
Fetal Bovine Serum, Qualified Standard	12483-020	20%	ThermoFisher
Ascorbic Acid, Reagent Grade, LabChem™	LC115309	100 mM	Fisher Scientific
Primocin™	ant-pm-1	100µg/mL	InvivoGen
Ethanol	E109	70%	Biochemistry Store University of Alberta (House Brand)
PBS (1x)	70011044	-	ThermoFisher
TrypLE™ Select 10x	A12177-02	-	ThermoFisher

**Table 4.2.** Special Equipment Used in Basic Protocol 1.

Article	Cat. No.	Company
5ml syringe with a blunt tip	-	-
Surgical Curettage	-	-
75cm <sup>2</sup> cell culture flask	156499	ThermoFisher

## Bone Marrow Collection

1. Attain written informed consent from patients undergoing cardiac surgery with a sternotomy for bone marrow collection under the approval of the local research ethics board.

2. Once the sternotomy is performed and hemostasis is achieved with cautery to the edges of the sternum, using a 5 mL syringe with a blunt needle tip or a surgical curettage to collect the discharging bone marrow from between the edges of the manubrium (Figure 4.1).
3. Collect 0.3 mL to 1 mL of bone marrow. Once drawn, store the bone marrow inside the syringe at room temperature not exceeding 4 hours.

*If the sample is expected to be stored for more than 4 hours, store in ice until further use.*

**Figure 4.1.** Sternal bone marrow harvest with a 5ml blunted tip syringe following a sternotomy.



## MSC Isolation and Culturing

1. Prepare a complete Dulbecco's Modified Eagle Medium Nutrient Mixture (DMEM F12) supplemented with 20% Fetal Bovine Serum (FBS), 100 mM ascorbic acid, and 100µg/mL Primocin. Warm the completed media in a 37°C water bath.
2. Spray the 5 mL syringe, the complete DMEM F12 container, and a 75cm<sup>2</sup> cell culture flask with a vented cap with 70% ethanol before placing them in a laminar flow hood.
3. Using an electronic pipette controller, pipette 15 ml of the complete DMEM F12 into the culturing flask.
4. Carefully push the bone marrow sample from the syringe into the flask ensuring to draw back any large clumps of marrow and residual bone back to the syringe and push out again to spread the sample around the flask.

*Ensure even distribution of the marrow to maximize the MSC's expansion potential. Avoid leaving a large clump of bone fragments in the flask.*

5. Gently shake the flask in an up and down and sideways motion to ensure the sample has covered the bottom of the flask.

*Avoid shaking the flask in a circular motion as cells do not distribute evenly.*

6. Place the flask in a 37°C, 5% CO<sub>2</sub> incubator for >18 hours.
7. Aspirate the media at the corner of the flask with a vacuum pipette to suction off any media and samples that have not adhered to the plastic.
8. Wash the adhered cells on the flask with 15 mL of 1x PBS and gently shake the flask. Then, aspirate the 1X PBS at the corner of the flask.
9. Add fresh 15 mL of the complete DMEM F12 into the culturing flask and incubate further for >18 hours.

10. Check for the confluency of the MSCs under a light microscope.
11. Repeat steps 7-10 every 3 days until the confluency has reached 85%.

### **MSC Expansion**

1. Aspirate old DMEM F12 media and wash the cells with 15 mL of 1X PBS.
2. Add 15 mL of 10X TrypLE solution that has been sitting in a 37°C water bath for 20 minutes to the flask to lift the plastic adhered MSCs.
3. Incubate the flask in a 37°C, 5% CO<sub>2</sub> incubator for 30min.
4. Check the MSCs have lifted off of the flask using a light microscope.

*Lifted MSC will confer a round shape as opposed to a spindle-shaped plastic adhered MSC cells.*

5. Add 15 mL of complete DMEM F12 that has been sitting in a 37°C water bath to the flask.
6. Pipette the contents in the flask into a 50 mL conical tube and centrifuge at 400 x g for 15 minutes at 18C.
7. Remove the supernatant without disturbing the pellet. Resuspend the pellet with 20 mL of 1X PBS and mix to disrupt the pellet. Centrifuge again at the same setting.
8. Remove the supernatant and resuspend the cells with complete DMEM F12 of appropriate volume and seed the cells into the desired number of flasks containing 15 mL of complete DMEM F12.
9. Repeat steps 7-10 until the second iteration of MSC Expansion.

### **Basic Protocol 2: Protocol for MSC Surface Phenotyping**

International Society of Cellular Therapy (ISCT) lists surface phenotyping as one of three MSC characterization criteria. MSCs should be positive for CD73, CD90, and CD105, but be

negative for CD34, CD45, CD11b or CD14, CD19 or CD79 $\alpha$ , and HLA-DR. This protocol which has been adopted by the BD Stemflow™ Technical data sheet describes surface phenotyping of MSC derived from sternal bone marrow.

## Materials List

**Table 4.3.** Solutions and Reagents Used in Basic Protocol 2.

Article	Cat. No.	Final Conc.	Company
TrypLE™ Select 10x	A12177-02	-	ThermoFisher
Stain Buffer (FBS)	554656	-	BD Pharmingen™
Human MSC Analysis Kit	562245	-	BD Stemflow™
FITC Mouse Anti-Human CD90	51-9007657	5 $\mu$ l	BD Stemflow™
PE Mouse Anti-Human CD44	51-9007656	5 $\mu$ l	BD Stemflow™
PerCP-Cy™5.5 Mouse Anti-Human CD105	51-9007648	5 $\mu$ l	BD Stemflow™
APC Mouse Anti-Human CD73	51-9007649	5 $\mu$ l	BD Stemflow™
hMSC Positive Isotype Control Cocktail	51-9007664	20 $\mu$ l	BD Stemflow™
PE hMSC Negative Isotype Control Cocktail	51-9007662	20 $\mu$ l	BD Stemflow™
hMSC Positive Cocktail	51-9007663	20 $\mu$ l	BD Stemflow™
PE hMSC Negative Cocktail	51-9007661	20 $\mu$ l	BD Stemflow™

## Surface Phenotyping

1. Detach MSCs from plastic using TrypLE™ Select 10x and resuspend at a concentration of  $1 \times 10^7$  cells/ml in BD Pharmingen™ Stain Buffer.
2. Add to labelled tubes the antibodies from the BD Stemflow™ Human MSC Analysis Kit: FITC Mouse Anti-Human CD90 (5 $\mu$ l), PE Mouse Anti-Human CD44 (5 $\mu$ l), PerCP-Cy™5.5 Mouse Anti-Human CD105 (5 $\mu$ l), APC Mouse Anti-Human CD73 (5 $\mu$ l), hMSC Positive Isotype Control Cocktail (20 $\mu$ l), PE hMSC Negative Isotype Control Cocktail

(20 $\mu$ l), hMSC Positive Cocktail (20 $\mu$ l) containing CD90 FITC, CD105 PerCP-Cy5.5, CD73, APC, and PE hMSC Negative Cocktail (20 $\mu$ l) containing CD34 PE, CD11b PE, CD19 PE, CD45 PE, HLA-DR PE.

3. Add 100  $\mu$ l of the prepared cell suspension to the tubes outlined in step 2.
4. Incubate the tubes in the dark for 30 minutes on ice.
5. Wash the cells twice with BD Pharmingen™ Stain Buffer and resuspend at 300-500  $\mu$ l in BD Pharmingen™ Stain Buffer.
6. Analyze cells on a flow cytometer.

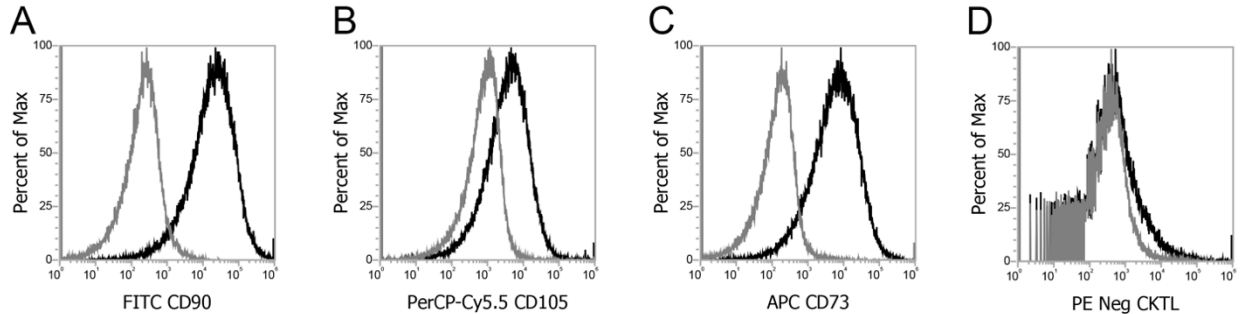


**Figure 4.2.** Surface phenotyping under flow cytometry for positive cell surface antigen CD 90 (A), CD105 (B), CD 73 (C) expression and absence of negative cell surface antigen in a negative cocktail of CD 34, CD 11b, CD19, CD45, and HLA-DR (D) expression in bone marrow–derived MSCs

### **Basic Protocol 3: Differentiation of MSCs into Adipogenic, Osteogenic and Chondrogenic Lineages**

This protocol demonstrates the third criteria of the International Society of Cellular Therapy (ISCT)'s MSC characterization where MSC must differentiate into adipocytes, osteoblasts, and chondroblasts in vitro. This protocol has been adapted from the StemPro® MSC differentiation kit protocol.

## Materials List

**Table 4.** Solutions and Reagents Used in Basic Protocol 3.

Article	Cat. No.	Final Conc.	Company
Complete Adipogenesis Differentiation Medium	A1007001	-	ThermoFisher
StemPro® Adipogenesis Differentiation Basal Medium	A10410-01	1X	ThermoFisher
StemPro® Adipogenesis Supplement	A10065-01	1X	ThermoFisher
Gentamicin Reagent	15710	5 µg/mL	ThermoFisher
Complete Osteogenesis Differentiation Medium	A10072-01	-	ThermoFisher
StemPro® Osteocyte/Chondrocyte Differentiation Basal Medium	A10069-01	1X	ThermoFisher
StemPro® Osteogenesis Supplement	A10066-01	1X	ThermoFisher
Gentamicin Reagent	15710	5 µg/mL	ThermoFisher
Complete Chondrogenesis Differentiation Medium	A10071-01	-	ThermoFisher
StemPro® Osteocyte/Chondrocyte Differentiation Basal Medium	A10069-01	1X	ThermoFisher
StemPro® Chondrogenesis Supplement	A10064-01	1X	ThermoFisher
Gentamicin Reagent	15710	5 µg/mL	ThermoFisher
Dulbecco's Modified Eagle Medium Nutrient Mixture DMEM F12	11330-032	-	ThermoFisher
Fetal Bovine Serum, Qualified Standard	12483-020	20%	ThermoFisher
Ascorbic Acid, Reagent Grade, LabChem™	LC115309	100 mM	Fisher Scientific
Primocin™	ant-pm-1	100µg/mL	InvivoGen
Paraformaldehyde (PFA)	28906	4%	ThermoFisher
PBS (1x)	70011044	-	ThermoFisher
HCS LipidTOX™ Green Neutral Lipid Stain	H34475	1:100 dilution	InvivoGen
DAPI (4',6-Diamidino-2-Phenylindole, Dihydrochloride) Stain	D1306	-	InvivoGen
Alizarin Red S	A5533-25G	2%	Millipore Sigma
Alcian-Blue Staining Solution	TMS-010-C	1%	Millipore Sigma

## **Adipogenesis Differentiation**

1. Prepare a complete Adipogenesis Differentiation Medium comprised of 90ml StemPro® Adipocyte Differentiation Basal Medium 1x concentration, 10ml StemPro® Adipocyte Supplement 1x concentration, 50 µL Gentamicin reagent (10 mg/mL) 5 µg/mL.
2. Collect MSCs from passage 1 and resuspend with the appropriate amount of pre-warmed complete DMEM F12 medium from Basic Protocol 1.
3. Seed MSCs onto a 12-well plate at  $1 \times 10^4$  cells/cm<sup>2</sup>.
4. After 1-4 days of incubation at 37°C, 5% CO<sub>2</sub>, replace complete DMEM F12 media with Complete Adipogenesis Differentiation Medium and continue to incubate for 7-14 days with refeeding every 3 days.
5. After 7-14 days of incubation, fix the cells with 4% PFA solution for 30 minutes.
6. Rinse with PBS x1 solution twice and Add LipidTOX™ to the cultures for staining of the lipid vacuoles for 15-30 minutes.
7. Add DAPI stain for counterstain.
8. Capture images under a fluorescent microscope for qualitative analysis.

## **Osteogenesis Differentiation**

1. Prepare a complete Osteogenesis Differentiation Medium comprised of 90ml StemPro® Osteocyte/Chondrocyte Differentiation Basal Medium 1x concentration, 10ml StemPro® Osteogenesis Supplement 1x concentration, 50 µL Gentamicin reagent (10 mg/mL) 5 µg/mL.
2. Collect MSCs from passage 1 and resuspend with the appropriate amount of pre-warmed complete DMEM F12 medium from Basic Protocol 1.
3. Seed MSCs onto a 12-well plate at  $5 \times 10^3$  cells/cm<sup>2</sup>.

4. After 1-4 days of incubation at 37°C, 5% CO<sub>2</sub>, replace growth media with Complete Osteogenesis Differentiation Medium and continue to incubate for >21 days with refeeding every 3 days.
5. After >21 days of incubation, fix the cells with 4% PFA solution for 30 minutes.
6. Rinse twice with distilled water and add 2% Alizarin Red S staining solution for 2-3 minutes.
7. Capture images under a light microscope for qualitative analysis.

### **Chondrogenesis Differentiation**

1. Prepare a complete Chondrogenesis Differentiation Medium comprised of 90ml StemPro® Osteocyte/Chondrocyte Differentiation Basal Medium 1x concentration, 10ml StemPro® Chondrogenesis Supplement 1x concentration, 50 µL Gentamicin reagent (10 mg/mL) 5 µg/mL.
2. Collect MSCs from passage 1 and resuspend with the appropriate amount of pre-warmed complete DMEM F12 medium from Basic Protocol 1.
3. Generate micro mass cultures of  $1.6 \times 10^7$  cells/mL by seeding 5µL droplets of cell solution on a 12-well plate.
4. Add complete chondrogenesis media to the wells after 2 hours under high humidity conditions and refeed every 3 days.
5. After 14 days of incubation at 37°C, 5% CO<sub>2</sub>, rinse with PBS and fix cells with 4% PFA solution for 30 minutes.
6. Add 1% Alcian Blue staining solution in 0.1 N HCL for 30 minutes
7. Visualize under a light microscope for qualitative analysis.

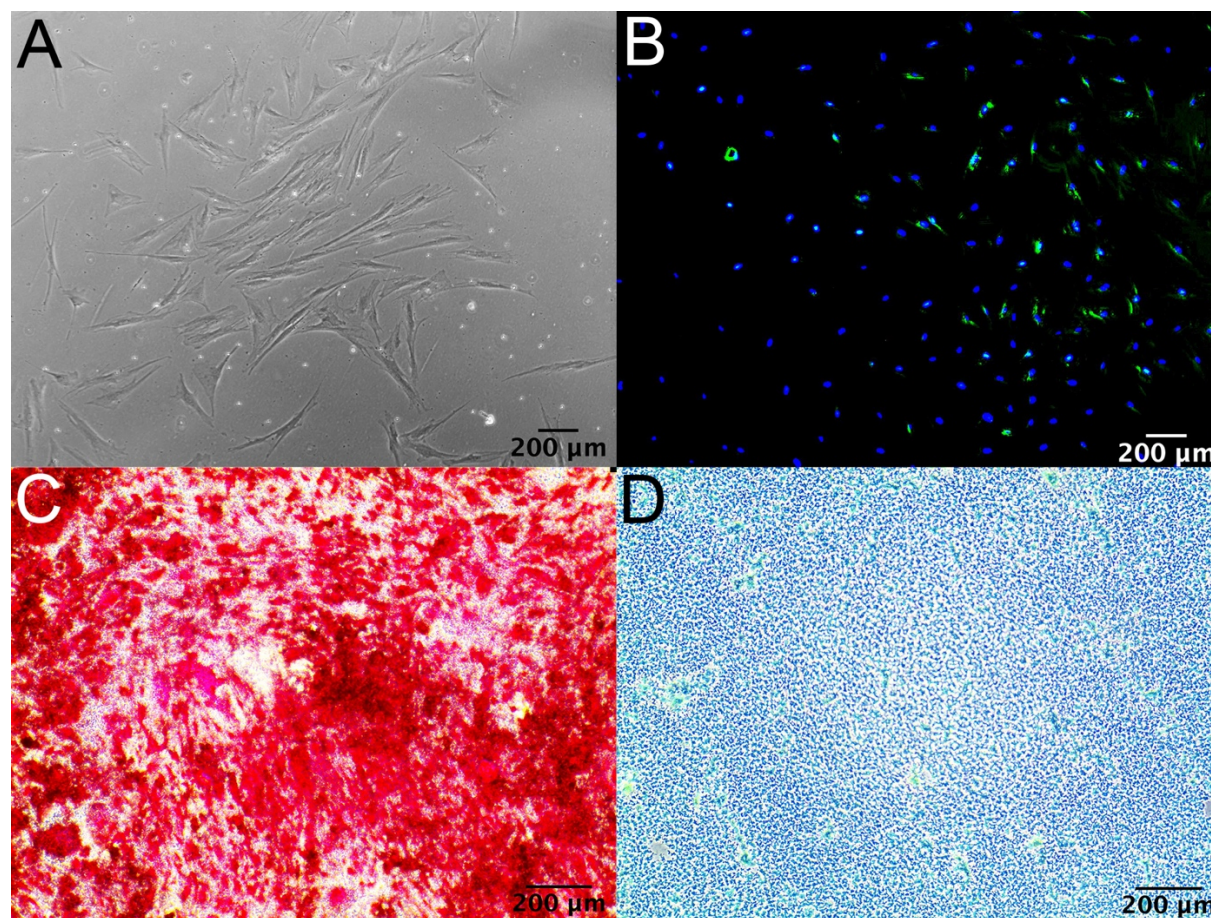


**Figure 4.3.** (A) Micrograph representing bone marrow derived MSCs. (B) Adipocyte differentiation of MSCs with LipidTOX™ Stain. (C) Osteocyte differentiation of MSCs with Alizarin Red S stain. (D) Chondrocyte differentiation of MSCs with Alcian Blue stain

## Reagents and Solutions

Table 4.5 lists recipes for media and solutions used in this article.

**Table 4.5.** Media and Solutions Used in Basic Protocols 1, 2, and 3.

Ingredient	Company, Cat. No.	Final Conc.	Comment
<b>Alcian-Blue Staining Solution</b>			
Alcian-Blue <sup>a</sup>	Millipore Sigma, TMS-010-C	1%	-
<b>Adipogenesis Differentiation Medium</b>			
StemPro® Adipogenesis	ThermoFisher,	1X	-

Differentiation Basal Medium <sup>b</sup>	A10410-01		
StemPro® Adipogenesis Supplement <sup>c</sup>	ThermoFisher, A10065-01	1X	-
Gentamicin Reagent	ThermoFisher, 15710	5 µg/mL	-
<b>Alizarin Red S Staining Solution</b>			
Alizarin Red S <sup>d</sup>	Millipore Sigma, A5533-25G	2%	-
<b>Chondrogenesis Differentiation Medium</b>			
StemPro® Osteocyte/Chondrocyte Differentiation Basal Medium <sup>b</sup>	ThermoFisher, A10069-01	1X	-
StemPro® Chondrogenesis Supplement <sup>c</sup>	ThermoFisher, A10064-01	1X	-
Gentamicin Reagent	ThermoFisher, 15710	5 µg/mL	-
<b>Complete Medium<sup>e</sup></b>			
Dulbecco's Modified Eagle Medium Nutrient Mixture DMEM F12	ThermoFisher, 11330-032	-	-
Fetal Bovine Serum, Qualified Standard <sup>f</sup>	ThermoFisher, 12483-020	20%	-
Ascorbic Acid, Reagent Grade, LabChem <sup>TMd</sup>	Fisher Scientific, LC115309	100 mM	-
Primocin <sup>TMg</sup>	InvivoGen, ant-pm-1	100µg/mL	-
<b>LipidTox Stain</b>			-
HCS LipidTOX <sup>TM</sup> Green Neutral Lipid Stain <sup>h</sup>	InvivoGen, H34475	1:100 dilution	Prepare a volume to completely cover cells
<b>Osteogenesis Differentiation Medium</b>			-
StemPro® Osteocyte/Chondrocyte Differentiation Basal Medium <sup>b</sup>	ThermoFisher, A10069-01	1X	-
StemPro® Osteogenesis Supplement <sup>c</sup>	ThermoFisher, A10066-01	1X	-
Gentamicin Reagent	ThermoFisher, 15710	5 µg/mL	-
<b>Paraformaldehyde (PFA) 4%<sup>i</sup></b>			-
16% Formaldehyde	ThermoFisher, 28906	4%	Dilute in PBS

			ThermoFisher, 70011044
<b>Staining Buffer Solution<sup>j</sup></b>			-
Stain Buffer (FBS)	BD Pharmingen™, 554656	-	-
<b>Trypsin Solution</b>			-
TrypLE™ Select 10x <sup>k</sup>	ThermoFisher, A12177-02	-	-

<sup>a</sup> Store at room temperature up to 4 months from date of receipt.

<sup>b</sup> Store at 2°C to 8°C; protected from light for up to 12 months.

<sup>c</sup> Store at -20°C to -5°C in the dark for up to 12 months.

<sup>d</sup> Store at room temperature

<sup>e</sup> Store at 4°C and warm in 37°C water bath for 15-20 min before use.

<sup>f</sup> Store at -20°C and warm in 37°C water bath for 15-20 min before use.

<sup>g</sup> Store at 4°C for 3 months or at -20 °C for long-term storage

<sup>h</sup> Store at -20°C protected from light

<sup>i</sup> Store at -20°C in 1ml aliquots and use within 6 months

<sup>j</sup> Store undiluted at 4°C

<sup>k</sup> Store at 15°C to 30°C protected from light for up to 24 months

## Discussion

### *Background Information*

Autologous bone marrow harvest for non-clinical research has been strictly limited due to the significant ethical challenge associated with the invasive nature of the procedure. Herein, we demonstrate a case of using sternal bone marrow from patients already undergoing a sternotomy for cardiac surgery. The collection of bone marrow using a surgical curettage or a blunt-tip needle syringe from an open sternum bypasses the ethical challenge of causing an additional risk to the patient as they are already scheduled to undergo cardiac surgery. Biopsy or collection of bone marrow from a sternum via aspirations in humans have been described previously as an

alternative to iliac crest aspirations[140, 142, 143], however, possibilities of serious complications such as aortic dissection [144] and pericardial tamponade [145] have limited this practice to experienced clinicians. It was also reported to induce significant anxiety and pain among patients[146]. In contrast, bone marrow collection from an open sternum during cardiac surgery is a controlled procedure that does not pose any additional risks to the patient.

Using our protocols, we also demonstrate the ability to conduct basic science research using autologous MSCs such as tissue engineering small biomaterials. We have previously shown that bovine pericardial tissue-engineered heart valves that are reseeded with autologous MSCs have reduced xenoreactive immune response compared to native bovine pericardial valves when exposed to autologous human blood [147, 148]. We first decellularized the native bovine pericardial tissue using detergents to leave only the extracellular matrix scaffold and recellularized the valve with human MSCs which we cultured from the sternal bone marrow. This shows the feasibility of conducting basic science and translational research using a minute quantity of bone marrow obtained from the sternum in addition to the already reported method of extracting and processing bone marrow aspirations in orthopedic settings using posterior superior iliac spine with 30 mL – 120 mL of bone marrow aspirate [139, 149-151]. Furthermore, the utility of MSCs is wide-ranging although largely still in various stages of research. The use of MSCs allows for several potential advantages. MSCs have immune-modulatory and anti-inflammatory properties which allow for a reduction in the immune response to a variety of implanted grafts [152, 153]. The incorporation of MSCs with various tissues or devices may attenuate immune responses and increase the durability of implanted materials. MSCs have also been shown to allow for remodelling of multiple systems including the myocardium, allowing for regeneration of damaged or fibrotic myocardial tissue [154, 155]. MSCs have also

demonstrated utility in autoimmune disease, hepatic dysfunction, malignancy among others [153, 156]. While the potential utility of MSCs is vast it is important to identify efficient and effective ways to isolate and culture these cells. Our described method allows for the collection and culture of MSCs without an additional invasive procedure and using a relatively small amount of collected marrow.

### *Critical Parameters and Troubleshooting*

Acquiring an adequate quantity of sternal bone marrow and the initial plating of the limited collected amount becomes critical in the success of the adequate expansion of the MSC. The hemostasis of the sternal bone marrow is conventionally achieved immediately following a sternotomy with bone wax at our institution. Despite patient consent, the patient's surgery is of priority and the collection of bone marrow has to be achieved fairly quickly before the application of the bone wax. Despite the curettage and suction with a blunt tip syringe, bone marrow collection is usually limited to 0.3-1.0ml per patient. Increasing the time spent collecting the bone marrow in the OR delays the time of surgery thus the research team and the surgical team need to establish appropriate time spent harvesting the marrow before the surgery.

In the case of a limited amount of bone marrow collected, adequate plating using the detailed steps described in Basic Protocol 1 becomes essential. Going through an additional step of cell quantification before bone marrow culturing and expansion, as described in other protocols, become impractical due to the limited amount of sample being able to be collected from the sternum. While the initial cell count may not be possible, we demonstrate in figure 4.4 and supplementary table 4.7 that quantification after 2 rounds of expansion is still possible.

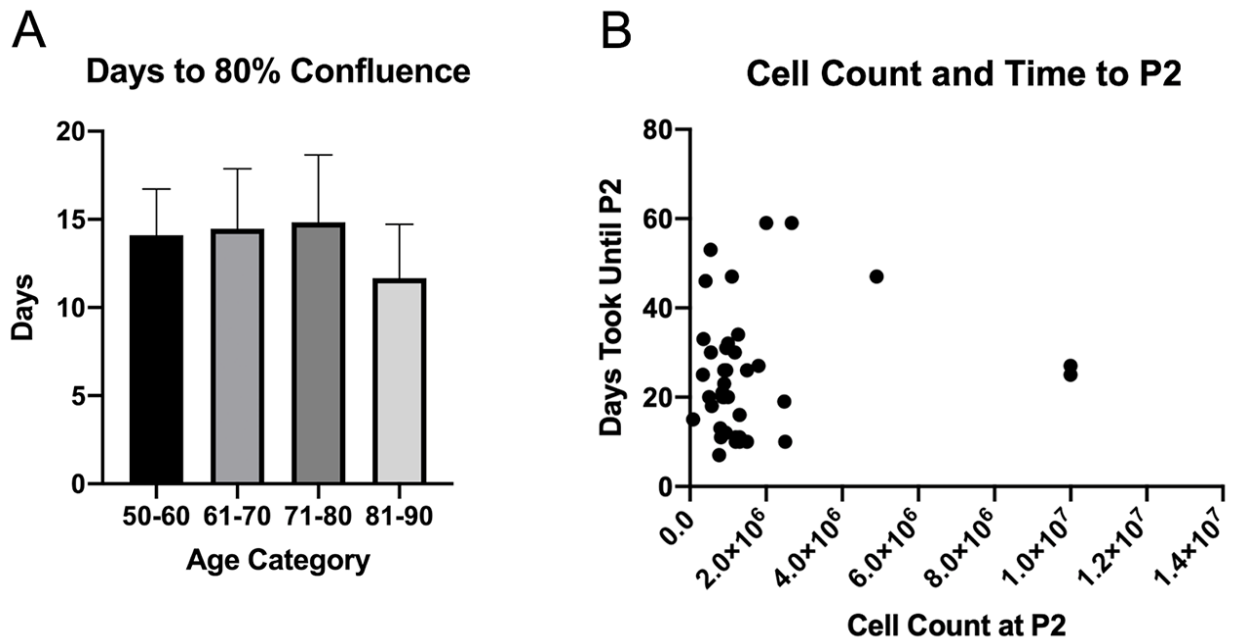


**Figure 4.4.** (A) Time took for MSCs to reach 80% confluency since the date of collection stratified based on age groups (50-60, N=9; 61-70, N=19; 71-80, N=19; 81+, N=3). (B) Cell count at the time of P2 and time took to P2 split of MSCs

**Table 4.7** Cell Count and Time Took to P2 Split of MSCs since Harvest

Patient Number	Cell Count at P2	Days Took to P2
Patient 1	356,000	33
Patient 2	410,000	46
Patient 3	800,000	13
Patient 4	940,000	12
Patient 5	337,000	25
Patient 6	1,300,000	16
Patient 7	900,000	23
Patient 8	550,000	30
Patient 9	1,300,000	10

Patient 10	1,200,000	10
Patient 11	2,500,000	10
Patient 12	1,000,000	20
Patient 13	570,000	18
Patient 14	1,300,000	11
Patient 15	500,000	20
Patient 16	1,200,000	11
Patient 17	10,000,000	27
Patient 18	10,000,000	25
Patient 19	812,000	11
Patient 20	1,500,000	10
Patient 21	768,000	7
Patient 22	1,500,000	26
Patient 23	1,260,000	34
Patient 24	2,480,000	19
Patient 25	1,000,000	32
Patient 26	1,800,000	27
Patient 27	905,000	20
Patient 28	80,000	15
Patient 29	940,000	12
Patient 30	955,000	26
Patient 31	860,000	20
Patient 32	953,000	31
Patient 33	900,000	26
Patient 34	850,000	21
Patient 35	1,180,000	30

Patient 36	2,000,000	59
Patient 37	2,675,000	59
Patient 38	540,000	53
Patient 39	1,100,000	47
Patient 40	4,900,000	47
Mean	1,628,025	25
Median	977,500	22

Our culturing technique may also differ from other labs using a different formation of cell culture media. Although several studies have shown usage of 20% FBS on human MSC culturing [157-160], others have shown that 10% FBS also work effectively on culturing [161-164]. The usage of human serum versus FBS remains contentious as studies have heterogeneous bone marrow sample harvest sites, donor sera, and sample numbers [157]. When comparing their proliferative effects of human mesenchymal cells, Kuznetsov et al. have shown the superiority of FBS over human serum [159], while Yamamoto et al [164]. and Spees et al [158]. have shown similar effects. On the other hand, Stute et al. Shadadfar et al. and Kobayashi et al. have demonstrated increased proliferation of human MSC with human serum use over FBS. With the increased concentration of FBS and primocin, there is a risk of mycoplasma contamination, thus the proliferation of MSC should always be weighed against the risk of contamination and strict rules for a good aseptic technique must be followed and the sources of aerosol contaminations should be carefully controlled [161-163].

Table 4.6 lists possible problems that can occur with the culturing, expansion, or differentiation as well as their possible causes and solutions.

**Table 4.6.** Troubleshooting

Observation	Possible cause	Remarks
Inadequate growth for MSC differentiation despite adequate cell count of the micro mass	Inadequate oxygenation due to too much differentiation media in the culturing wells.	Be sure to only refeed the cells with 1-2mls of differentiation media.
Pockets of MSC expansion in the flask, or inadequate growth	Clumping of bone marrow on initial sample plating, circular shaking motion of the flasks, inadequate sample quantity, patient dependent factors.	<p>Make sure all large clumps of marrow or residual bones are evenly spread out throughout the flask.</p> <p>Avoid the circular shaking motion and use up and down and sideways motion when shaking the flasks.</p> <p>Make sure the bone marrow sample contains at least 0.3ml of marrow upon harvesting.</p> <p>Exclude patients with corticosteroid use or hematological diseases.</p>
Cells are not lifting after trypsinization	Cold TrypLE 10x Select, inadequate time for cells to lift after exposure with trypsin, Using TrypLE 1x Select.	<p>Ensure both TrypLE 10x Select is sitting in the 37°C water bath for 20 minutes before use.</p> <p>Make sure the trypsinized cells are placed in a 37°C, 5% CO<sub>2</sub> incubator for 30min before checking whether they lifted.</p> <p>Use TrypLE 10x Select as opposed to 1x as the trypsin concentration needs to be strong enough to lift the cells.</p>

### *Understanding results*

While the immediate therapeutic application of autologous MSCs from the time of collection may be limited due to the quantity of the sample collected, adequate culturing and expansion of MSCs following the harvest can still be achieved promptly with adequate cell counts (figure 4.4). Additionally, the age of the patient from which the sternal bone marrow MSC was collected should not determine the rate of growth of the cells, thus producing relatively consistent results. Using our protocol, MSC were isolated and expanded from the sternal bone marrow of 50 patients. The patients were divided into different age groups (50-60, n=9; 61-70, n=19; 71-80, n=19; 80-90, n=3). There was no statistically significant difference in the days took to the first split of MSC cells at 80% confluency between the different patient age groups ( $p = 0.523$ ). The mean MSC cell count and the days took to the time of the second split at 80% confluency were 1,628,025 and the mean time took to reach P2 was 24.8 days in our samples. The variability in the cell count and time to expansion will vary depending on multiple factors including the quantity of the marrow collected, plating techniques, and patient-dependent variabilities. Setting a clear exclusion criterion for patients such as corticosteroid use or those with the hematological disease will further reduce the variability encountered. Importantly, we were still able to meet the ISCT guidelines for MSC definition with the collected marrow and isolated MSC, which require  $1 \times 10^7$  MSC cells for surface phenotyping (Figure 4.2), and MSC differentiation into adipocytic, osteocytic, chondrocytic lineages (Figure 4.3).

### *Time Considerations*

The entire process of demonstrating that the sternal bone marrow sample meets the MSC characterization criteria by the International Society of Cellular Therapy (ISCT) will depend largely on Basic Protocol 1 as Basic Protocol 2 and 3 have specific time frames set whereas Basic Protocol 1 depends on patient dependent factors that vary the time to MSC expansion. We demonstrate in figure 3 the days to 80% confluence after initial sample collection and cell count and time to second split P2 using our N=50 sternal bone marrow samples. 50-60 age group reached 80% confluency in  $14.1 \pm 2.6$  days, 61-70 in  $14.5 \pm 3.4$  days, 71-80 in  $14.8 \pm 3.8$ , and 81-90 in  $11.7 \pm 3.1$  days (Figure 4A). If appropriate cells are acquired by this time for Basic Protocol 2 and 3, additional >25 days would take until all the staining are complete for MSC differentiation qualitative analysis.

**Chapter 5. Structural Valve Deterioration is Linked to Increased Immune  
Infiltrate and Chemokine Expression**

*Journal of Cardiovascular Translational Research*

2020

DOI: 10.1007/s12265-020-10080-x

## **Abstract**

We aim to investigate whether structural valve deterioration (SVD) of bioprosthetic xenogenic tissue heart valves (XTHVs) is associated with increased immune cell infiltration and whether co-expression of several chemokines correlate with this increase in immune infiltrate. Explanted XTHVs from patients undergoing redo valve replacement for SVD were obtained.

Immunohistochemical, microscopic and gene expression analysis approaches were used. XTHVs (n=37) were obtained from 32 patients (mean 67.7-years) after a mean time of 11.6-years post-implantation. Significantly increased immune cellular infiltration was observed in the explanted SVD valves for all immune cell types examined, including T-cells, macrophages, B-cells, neutrophils, and plasma cells, compared to non-SVD controls. Furthermore, a significantly increased chemokine gradient in explanted SVD valves accompanied immune cell infiltration. These data suggest development of SVD is associated with significantly increased burden of immune cellular infiltrate correlated to the induction of a chemokine gradient around the XHTV, representing chronic immune rejection.

## Introduction

Valvular heart disease (VHD) continues to affect millions of people worldwide, having a significant impact on survival and quality of life[10, 11]. Due to lack of medical treatment for certain types of VHD, the burden of management falls on options such as valve replacement. The most common type of prosthetic valve implanted are glutaraldehyde-fixed xenogenic tissue heart valves (XTHV)[165]. Despite widespread availability and ease of implantation, XTHVs suffer from the development of structural valve deterioration (SVD)[166]. SVD is defined as intrinsic permanent changes of the XTHV leading to morphologic leaflet degeneration and hemodynamic dysfunction, typically manifested as increasing transvalvular gradients[3]. Several hypotheses have been established regarding the mechanism of SVD, including a chronic immune-mediated rejection of the foreign XTHV. There is increasing evidence from laboratory and clinical investigations that suggests XTHVs are immunogenic and generate an immune response that has been implicated in the failure of these grafts [4-6, 33].

It has been postulated that the immune system recognizes and responds to XTHVs by initiation of the innate immune system with subsequent adaptive immune activation. Two important effector cells in the innate immune response are neutrophils and macrophages. The initial event in development of SVD is hypothesized to be activation of neutrophils and macrophages that leads to production of inflammatory molecules, leading to a cascade of immune activation [38]. Activation of the adaptive immune response follows, characterized by proliferation of T-cells, B-cells, and differentiation to plasma cells leading to antibody production[44, 167]. While prior studies have demonstrated the presence of innate and adaptive immune cell infiltrate in explanted SVD valves, one of the major limitations with these prior studies has been determining how these immune cells are drawn towards XTHVs. Since cells of

innate and adaptive immunity are controlled by chemokine gradients throughout the body[168-170], it is plausible that a chemokine gradient may be correlated to infiltration of immune cells into XTHVs developing SVD. Preventing the generation of this chemokine gradient with targeted immunomodulation may represent one potential therapy to avoid development of SVD in XTHVs.

The purpose of this study was to investigate whether SVD of XTHVs is associated with an increased infiltration of cells of adaptive immunity into XTHVs. As well as to determine whether this infiltration is complemented by a co-expression of chemokines that are known to control migration of cells of immunity. We hypothesized that explanted XTHVs from human patients developing SVD will contain significantly greater adaptive immune cell infiltrate accompanied by an increased chemokine gradient compared to normally functioning human heart valves.

## **Methods**

### **Patients and Explanted Valves**

Explanted aortic or mitral XTHVs from patients undergoing redo valve replacement for SVD were obtained from the Division of Anatomical Pathology at the University of Alberta Hospital in Edmonton, Alberta, Canada. Patients with a diagnosis of infective endocarditis and transplant recipients were excluded from this study. Aortic or mitral XTHVs were all obtained during surgical explant. At the time of explant, the valve is sent for routine pathology assessment where it is stored as a formalin-fixed (10%), paraffin embedded (FFPE) block. A control group comparison arm included aortic or mitral valves explanted from human hearts without valvular disease considered for transplantation that were not utilized. Patient and procedural data were

collected from retrospective chart reviews. The Research Ethics Board at the University of Alberta approved the research protocol, including waiver of individual consent.

### **Immunohistochemical Analysis**

All samples obtained were stored as per institutional protocols as FFPE blocks. These blocks were retrieved and serially sectioned (5- $\mu$ m) for histologic and immunohistochemical examination. Immunohistochemistry involved standard staining techniques with biotinylated secondary antibodies, a peroxidase avidin-biotin complex, and 3,3' diaminobenzidine as the chromogen.

Hematoxylin-eosin and chloroacetate esterase stains (for confirmation of presence of neutrophils and plasma cells) were prepared from the FFPE blocks using standard procedures. Primary monoclonal antibodies for T-cells (anti-CD3; clone 2GV6, Roche), B-cells (anti-CD20; clone L26, Dako), and macrophages (anti-CD68; clone KP1, Dako) were used.

### **Tissue Analysis**

Samples were examined with a light microscope, and images captured with a digital camera. Cell density was obtained from sampling of the entire sample area from representative tissue cross-sections from each group. Cell counts were obtained from 1, 5 and 10 high powered fields (HPFs), averaged per HPF, and the mean cell count per HPF recorded.

### **Gene Expression Analysis**

RNA extraction and gene expression analysis were performed as previously described[171, 172]. Briefly, three consecutive 20- $\mu$ m sections were obtained from each FFPE block, and RNA was isolated using the RNeasy FFPE Kit (Qiagen, Toronto, ON). RNA

concentration and purity were measured with a NanoDrop 2000c spectrophotometer (Thermo Fisher Scientific, Waltham, MA).

Oligonucleotide probes were manufactured for the following 9 genes: BTLA, CTLA4, CXCL1, CXCL9, CXCL10, CXCL13, CXCL16, CXCR3, IFNG (Integrated DNA Technologies, Coralville, IA). Three housekeeping genes were also included for data normalization purposes (GAPDH, RPL7, SDHA). These genes were chosen as a broad screen of pro-inflammatory gene expression (including chemokines) that encompasses a wide variety of immune cell types. BTLA and CTLA4 are lymphocyte negative regulators. Chemokines CXCL1, CXCL10, CXCL13, CXCL16 and CXCL9 are chemoattractants for neutrophils, T-cells, NK cells, B-cells and macrophages, respectively. CXCR3 is the receptor for CXCL9/10/11 while IFNG is a pro-inflammatory cytokine. Gene expression was then quantified using NanoString nCounter (NanoString Technologies, Seattle, WA).

Quality control assessment and data normalization were performed using nSolver Analysis Software Version 4.0 (NanoString Technologies). Gene expression data was corrected to GAPDH expression and were generated using R version 3.4.3 (R Foundation for Statistical Computing, Vienna, Austria). Raw gene expression counts for all SVD samples examined are shown in Table 5.1 and for all normally functioning human heart valves in Table 5.2.

Sample	BTL A	CTLA 4	CXCL 1	CXCL 10	CXCL 13	CXCL 16	CXCL 9	CXCR 3	IFN G
U11-3648	25.29	7.78	163.44	44.75	1.95	782.2	103.13	17.51	27.2 4
U12-18204	1.92	4.79	5466.5 5	115.98	89.14	1968.84	161.99	2.88	1.92
U12-9021	2.26	11.28	189.47	42.86	2.26	1883.44	20.3	4.51	2.26
U13-12126- 2	3.83	5.11	59.44	14.7	3.2	2223.48	12.78	2.56	2.56
U13-14334	17.16	5.72	57.21	28.6	45.77	303.2	97.25	17.16	11.4 4
U13-2601	4.72	1.18	17.71	3.54	4.72	161.73	37.78	5.9	3.54
U13-823	14.64	7.32	73.2	7.32	21.96	424.55	109.8	7.32	7.32
U14-9868	2.23	15.6	298.68	15.6	2.23	1181.37	71.33	4.46	2.23
U15-6351	7.37	24.45	923.17	6.98	4.66	1365.55	39.58	16.69	10.0 9
U15-869	3.74	3.74	111.19	21.49	2.34	687.68	90.16	8.41	4.67
U16-12613- 1A	14.56	14.56	131	43.67	14.56	1470.07	116.44	29.11	14.5 6
U16-12618- 1A	24.75	51.69	99.93	55.76	101.49	405.66	304.16	32.26	10.6 5
U16-12618- 2A	26.62	35.3	100.5	109.48	187.54	356.84	577.89	43.37	8.67
U16-12664	4.54	12.38	84.6	22.28	9.9	836.89	33.01	11.97	3.3
U16-1388	4.17	4.17	175.26	4.17	4.17	1301.96	45.9	4.17	4.17
U16-14697	1.46	1.46	29.28	2.93	1.46	383.63	20.5	1.46	1.46
U16-15978	11.77	7.85	70.65	11.77	3.92	345.39	70.65	11.77	19.6 2

U16-17521	7.12	28.47	99.63	71.16	14.23	1259.6	64.05	21.35	21.35
U16-20519-1A	5.65	11.3	84.76	8.48	8.48	356	98.89	14.13	14.13
U16-20952	1.61	5.62	140.58	32.94	1	535.54	53.02	8.03	2.41
U16-21710	4.09	4.43	3288.34	19.75	29.62	1524.85	6.47	4.09	1.7
U16-24040	5.58	3.72	130.31	7.45	1.86	1435.32	26.06	16.75	1.86
U16-3255	10.19	7.65	71.36	53.52	6.37	689.41	101.95	11.47	8.92
U16-7553	13.66	1.71	38.24	18.44	2.05	603.71	49.51	7.85	1.71
U16-7658-1A	12.52	7.82	59.46	7.04	47.72	179.55	37.16	9.78	1.17
U16-9188	1.23	11.07	100.84	9.02	1	1464.16	47.14	6.56	3.28
U16-9779	18.58	37.15	315.79	55.73	37.15	1170.27	92.88	18.58	18.58
U17-1810	11.81	10.13	52.32	38.26	1	224.48	22.5	16.88	17.44
U17-4191-1A	32.44	16.22	48.66	16.22	8.11	178.43	81.1	24.33	48.66
U17-5383	8.28	8.28	57.93	8.28	8.28	554.46	74.48	24.83	24.83
U17-7598	34.12	11.37	22.75	34.12	11.37	1012.32	113.74	11.37	22.75

**Table 5.1.** Raw gene expression counts for all SVD samples used.

Sample	BTL A	CTLA 4	CXCL 1	CXCL1 0	CXCL1 3	CXCL1 6	CXCL 9	CXCR 3	IFN G
H001 MV	1.47	4.42	16.21	4.42	1.47	58.94	36.84	2.95	5.89
H039 MV A	1	1	3.63	1.04	1.04	59.16	4.15	1	1
H039 MV P	3.56	1.78	3.26	1.19	2.37	61.4	13.35	4.45	1.19
H040 MV A	1	1	3.09	1	1	63.3	3.28	2.12	1
H040 MV P	1.07	1.07	8.54	1.07	1.07	87.54	11.74	4.27	1.07
H008 MV	1	1.22	9.33	2.03	1	66.97	5.28	1.62	1
H032 MV A	1	1.16	2.31	1.73	1	90.73	11.56	3.47	1
H032 MV P	1	1	1.61	1	1	13.71	3.23	1	1
H033 MV A	1	1	5.3	1	1	48.62	9.72	1.77	1
H033 MV P	1	1	1.54	1	1	15.38	9.22	1	1
H034 MV A	2.86	1.43	15.71	4.29	1.43	108.56	15.71	10	2.86
H034 MV P	3.5	1	8.4	2.1	1	110.66	8.4	6.3	1

**Table 5.2.** Raw gene expression counts for all normal human heart valve samples used.

## Statistical Analysis

Continuous data is expressed as mean $\pm$ standard error of the mean. Two-sample t-testing was used to compare between groups when  $n>5$ , while Wilcoxon test was used to compare between groups when  $n<5$ . All tests were considered significant with a  $p<0.05$ . All statistical analysis and figures were performed using GraphPad Prism version 8.4.1.

## Results

### Xenogenic tissue heart valves deteriorate in non-immune suppressed patients

From 2000 to 2016, 37 XTHVs were obtained from 32 adult patients undergoing aortic or mitral XTHV explant for SVD. As described in the methods section, the comparison arm included 19 valves explanted from human hearts without valvular disease considered for transplantation that were not utilized.

Characteristics		
Mean latency time (years)	11.6 +/- 0.5	
Average Patient Age (years)	67.7	
	<b>No. of Patients</b>	<b>% Affected (n=32*)</b>
Valve Type		
Mitral Valve	11	
Aortic Valve	25	
Unknown	1	
Comorbidities		
Hypertension	20	63

Dyslipidemia	13	41
Smoking History	12	38
Renal Insufficiency	7	22
Obesity	6	19
Hypothyroidism	4	13
Type 2 Diabetes Mellitus	3	9
Hodgkin's Lymphoma	1	3
Medications		
Statins	30	94
ASA	26	81

**Table 5.3.** Patient characteristics

Baseline patient characteristics in the SVD cohort demonstrate that the mean time from initial XTHV implantation to development of SVD requiring reoperation was 11.6-years with an average patient age of 67.7-years. The most common XTHV explanted was from the aortic position (25/37; 68%). 13% (4/32) of patients had hypothyroidism, 9% (3/32) had type 2 diabetes mellitus and 3% (1/32) had prior Hodgkin's lymphoma. No patients were actively receiving any immunosuppressive medication, although 94% (30/32) were taking a statin. Clinical details for the comparison arm were not available due to organ donor confidentiality.

#### **Non-structural valve deteriorated controls are not infiltrated by cells of adaptive immunity**

Normal functioning controls were valves explanted from human hearts without valvular disease, considered but not utilized for transplantation. The definition of 'normal functioning' valve was defined as a valve having less than mild aortic/mitral valve stenosis or regurgitation. Mild aortic valve stenosis was defined as a valve area of 1.5 cm<sup>2</sup> or a mean valve gradient of 25

mmHg. Mild mitral valve stenosis was defined as a valve area of 1.5 cm<sup>2</sup> or a mean valve gradient of 5 mmHg. Mild aortic valve regurgitation was defined on colour Doppler jet as a width less than 25% of the left ventricular outflow tract. Finally, mild mitral valve regurgitation was defined on colour Doppler jet as a width less than 20% of the left atrial area. All 19 control valves had less than mild stenosis and/or regurgitation.

Control valves exhibited minimal neutrophil or plasma cell infiltration on H&E staining (Figure 5.1A). To further describe control valve adaptive immune cell infiltration, we stained valves for CD3<sup>+</sup> T-cells. CD3<sup>+</sup> infiltration into control valves was nominal (Figure 5.1B). Consistent with other cells of adaptive immunity, CD20 stain for B-cells (Figure 5.1C) and CD68 stain for macrophages (Figure 5.1D) showed insignificant infiltration into normal functioning control valves. Taken together, these data suggest that normally functioning, non-structural valve deteriorated valves are not associated with infiltration by cells of innate or adaptive immunity.

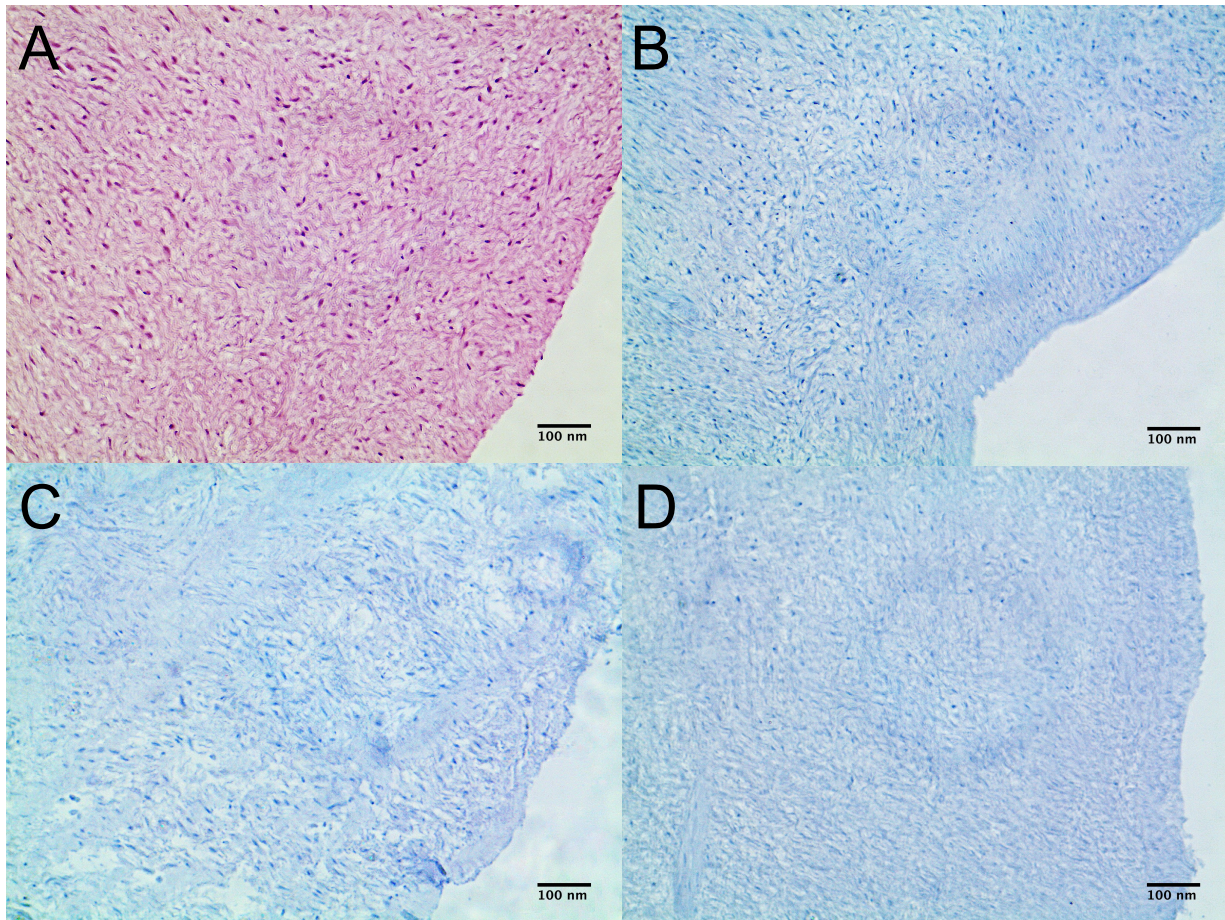


**Figure 5.1.** Representative histology of normal human heart valves with hematoxylin and eosin stain for neutrophil and plasma cell identification (A), CD3 stain for T-cell identification (B), CD20 stain for B-cell identification (C), and CD68 stain for macrophage identification (D)

**Structural valve deterioration of xenogenic tissue heart valves is associated with increased immune cellular infiltrate**

We hypothesized that immune cellular infiltrate of XTHVs that have undergone SVD will be significantly increased when compared to normally functioning controlled valves. This hypothesis is in some measure based on previous studies with limited human valve explants that have detected some cells of adaptive immunity related to SVD on XTHVs[6, 7, 9, 173]. To test this hypothesis, we utilized 37 XTHVs from 32 adult patients (Table 5.1) undergoing aortic or mitral XTHV explantation for SVD. We observed increased neutrophil, plasma cell, T-cell, B-cell and macrophage infiltration in the explanted SVD valves (Figure 5.2A, B, C, and D, respectively).

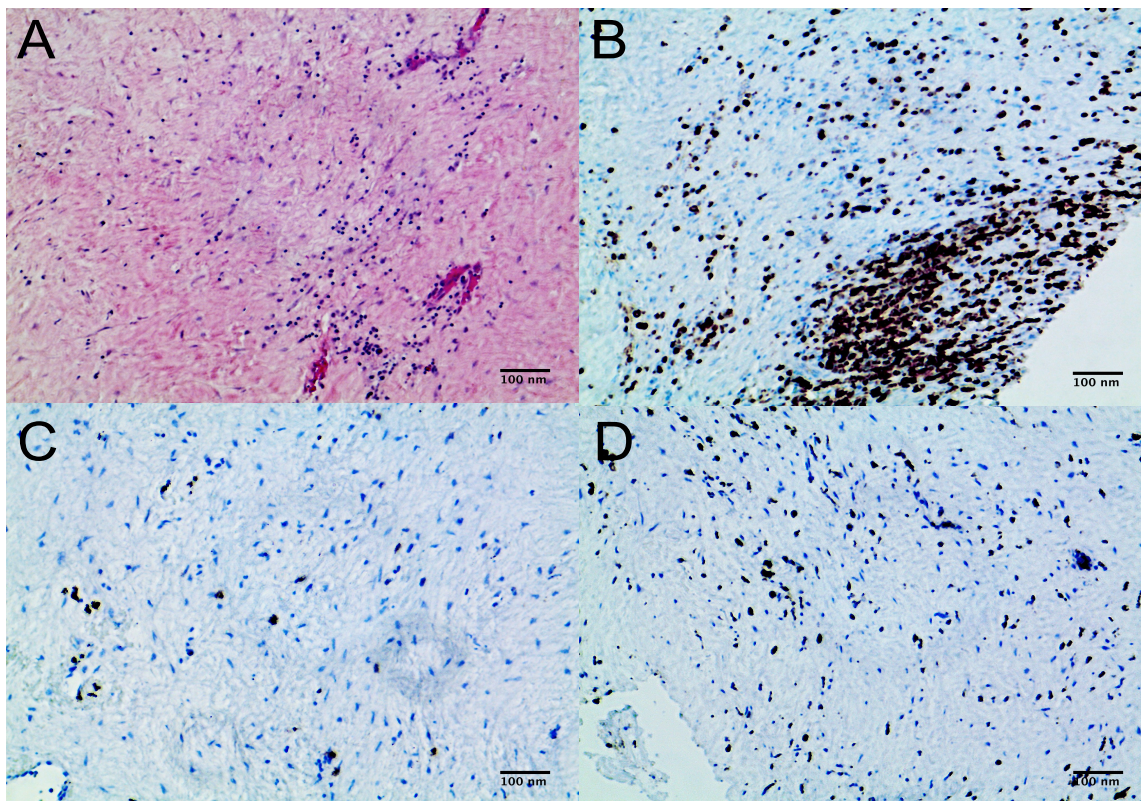


**Figure 5.2.** Representative histology of explanted xenogenic tissue heart valves for structural valve deterioration with hematoxylin and eosin stain for neutrophil and plasma cell identification (A), CD3 stain for T-cell identification (B), CD20 stain for B-cell identification (C), and CD68 stain for macrophage identification (D)

We observed that XTHVs explanted for SVD exhibited significantly higher rates of neutrophil ( $0.7 \pm 0.2$  cells/HPF v.  $0.0$  cells/HPF, XTHVs v. control valves,  $p < 0.001$ ; Figure 5.3A)

and plasma cell ( $3.7 \pm 0.6$  cells/HPF v.  $0.3 \pm 0.1$  cells/HPF, XTHVs v. control valves,  $p < 0.001$ ; Figure 5.3B) infiltration compared to control valves. Moreover, CD3<sup>+</sup> T-cell infiltration compared to control valves ( $7.6 \pm 1.3$  cells/HPF v.  $0.2 \pm 0.1$  cells/HPF, XTHVs v. control valves,  $p < 0.001$ ; Figure 5.3C), CD20<sup>+</sup> B-cells ( $1.0 \pm 0.4$  cells/HPF v.  $0.0$  cells/HPF, XTHVs v. control valves,  $p < 0.001$ ; Figure 6.3D), and CD68<sup>+</sup> macrophages ( $11.8 \pm 2.0$  cells/HPF v.  $0.4 \pm 0.2$  cells/HPF, XTHVs v. control valves,  $p < 0.001$ ; Figure 5.3E) showed significantly higher rates of infiltration when compared to control valves. Taken together, these data suggest that development of SVD in XTHVs is associated with a significantly increased burden of immune cellular infiltrate when compared to normal functioning control valves.

### **Increased chemokine gradient accompanies infiltration by the cells of adaptive immunity**

Chemokines are a large family of small cytokines considered pro-inflammatory that are able to control the migration and infiltration of immune cells of innate and adaptive immunity[174]. We examined whether increased immune cell infiltration into XTHVs that have developed SVD correlates with an increased co-expression of chemokines, since it has been shown that T-cell migration, along with other cells of adaptive immunity, throughout the body are controlled by chemokine gradients[168-170]. Interestingly, the lymphocyte negative regulators, BTLA (Figure 5.4A) and CTLA4 (Figure 5.4B), were both significantly upregulated in the explanted SVD valves compared to the control valves ( $p < 0.001$ ). As well, we observed that co-expression of the chemokines CXCL1 (a neutrophil chemoattractant, Figure 5.4C), CXCL10 (a T-cell chemoattractant, Figure 5.4D), and CXCL13 (a NK cell chemoattractant, Figure 5.4E) correlate with a significantly increased cellular infiltration on SVD-XTHVs when compared to control valves ( $p < 0.001$ ). This finding is consistent with the significant increase in CXCL16 (a B-cell chemoattractant, Figure 5.4F), CXCL19 (a macrophage chemoattractant,

Figure 5.4G) and CXCR3 (the chemokine receptor for CXCL9/10/11, Figure 5.4H) when compared to control valves ( $p < 0.001$ ). Since CXCL10, CXCL16 and CXCL19 are interferon-stimulated genes, we also looked at the gene expression of IFNG. Indeed, IFNG gene expression is significantly higher on explanted SVD valves when compared to control valves (Figure 5.4I,  $p < 0.001$ ). Taken together, these data suggest that SVD of XTHVs is correlated to the induction of a chemokine gradient around the xenograft.

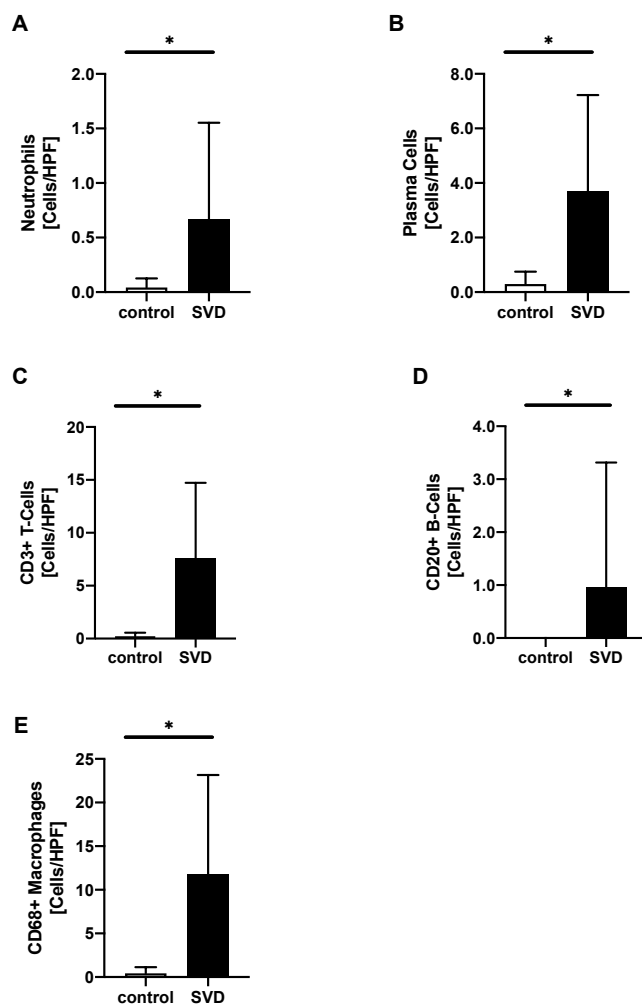


**Figure 5.3.** Quantification of immunohistochemical analysis for neutrophils (A), plasma cells (B), T-cells (C), B-cells (D) and macrophages (E). All cell counts are presented as number of cells counted per high powered field

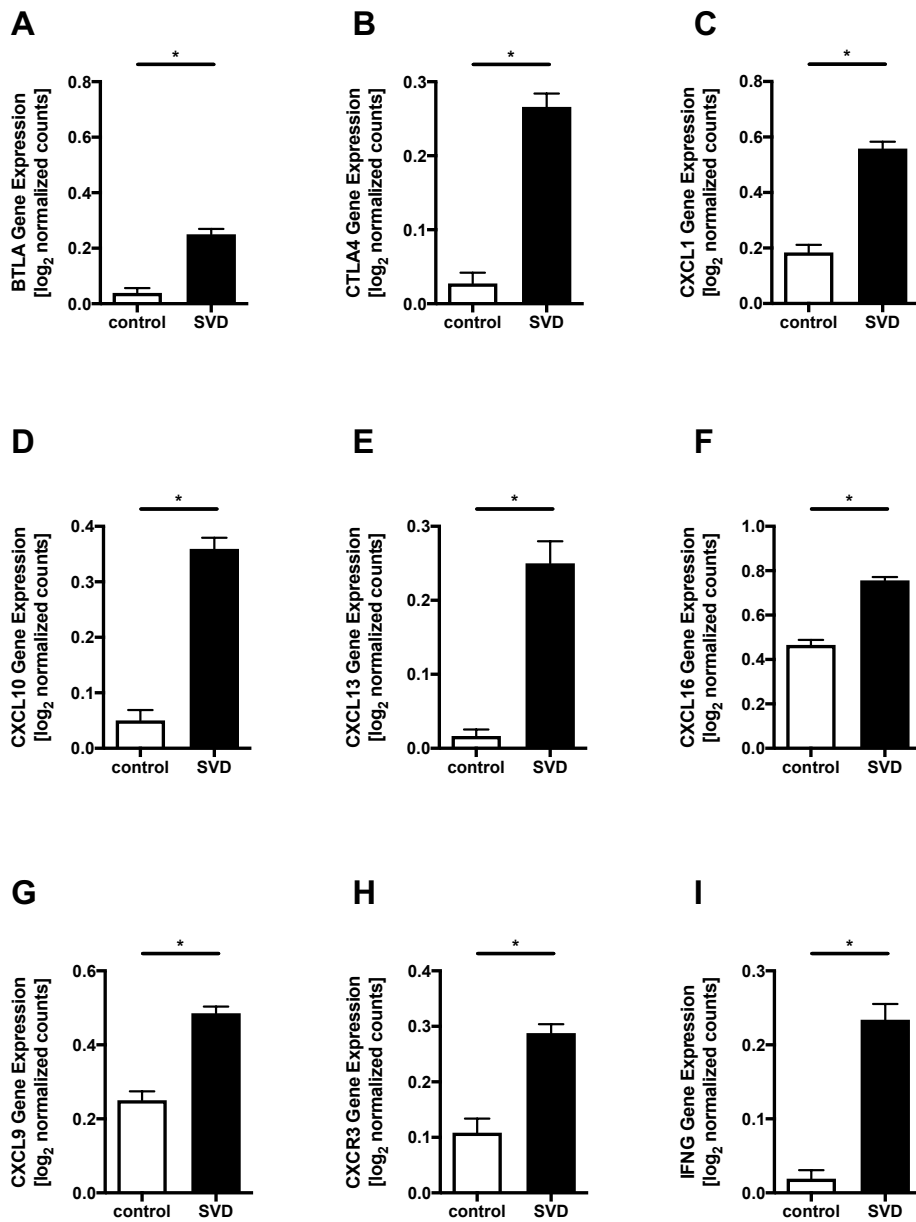


**Figure 5.4.** Quantification of mRNA transcripts using Nanostring technology for a screening panel of nine gene products including, BTLA (A), CTLA4 (B), CXCL1 (C), CXCL10 (D), CXCL13 (E), CXCL16 (F), CXCL9 (G), CXCR3 (H) and IFNG (I). All gene expression is presented as log<sub>2</sub> normalized counts and corrected for GAPDH expression

## Discussion

We investigate whether SVD of XTHVs is associated with an increase in infiltration of the valve tissue with cells of adaptive immunity. Additionally, we studied whether co-expression of several chemokines, responsible for immune cell migration, correlate with this increase in cellular immune infiltrate. Our results demonstrated both a qualitative and quantitative increase in immune cell infiltrate, primarily composed of macrophages and T-cells, found in explanted XTHVs developing SVD compared to normally functioning human valves. As expected, explanted SVD valves show greater recruitment of cells from adaptive immunity that is accompanied by increased chemokine expression. These data show that SVD in XTHVs may be related to the recruitment of immune cellular infiltrate to the valve and a possible mechanism of this recruitment is the existence of a chemokine gradient. This chemokine gradient may represent a potential therapeutic target to mitigate the development of SVD and prevent reoperative risk in patients undergoing valve replacement surgery with a XTHV.

We have previously observed a decreased rate of SVD development amongst solid-organ transplant recipients undergoing valve replacement with a XTHV post-transplantation[175]. In fact, we found that no patient required a redo valve replacement for SVD despite rates as high as 0.36%/patient-year being reported[176]. These data suggest that the rate of SVD may be lower in transplant recipients undergoing immunosuppressive therapy. Therefore, we and others hypothesize that SVD may be driven primarily by immune-mediated processes since the rates of SVD are reduced in those patients receiving immunosuppressive therapy [6, 7, 9, 173, 175, 177].

Given the lack of SVD in immunosuppressed patients, we first sought to characterize how SVD occurs in non-immune suppressed patients at our centre. To do this, we examined clinical baseline characteristics of explanted valves from human patients developing SVD. Our

results showed that the mean time from initial XTHV implantation to development of SVD requiring reoperation and explant was 11.6-years, occurring at an average patient age of 67.7-years. These results are consistent with the literature, demonstrating an average time to development of SVD ranged from 5.9-years to 12-years[6, 7, 9, 173]. Reoperation to replace a dysfunctional XTHV developing SVD is associated with increased morbidity and mortality for the patient[178]. Thus, investigating the causes of SVD is an important undertaking to prevent this reoperative risk for patients.

Since non-immune suppressed patients develop SVD and immunosuppressed patients do not develop SVD[175], we wanted to examine SVD valves for the presence of immune cell infiltrate in an effort to elucidate possible causes of SVD. Although previous studies have shown presence of immune cell infiltrate on valves that have been explanted for SVD, these studies lacked a robust examination of immune cells, suffered from few valve samples and none had normally functioning valve controls. Butany et al examined 163 explanted porcine valves and found significant morphological changes including calcification, tears, pannus formation and thrombus in the >65% of the XTHVs, however they did not examine for infiltrating cells[173]. Shetty et al found cellular infiltrate composed primarily of macrophages in explanted XTHVs, particularly associated with areas of calcification and lipid accumulation[9]. More recently, Manji et al and Sellers et al provided further contemporary evidence of immune involvement in development of SVD[6, 7]. In the former, cellular infiltrate was found in all but one explanted XTHV and was composed primarily of macrophages, with no T-cell or B-cell infiltration[6]. In the latter, transcatheter aortic heart valves were analyzed, finding fibrosis, calcification and polymorphonuclear cell infiltration[7].

Our findings are different from these previous studies as we were able to make comparisons of SVD valves to normally functioning human heart valve controls to illustrate differences in infiltration. The gold-standard control arm to use for this study would be normally functioning XTHVs that have been implanted for a similar duration. However, there is no surgical indication to remove these normally functioning valves for analysis making them very challenging to obtain. It is well established that chronic allograft dysfunction in solid organ transplantation is correlated to immune cell infiltration and that normally functioning allografts exhibit reduced rates of immune infiltrate [179, 180]. Since XTHVs are implanted intravascularly in direct contact with blood, it is plausible to expect normally functioning, non-SVD XTHVs to exhibit reduced immune infiltrate in comparison to abnormally functioning, SVD XTHVs, similarly to chronic rejection in transplantation. In fact, several preclinical studies support the notion that less immune cell infiltration and calcification and normal transvalvular gradients occur in normally functioning xenograft valve implants [45, 46, 181]. With that in mind, we chose to highlight the importance of function by comparing our abnormally functioning XTHVs to normally functioning human heart valves, intending to support the concept that development of dysfunction is correlated to immune infiltration. The use of normally functioning human heart valves serves as a negative control, where one would not expect to any immune infiltration, consistent with what is demonstrated here. The addition of a positive control, namely explanted diseased native heart valve tissue, would be informative to include in future studies as it is likely that immune cells could be found in a similar mechanistic process. Support for this notion has recently been examined by Erkhem-Ochir and colleagues [182].

We observed significantly increased immune cellular infiltration in the explanted SVD valves compared to the control valves for all immune cell types examined. Macrophages and T-cells represented the most common cell types present, while neutrophils and B-cells were rarely present. The increased presence of macrophages and T-cells suggest a response similar to a chronic immune rejection, as opposed to an acute response, where more polymorphonuclear cells such as neutrophils would be expected[37]. While only a small number of plasma cells were identified, they play a critical role in the production of antigen-specific humoral immune responses. Plasma cells can produce significant quantities of antigen-specific antibody into the microenvironment, propagating a chronic immune rejection to XTHVs[183].

Previous studies have consistently demonstrated polymorphonuclear cell infiltration in explanted SVD valves, however, they have largely failed to show adaptive immune cell infiltration such as T-cells and B-cells. In contrast, the current study suggests that XTHVs developing SVD contain a large burden of adaptive immune cells. One reason for this difference is potentially due to prior studies not staining specifically for T-cells, B-cells and plasma cells. Further, differences in time to onset of SVD and subsequent explantation of the XTHV may have an impact on reliable detection of adaptive immune cells which may be exhibiting transient infiltration [6].

The probable event that initiates immune cell infiltration is the post-translational modification  $\alpha(1,3)$ -galactose (alpha-gal) that is found in all non-primate mammals and new world primates[34, 35]. From exposure to natural gut bacteria all humans develop anti-alpha-gal antibodies, constituting 1-8% of IgM and 1-2.5% of IgG's found in human circulation[36]. The alpha-gal epitope interacts with these natural preformed IgG antibodies, activating the classic complement pathway and subsequent tissue damage [37].

Lastly, since it has been shown that cells of adaptive immunity throughout the body are controlled by chemokine gradients [168-170], we examined whether increased immune cell infiltration into XTHVs that have developed SVD correlates with an increased co-expression of chemokines. Indeed, we observed a significantly increased chemokine gene transcript levels in SVD valves compared to controls. We successfully isolated the mRNA gene transcripts from the FFPE blocks and from the normally functioning human heart valves (tables 5.1 and 5.2) and quantified using Nanostring. To the best of our knowledge, our study provides the first evidence that these infiltrating adaptive immune cells are actively transcribing chemokine gene products associated with SVD of XTHVs. This finding provides evidence that there is in fact an active, chronic pro-inflammatory immune response occurring in response to XTHVs. Specifically, the identification of the T-cell and macrophage chemoattractants CXCL10 and CXCL9 may represent effective future targets to mitigate this immune response.

### **Study Limitations**

The explanted XTHVs used in this study were all obtained from surgical explantation from patients with symptomatic SVD, thus we cannot make any conclusions regarding initiation of early SVD. As discussed above, the gold-standard control arm to use for this study would be non-SVD XTHVs, however, there is no surgical indication to remove these normally functioning valves for analysis. Finally, the present analysis cannot prove a direct link between immune cell infiltration, subsequent chemokine gene expression and development of SVD. Further studies are needed to establish the initiation of SVD and to elucidate the interplay between the immune cells implicated by the present analysis.

## **Conclusion**

Our results suggest that SVD is a chronic immune mediated rejection of XTHV tissue. We demonstrate both a qualitative and quantitative increase in immune cell infiltrate, primarily composed of macrophages and T-cells, found in explanted XTHVs developing SVD compared to normal human valves. Furthermore, the immune cells present are actively transcribing chemokine genes, propagating development of SVD via generation of a chemokine gradient. The chemokine gene expression quantified in the present study may be effective targets for future immunomodulating therapeutics to mitigate development of SVD.

**Chapter 6. Recellularization of Bovine Pericardium with Autologous  
Mesenchymal Stem Cells Attenuates Initial Immune Activation**

## **Abstract**

**Objectives:** The purpose of this study is to address the significant gap in knowledge by examining the effects of autologous MSC recellularized tissue on the immune response. We hypothesized that autologous MSC recellularization of bovine pericardium will result in a reduction in pro-inflammatory cytokine production equivalent to autologous human pericardium.

**Methods:** Bone marrow, human pericardium and whole blood was collected from adult patients undergoing elective cardiac surgery. Decellularized bovine pericardium underwent recellularization with autologous MSCs, followed by co-incubation with autologous whole blood. Immunohistochemical, microscopic and quantitative immune analysis approaches were used.

**Results:** We show that bovine pericardium, exposed to human whole blood, results in a significant amount of TNF-a and IL-1b production. When decellularized bovine pericardium is recellularized with autologous MSCs and exposed to human whole blood, there is a significant reduction in TNF-a and IL-1b production. Importantly, recellularized bovine pericardium exposed to human whole blood had an equivalent production of TNF-a and IL-1b when compared to autologous human pericardium exposed to human whole blood.

**Conclusions:** Our results suggest that preventing initial immune activation with autologous MSC recellularization may be an effective approach to decrease the recipient immune response, thus preventing recipient immune recognition of XTHVs, and potentially leading to a reduction in SVD incidence.

## Introduction

The prevalence of valvular heart disease (VHD) in industrialized countries is predicted to be at 2.5%, and over 250,000 valve replacement surgeries are estimated to take place worldwide in a given year [184-188]. Today, xenograft tissue heart valves (XTHV) constructed out of bovine pericardium are the most prevalent option used for surgical valve replacements [165, 189-191]. While not requiring long-term anticoagulation, XTHVs undergo time-dependent structural valve deterioration (SVD) that is characterized by degeneration and/or hemodynamic dysfunction of the valve [3]. This degeneration is especially accelerated in pediatric and young adult populations as xenograft failure rate can be 50% as early as 5 years after implantation [192, 193]. We have previously observed a decreased rate of SVD in solid-organ transplant recipients undergoing valve replacement with XTHV post-transplantation, suggesting that the rate of SVD may be lower in patients receiving immunosuppressive therapy [175]. Thus, we and others have hypothesized that the development of SVD is a result of a chronic, immune-mediated rejection to the foreign XTHV tissue [4-6, 33, 175, 194].

With this hypothesis in mind, we investigated whether SVD of XTHVs is associated with increased immune cell infiltration and whether co-expression of several chemokines correlate with this increase in immune infiltrate [194]. We found significantly increased immune cellular infiltration in explanted SVD valves for all immune cell types examined, associated with a significantly increased pro-inflammatory cytokine and chemokine gradient. These data suggest development of SVD is associated with immune cellular infiltrate correlated to the induction of a chemokine gradient around the XHTV, representing chronic immune rejection. The post-translational modification  $\alpha(1,3)$ -galactose (alpha-gal), found in all non-primate mammals and new world primates, is the most likely initial epitope leading to immune activation [34, 35].

Autologous mesenchymal stem cell (MSC) recellularization is a method of concealing a xenogenic scaffold with the intention of preventing recipient immune recognition. Despite being at early stages of development with limited clinical applications, MSC demonstrated multipotency, immunomodulatory, and trophic effects have garnered interest among researchers and clinicians to explore their use in treating a wide variety of conditions [195, 196]. While recellularization has been used to repopulate acellular xenogenic matrices, the immune responses generated by these tissues has not been investigated and it remains unclear what effect an autologous recellularized xenograft has on the immune response in the host. As such, there is a significant gap in knowledge regarding the role of autologous recellularized tissue in attenuating the immune response. Preventing initial immune activation with autologous MSC recellularization may be an effective approach to decrease the recipient immune response, thus preventing recipient immune recognition of XTHVs and potentially leading to a reduction in SVD incidence.

The purpose of this study is to address the significant gap in knowledge by examining the effects of autologous MSC recellularized tissue on the immune response. We hypothesized that autologous MSC recellularization of bovine pericardium will result in a reduction in pro-inflammatory cytokine production equivalent to autologous human pericardium.

## **Methods**

### **Patient Population**

Patients undergoing elective cardiac surgery at the Mazankowski Alberta Heart Institute in Edmonton, Alberta, Canada were consented pre-operatively (**Table 6.1**). Once the sternotomy was performed and hemostasis achieved with cautery to the edges of the sternum, a 5 mL syringe with a blunt needle tip or a surgical curettage were used to collect the discharging bone marrow

from between the edges just below the manubrium, collecting 0.3 – 1 mL of bone marrow. Once drawn, the sample was stored at room temperature not exceeding 4 hours. Intra-operatively, human pericardium (5cm x 5cm) and 20mL of heparinized whole blood were collected. Written informed consent for research participation containing the purpose of study, procedural details, risks and benefits, and confidentiality that was approved by the Health Research Ethics Board was provided and carefully explained to the patients prior to surgery. Exclusion criteria for patients included active malignancy, any hematologic disease, or infective endocarditis.

**Table 6.1.** Patient Characteristics

<b>Characteristics</b>	<b>No. of Patients</b>	<b>% Affected (n total=14)</b>
Gender - Male	8	57
Average Patient Age (years)	67.2 years	
<b>Comorbidities</b>		
Smoking hx	8	57
HTN	9	64
Dyslipidemia	7	50
hypothyroidism	2	14
Obesity	2	14
T2DM	4	29
polymyalgia rheumatica	1	7
<b>Medications</b>		
Corticosteroids	3	21
Chemotherapy drugs	0	0
Antibiotics	0	0

## **MSC Isolation and Culturing**

The sternal bone marrow collected was directly plated onto T75 plastic cell culture flasks (Thermo Fisher Scientific, Massachusetts, USA). The cells were incubated at 37°C with 5% CO<sub>2</sub> in DMEM F12 (Thermo Fisher Scientific, Massachusetts, USA) culture media completed with 20% fetal bovine serum, 0.2% ascorbic acid, and 0.2% primocin in order to only culture plastic adherent MSCs. The cells were washed with PBS and the media changed at 1 day after initial plating. The media was then changed every 3 days afterward and monitored regularly until the flask had reached 80% confluence. Cells were passaged by addition of 15ml of TrypLE Select Enzyme 10x (Thermo Fisher Scientific, Massachusetts, USA) and incubated for 30 minutes to detach the cells. Next, 15ml of complete DMEM F12 was then added and the cells and solution were transferred to a 50ml conical tube for centrifugation at 400g, 18°C for 15min. The solution was aspirated, the cells were resuspended in PBS and underwent 1 additional cycle of centrifugation. The cell pellet was then resuspended in DMEM F12 media and either plated onto multiple flasks until it reached 80% confluency or used immediately for recellularization.

## **MSC Surface Phenotyping and Differentiation**

A small sample of isolated and cultured MSCs were utilized to confirm surface phenotyping. MSC phenotype was confirmed by staining positively for CD44, CD90, CD105 and CD73, but negatively for CD34, CD11b, CD19, CD45 and HLA-DR. After antibody staining, the cells were then analyzed using an Attune NXT flow cytometer. To confirm their differentiation potential, MSCs were differentiated into adipocytic, osteoblastic and chondrocytic phenotypes.

## **Decellularization and Recellularization**

Fresh bovine pericardium was supplied by LivaNova (London, UK) and used as the xenogenic scaffold for this study. Initially, 5cm x 5cm pieces of bovine pericardium were decellularized. The tissue was first washed with 25mL of phosphate-buffered saline (PBS) and then washed with 1% sodium dodecyl sulfate (SDS) (Bio-Rad Laboratories, California, USA) while oscillating at 40rpm at room temperature. The SDS was changed every hour for 4 changes in total. The fourth addition of SDS was left for 20 hours. The next day the SDS was removed and 25mL of Triton-X 100 (Thermo Fisher Scientific, Massachusetts, USA) was added while oscillating at 40rpm at room temperature. After 1 hour the Triton-X 100 was removed and replaced. This was repeated for a total of 4 changes, and after the last change was left for 20 hours. The next morning the Triton-X 100 was removed, and the tissue was rinsed with PBS and double distilled water (DDH<sub>2</sub>O) until bubbles no longer formed. The tissue was then washed with 1% sodium chloride for 1 hour while oscillating at 40rpm at room temperature. The sodium chloride was removed, the tissue was again rinsed with PBS and DDH<sub>2</sub>O. After rinsing 25ml of DNAase and MgCl<sub>2</sub> was added and the tissue oscillated at 40rpm at 37°C. After aspirating, the tissues were rinsed twice with DDH<sub>2</sub>O, and 25ml of 1% PBS penicillin-streptomycin mixture was added, the tissue was left oscillating at 40rpm at 37°C for 30 minutes. Once decellularization was complete the tissue was stored in 1% Hank's balanced salt solution with primocin (InvivoGen, California, USA) in a 4°C fridge until use.

Recellularization began by incubating a 5cm x 5cm piece of tissue in 10mL of DMEM F12 culture media on a rotator at 37°C for 24h. The next day, approximately 1 million MSCs isolated as described above would be resuspended in 4mL of DMEM F12 culture media. The tissue was then placed into the media in a 5mL centrifuge tube (MTC Bio, New Jersey, USA),

including MSCs and was placed on a rotator at 37°C for 12h. The recellularized tissue was then ready for qualitative and quantitative analysis.

### **Tissue Exposure to Whole Blood**

The 20mL of whole blood collected intra-operatively was mixed with 20mL of DMEM F12 culture media. Next, 10mL of the whole blood and DMEM mixture was then moved into individual 15mL polypropylene centrifuge tubes (Thermo Fisher Scientific, Massachusetts, USA). To these tubes, native bovine pericardium (NBP), decellularized bovine pericardium (DBP), recellularized bovine pericardium (RBP) or autologous human pericardium were added. In order to provide a reference for the amount of immune activation generated by each of our experimental tissue groups, we performed *in-vitro* stimulation of whole blood alone with PMA (50ng/mL) and ionomycin (1ug/mL) as a positive control. The tubes were then placed onto a rotator and incubated at 37°C. At days 1, 3, and 5 after starting exposure, 2 mL of whole blood was collected from each tube and placed into a 2mL Eppendorf tube (Thermo Fisher Scientific, Massachusetts, USA). The samples were then centrifuged at 400g, 18°C for 15min. The serum was collected and move into a new tube, the pellet was discarded. The tubes containing the serum were flash-frozen in liquid nitrogen and stored at -80°C until enzyme-linked immunosorbent assay (ELISA) analysis.

### **Qualitative Analysis**

Tissue composition of NBP, DBP and RBP was analyzed qualitatively using standard immunohistochemical techniques. Hematoxylin-eosin, Gomori's trichrome, and elastic Verhoeff's van Gieson staining was performed to assess extracellular matrix (ECM) integrity. Confirmation of successful decellularization and recellularization was completed by 4',6-diamidino-2-phenylindole (DAPI) staining. Tissue samples at each stage of processing including

native, decellularized, and recellularized samples were stained with DAPI in order to identify the presence of original cells, the absence of those cells after decellularization, and presence of MSCs after recellularization. Representative samples of NBP, DBP and RBP were analyzed using scanning and transmission electron microscopy. Finally, immunofluorescence to detect the presence of the alpha-gal epitope was performed on NBP, DBP and RBP tissue samples.

### **Quantitative Analysis**

The serum containing cytokines that were stored at  $-80^{\circ}\text{C}$  was thawed and underwent ELISA analysis according to the manufacturer's recommended protocol for human TNF- $\alpha$  DuoSet ELISA Kit (Cat. No. DY210-05) and Human IL1 $\beta$  DuoSet ELISA kit (Cat. No. DY201-05) (R&D Systems, Minneapolis). Absorbance reading at 450 nm and 540 nm were performed using Synergy H4 hybrid reader (Biotek, Winooski, Vermont). Quantitative biochemical analysis was also performed to determine the impact of the decellularization and recellularization process. DNA was quantified to confirm the decellularization process removed all genetic material and the recellularization process restored it. Hydroxyproline (HYP) and glycosaminoglycan (GAG) content was similarly quantified to determine the impact of collagen content and chondroitin sulfate, respectively.

### **Statistical Analysis**

Continuous data is expressed as mean  $\pm$  standard error of the mean. Two-sample t-testing was used to compare between groups when  $n > 5$ , while Wilcoxon test was used to compare between groups when  $n < 5$ . All tests were considered significant with a  $p < 0.05$ . All statistical analysis and figures were performed and generated using GraphPad Prism version 9.0.0.

## Results

### **Bovine pericardium is immunogenic, stimulating an immune response similar to PMA/ionomycin stimulation**

As the majority of XTHVs implanted in humans are composed of bovine pericardium, we sought to first quantify the immune response generated to this tissue. We quantified the initial immune response based on the production of 2 cytokines: TNF-a and IL-1b. Both of these cytokines are pro-inflammatory, generated very rapidly by activated macrophages in the initial phase of immune activation [38]. Thus, analyzing TNF-a and IL-1b production acutely will allow us to evaluate the initial immune response to the tissue types examined. In order to provide a reference of a known immune activating stimulant to compare bovine pericardium to, we used phorbol 12-myristate 13-acetate (PMA) and ionomycin. PMA is a DAG mimic that recruits PKC and RasGRP to the cell membrane and ionomycin is a calcium ionophore that promotes signaling through the calmodulin-calcineurin pathway [197]. Both of these molecules force the activation of peripheral blood mononuclear cells to produce copious amounts of cytokine and stimulate proliferation [197].

We hypothesized that NBP would elicit an immune response equivalent to forced activation via PMA/ionomycin stimulation. To test this hypothesis, we performed *in-vitro* stimulation of human whole blood with PMA/ionomycin and compared the amount of cytokine production to that elicited by only NBP incubated with human whole blood (without PMA/ionomycin stimulation). Unstimulated whole blood did not result in the production of any cytokine. As expected, whole blood stimulated with a cocktail of PMA and ionomycin did result in significant production of TNF-a and IL-1b. We also observed significant production of TNF-a and IL-1b after exposure of whole blood to NBP alone. Importantly, the amount of TNF-a

production was equivalent between the stimulated group and the NBP alone group ( $1258 \pm 267$  pg/mL v.  $1298 \pm 419$  pg/mL, stimulated v. NBP group,  $p=0.81$ ) (**Figure 6.1A**). Similarly, the amount of IL-1b production was equivalent between the stimulated group and the NBP alone groups ( $431 \pm 77$  pg/mL v.  $387 \pm 51$  pg/mL, stimulated v. NBP group,  $p=0.65$ ) (**Figure 6.1B**). Taken together, these data suggest that NBP elicits an acute and robust immune response characterized by the production of TNF-a and IL-1b at equivalent levels as forced stimulation with known robust immune activators, PMA and ionomycin. The raw data for figure 6.1 has been tabulated in table 6.2 for TNF-a and table 6.3 for IL-1b.

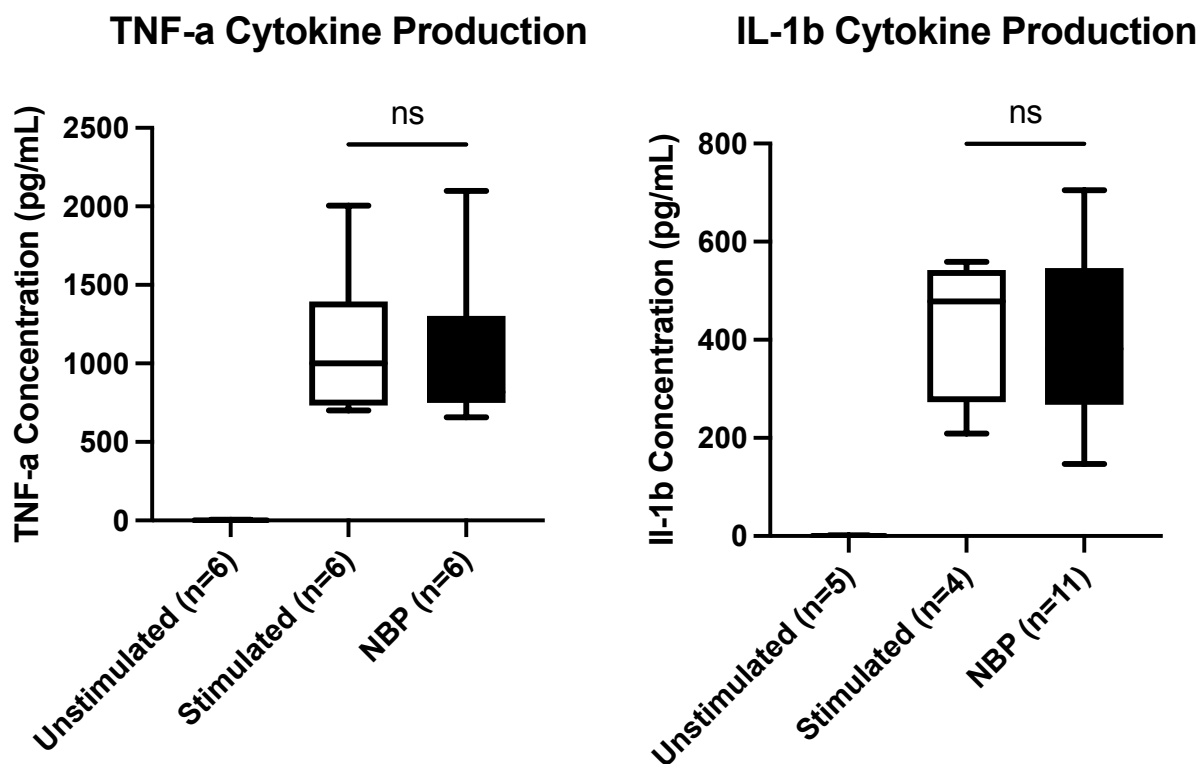


**Figure 6.1.** Production of pro-inflammatory cytokines TNF-a and IL-1b. Native bovine pericardium (NBP) produces a similar production of TNF-a and IL-1b as forced stimulation with PMA/ionomycin (Stimulated), while unstimulated whole blood does not result in any cytokine production.

TNF-a Raw Data		
Unstimulated (n=6)	Stimulated (n=6)	NBP (n=6)
0	2005.585	656.5
0	1093.073	849.2
0	743.2145	778.5
0	1191.95	787.3
4.456	909.437	2098
0.2105	700.271	1038.7

**Table 6.2.** Raw data for TNF-a presented as concentrations in pg/mL for each sample.

IL-1b Raw Data		
Unstimulated (n=5)	Stimulated (n=4)	NBP (n=11)
0	465.068	440.2725
0	559.2	267.3415
0	491.17	288.196
0.9	209.11	179.1365
1.754		342.5795
		705.08
		546.18
		146.8025
		552.355
		381.565
		401.58

**Table 6.3.** Raw data for IL-1b presented as concentrations in pg/mL for each sample.

## **Bovine pericardium can be decellularized and recellularized successfully without damaging the extracellular matrix**

Modification of xenogenic scaffolds with decellularization and recellularization has been proposed as one possible method of developing an immunologically acceptable future heart valve construct [198]. However, in order to do so, several key points must be addressed. First, complete decellularization must be achieved without any major biochemical damage to the components of the ECM. Second, recellularization of the acellular scaffold must quantitatively restore genetic material and be qualitatively evenly distributed across the scaffold. Finally, recellularization also must not adversely impact the biochemical structure of the scaffold. We assessed our decellularization and recellularization procedures using histology, electron microscopy and biochemical analysis.

Our decellularization and recellularization processes were assessed qualitatively using DAPI nuclear staining on NBP, DBP and RBP (**Figure 6.2A, B, and C**). As expected, the NBP contained a large number of cell nuclei (**Figure 6.2A**), which were completely eliminated after decellularization (**Figure 6.2B**). Following recellularization there was nearly equivalent nuclear material as the NBP (**Figure 6.2C**). The ultrastructure of the ECM was assessed with scanning (SEM) and transmission electron microscopy (TEM). SEM confirmed that the overall structure of the collagen and elastin of the ECM remained intact following decellularization and recellularization (**Figure 6.2D, E, and F**). TEM confirmed that the orientation of individual collagen fibres was not distorted, implying the ECM was structurally undisturbed (**Figure 6.2G, H, and I**).

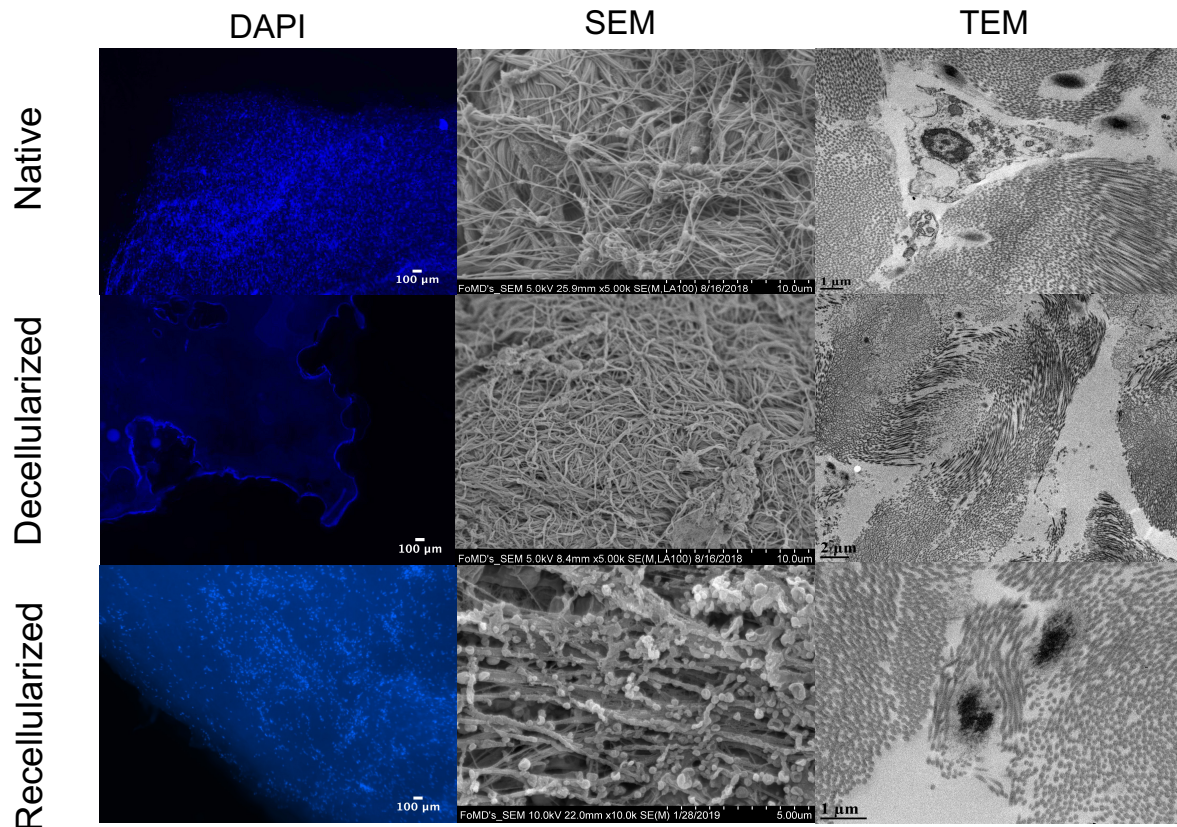


**Figure 6.2.** DAPI nuclei staining, SEM and TEM images assessing decellularization and recellularization procedure and impact on the ultrastructure of the extracellular matrix.

Gross histology was performed with H&E, elastic Verhoeff's van Gieson (eVG) and Gomori's trichrome staining. Intact ECM structure was observed in the NBP tissue prior to decellularization, in the DBP tissue after decellularization and in the RBP tissue after recellularization (**Figure 6.3A, B, and C**). Arrangement of elastin fibres was assessed with eVG staining and found to be grossly consistent before and after decellularization and recellularization (**Figure 6.3D, E, and F**). Finally, Gomori's trichrome staining was used to analyze gross collagen structure. No significant differences were observed in any tissue type before and after decellularization and recellularization (**Figure 6.3G, H and I**).

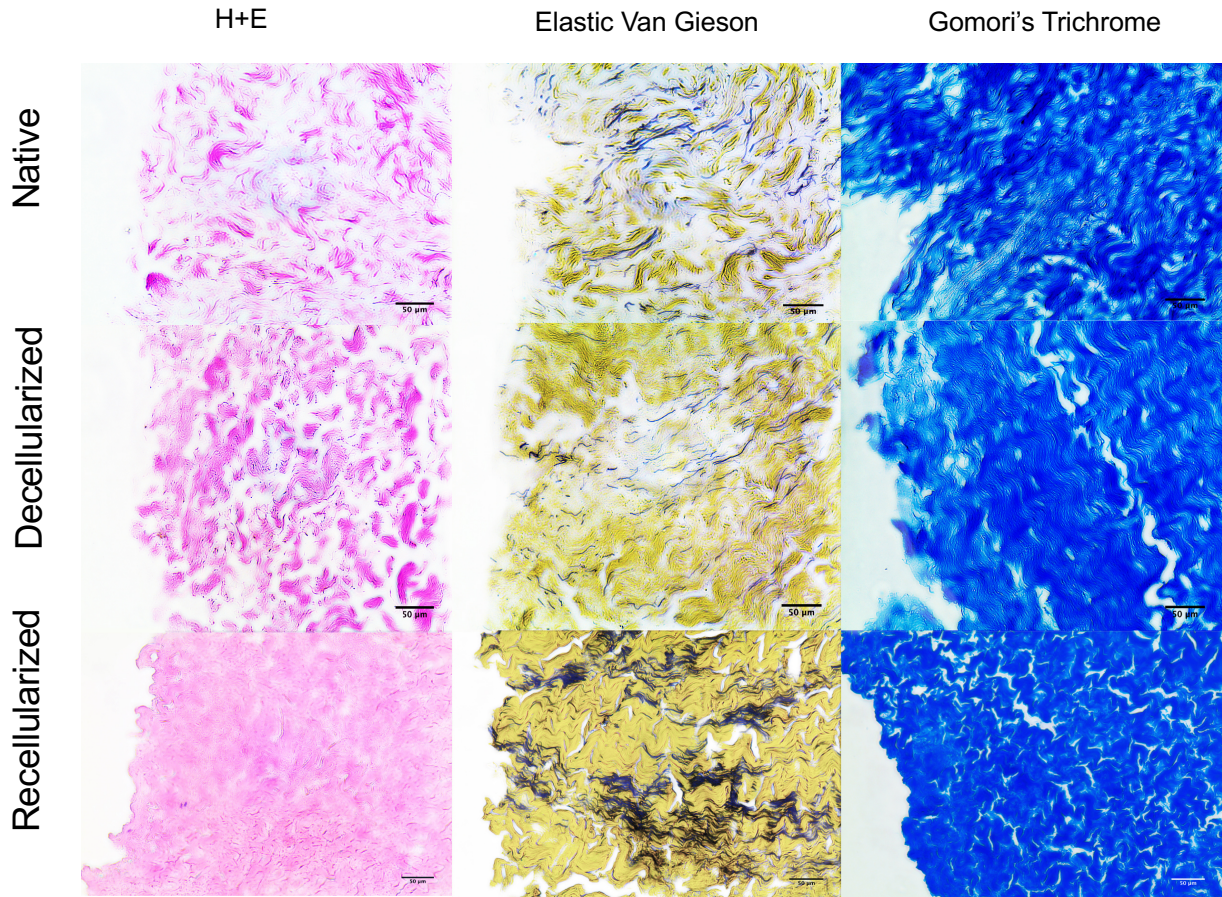


**Figure 6.3.** H&E, elastic van Gieson and Gomori's assessment on the distribution of elastin or collagen, respectively.

Biochemical quantification of DNA and ECM components hydroxyproline and glycosaminoglycans (GAG) in NBP, after decellularization (DBP), and after recellularization (RBP) was performed. DNA quantification confirms a significant reduction in genetic material following decellularization ( $30.9 \pm 5.5$  ng/uL v.  $6.8 \pm 1.0$  ng/uL, NBP v. DBP,  $p=0.003$ ), with a subsequent increase following recellularization ( $6.8 \pm 1.0$  ng/uL v.  $61.2 \pm 14.4$  ng/uL, DBP v. RBP,  $p=0.006$ ) to equivalent levels as NBP ( $30.9 \pm 5.5$  ng/uL v.  $61.2 \pm 14.4$  ng/uL, NBP v. RBP,  $p=0.09$ ) (**Figure 6.4A**). Hydroxyproline quantification confirms no significant change in collagen content following decellularization ( $1.1 \pm 0.3$  ug v.  $1.8 \pm 0.5$  ug, NBP v. DBP,  $p=0.23$ ) and recellularization ( $1.1 \pm 0.3$  ug v.  $1.4 \pm 0.4$  ug, NBP v. RBP,  $p=0.48$ ) (**Figure 6.4B**). GAG

quantification revealed a significant reduction in chondroitin sulfate content following decellularization ( $113.3 \pm 1.7$  ng/mL v.  $56.9 \pm 1.8$  ng/mL, NBP v. DBP,  $p < 0.0001$ ), with a subsequent increase following recellularization ( $56.9 \pm 1.8$  ng/mL v.  $144.9 \pm 2.4$  ng/mL, DBP v. RBP,  $p < 0.0001$ ) to levels higher than NBP ( $113.3 \pm 1.7$  ng/mL v.  $144.9 \pm 2.4$  ng/mL, NBP v. RBP,  $p < 0.0001$ ) (**Figure 6.4C**). The raw data for figure 6.4 has been tabulated in table 6.4 for DNA, table 6.5 for hydroxyproline, and table 6.6 for glycosaminoglycan content.

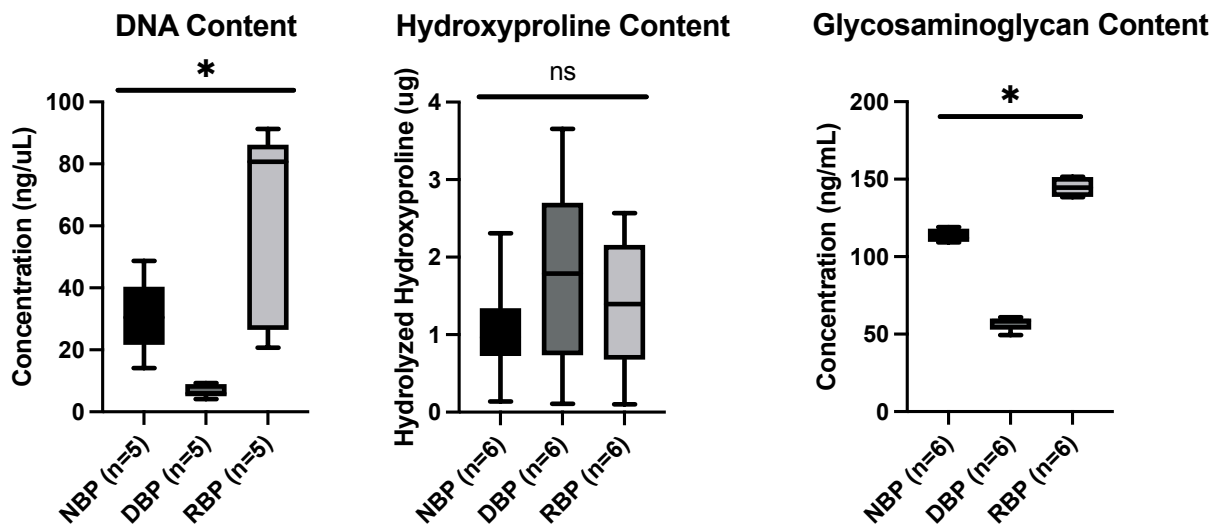


**Figure 6.4.** Biochemical quantification of DNA and ECM components hydroxyproline and glycosaminoglycans in NBP, after decellularization (DBP), and after recellularization (RBP).

DNA Raw Data		
NBP (n=5)	DBP (n=5)	RBP (n=5)
29.1675	5.935	80.6675
32.0275	9.30625	20.7025
48.695	8.635	81.1225
30.45	4.08425	91.3125
14.1	5.921	32.155

**Table 6.4.** Raw data for DNA presented as concentrations in ng/uL for each sample.

Hydroxyproline Raw Data		
NBP (n=6)	DBP (n=6)	RBP (n=6)
0.139	0.107	0.103
1.02	1.752	1.05
0.98	0.944	2.024
0.951	1.825	1.737
2.307	2.385	2.567
0.92	3.654	0.87

**Table 6.5.** Raw data for hydroxyproline presented as quantity in ug for each sample.

Glycosaminoglycan Raw Data		
NBP (n=6)	DBP (n=6)	RBP (n=6)
119.01	59.74	145.89
111.75	59.75	151.58
109.76	54.05	138.77
117.78	60.92	151.35
112.48	57.22	143.27
109.22	49.42	138.35

**Table 6.6.** Raw data for glycosaminoglycan presented as concentrations in ng/mL for each sample.

Taken together, these data suggest complete decellularization is achievable without any major biochemical damage to the components of the ECM. Further, recellularization of the decellularized scaffold quantitatively restores genetic material without adversely impacting the biochemical structure of the scaffold.

## Decellularization alone does not significantly reduce initial cytokine production

A modality to render xenogenic matrices immunoprivileged and possibly susceptible to further autologous-like regeneration has been offered by decellularization technology.

This extraction process has as rationale, the removal of all endogenous cell elements, as, for instance, cell membranes, organelles, and nucleic acids, which can adversely prompt inflammatory, immune, and calcific events. This cell removal is proposed to decrease the effects of acute and chronic rejection via an elimination of MHC I mediated immune responses [199]. However, the antigenic ECM composed of alpha-gal and other xenoantigens still poses a significant barrier to xenograft implants [56]. While prior studies have established various decellularization protocols, none have examined the effect of decellularized xenogenic tissue on immune activation in a human *in-vitro* model. We hypothesized that in spite of successful decellularization, an immune response would still be generated in response to an antigenic ECM.

To test this hypothesis, we performed *in-vitro* incubation of NBP with human whole blood and compared the amount of cytokine production to that elicited by DBP incubated with human whole blood. We also performed immunofluorescent staining for the alpha-gal epitope on NBP, after decellularization (DBP) and after recellularization (RBP). We observed a robust TNF- $\alpha$  cytokine production after 1-day of incubation, with no significant difference in the amount of cytokine produced to the decellularized tissue ( $1565 \pm 258$  pg/mL v.  $1092 \pm 298$  pg/mL, NBP v. DBP,  $p=0.26$ ) (**Figure 6.5A**). Production of TNF- $\alpha$  tapers off after 3-days ( $648 \pm 81.3$  pg/mL v.  $361 \pm 147$  pg/mL, NBP v. DBP,  $p=0.12$ ) (**Figure 6.5B**) and after 5-days ( $472 \pm 289$  pg/mL v.  $112.5 \pm 51.5$  pg/mL, NBP v. DBP,  $p=0.40$ ) (**Figure 6.5C**), with no significant difference in the amount of cytokine produced to decellularized tissue. Similarly, we observed a robust IL-1 $\beta$  cytokine production after 1-day of incubation, with no significant

difference in the amount of cytokine produced to the decellularized tissue ( $387 \pm 50.8$  pg/mL v.  $299 \pm 41.7$  pg/mL, NBP v. DBP,  $p=0.20$ ) (**Figure 6.5D**). Production of IL-1b remained sustained after 3-days ( $332 \pm 53.5$  pg/mL v.  $261 \pm 53.6$  pg/mL, NBP v. DBP,  $p=0.36$ ) (**Figure 6.5E**) and after 5-days ( $331 \pm 60.1$  pg/mL v.  $260 \pm 63.4$  pg/mL, NBP v. DBP,  $p=0.43$ ) (**Figure 6.5F**), with no significant difference in the amount of cytokine produced to decellularized tissue. The raw data for figure 6.5 has been tabulated in table 6.7 for TNF-a cytokine production, and table 6.8 for IL-1b cytokine production.

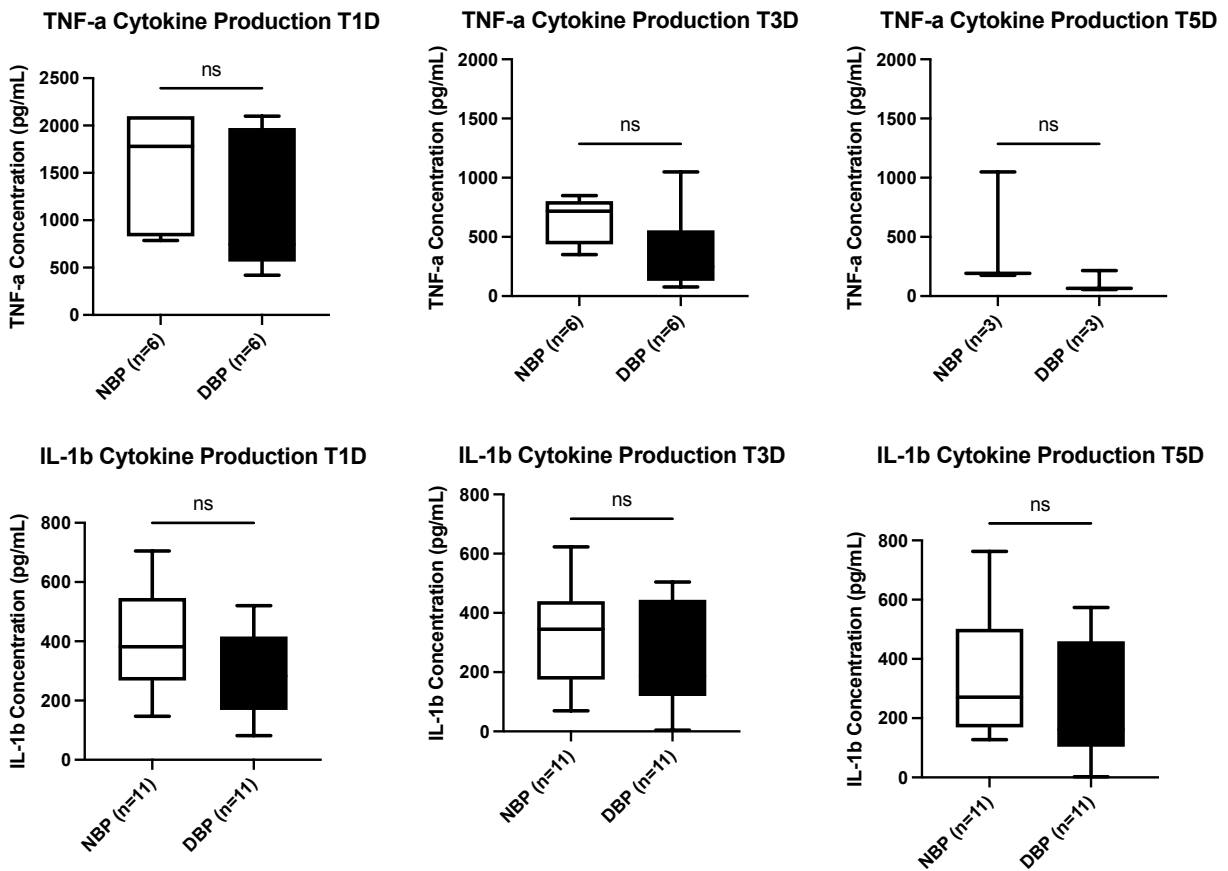


**Figure 6.5.** Decellularization alone does not significantly reduce initial pro-inflammatory cytokine production. Initial TNF-a cytokine production tapers off after 3 and 5-days of exposure to NBP and DBP, with significantly less production in the DBP group at 3-days. Initial IL-1b cytokine production is sustained and remains robust through 5-days, with no significant difference between NBP and DBP.

TNF-a Raw Data at T1D		TNF-a Raw Data at T3D		TNF-a Raw Data at T5D	
NBP (n=6)	DBP (n=6)	NBP (n=6)	DBP (n=6)	NBP (n=3)	DBP (n=3)
1462.8	647	656.5	145.9	192.1	56.3
843.3	420.2	849.2	78.1	1049.2	215.4
787.3	610.5	778.5	391.9	175.7	65.9
2098.4	843.3	787.3	149.6		
2098.4	1932	351.1	1049.2		
2098.4	2098.4	465.5	351.1		

**Table 6.7.** Raw data for TNF-a presented as concentrations in pg/mL for each sample at T1D, T3D and T5

IL-1b Raw Data at T1D		IL-1b Raw Data at T3D		IL-1b Raw Data at T5D	
NBP (n=11)	DBP (n=11)	NBP (n=11)	DBP (n=11)	NBP (n=11)	DBP (n=11)
440.2725	520.385	230.0415	186.7155	189.1305	114.4505
267.3415	283.4315	69.736	161.9415	209.1375	2.046
288.196	282.4555	299.692	444.3455	168.672	513.156
179.1365	250.5335	105.403	387.345	139.4965	14.8075
342.5795	168.265	439.8195	119.79	401.7975	161.7835
705.08	292.0925	555.13	4.046	763.27	573.552
546.18	416.475	433.76	472.125	501.795	430.655
146.8025	81.952	174.723	68.004	127.376	103.645
552.355	478.02	623.09	504.27	510.075	459.87
381.565	368.6155	344.945	369.57	270.755	359.82
401.58	142.843	372.93	147.999	354.885	121.0915

**Table 6.8.** Raw data for IL-1b presented as concentrations in pg/mL for each sample at T1D, T3D and T5D.

We hypothesized the residual immunogenicity seen in the DBP group is likely secondary to exposure of antigenic epitopes, namely alpha-gal. The alpha-gal epitope can be present on the ECM and not necessarily removed after decellularization [35, 48]. To test our hypothesis, we performed immunofluorescent staining to test for the presence or absence of the alpha-gal epitope. Immunofluorescent staining demonstrated the presence of the alpha-gal epitope on the NBP (**Figure 6.6A**) and that it remained present following decellularization (**Figure 6.6B**). In a cross-section after recellularization, there is reduced alpha-gal staining along the recellularized surface of the tissue (**Figure 6.6C**), suggesting the MSCs used are masking this epitope from antibody binding.

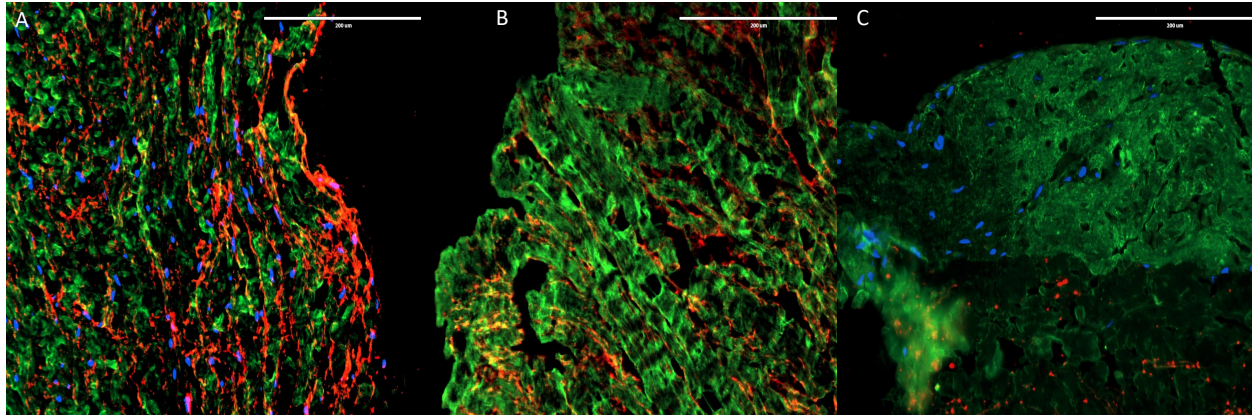


**Figure 6.6.** Immunofluorescent staining assessing presence of the alpha-gal epitope (red) on the NBP (A), DBP (B) and RBP (C). *Blue- DAPI nuclear stain; green- collagen, red- alpha-gal.*

Taken together, these data suggest that while decellularization is able to successfully remove all cellular material, the xenogenic ECM remains antigenic, resulting in sustained pro-inflammatory cytokine production. This antigenicity is likely in part related to residual alpha-gal epitope expression, and this expression may be partly masked by recellularization.

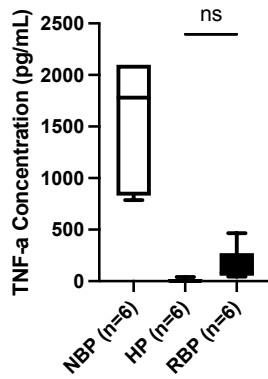
### **Autologous human MSC recellularization reduces initial cytokine production equivalent to that elicited by autologous human pericardium**

Recellularization of decellularized allogenic and xenogenic valve constructs to create a tissue engineered heart valve (TEHV) has been performed experimentally in both animal models and clinically in humans [82-85, 92, 94, 95, 200]. The most prominent cell type used for recellularization has been the MSC [201]. It has been proposed that MSCs mediate their immunomodulatory effects by interacting with cells from both innate and adaptive immunity, leading to skewing the immune response toward an anti-inflammatory phenotype, in part mediated by inhibition of TNF- $\alpha$  and IL-1 $\beta$  production [202, 203]. A core principle in immunology is that “self does not recognize self”, meaning that autologous tissue should not stimulate any meaningful immune activation. Therefore, we hypothesized that autologous MSC

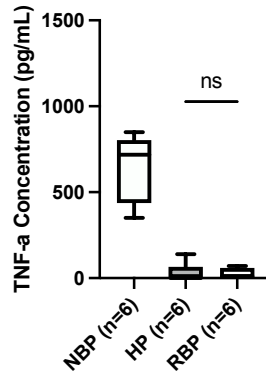
recellularization of bovine pericardium would result in attenuation of initial immune activation, with equivalent immune activation compared to that produced by autologous human pericardium.

To test this hypothesis, we performed *in-vitro* incubation of human pericardium (HP) incubated with autologous human whole blood and compared the amount of cytokine production to that elicited autologous human MSC recellularized bovine pericardium (RBP) incubated with autologous human whole blood. Cytokine production elicited by NBP was used as a reference for robustly stimulated cytokine production (**Figure 6.7**). We observed no significant difference in TNF- $\alpha$  cytokine production after 1-day of incubation between HP and RBP ( $8.35 \pm 6.65$  pg/mL v.  $157.1 \pm 66.3$  pg/mL, HP v. RBP,  $p=0.07$ ) (**Figure 6.7A**). Similarly, no significant difference in TNF- $\alpha$  cytokine production after 3-days of incubation ( $36.1 \pm 27.1$  pg/mL v.  $24.3 \pm 12.7$  pg/mL, HP v. RBP,  $p=0.83$ ) (**Figure 6.7B**) or after 5-days of incubation ( $3.14 \pm 1.95$  pg/mL v.  $13.6 \pm 8.63$  pg/mL, HP v. RBP,  $p=0.26$ ) (**Figure 6.7C**) between HP and RBP. When examining for IL-1 $\beta$  cytokine production, we also observed no significant difference after 1-day of incubation ( $15.9 \pm 9.26$  pg/mL v.  $31.9 \pm 12.2$  pg/mL, HP v. RBP,  $p=0.37$ ) (**Figure 6.7D**). Further, no significant difference in IL-1 $\beta$  cytokine production after 3-days of incubation ( $18.8 \pm 7.65$  pg/mL v.  $34.2 \pm 14.6$  pg/mL, HP v. RBP,  $p=0.33$ ) (**Figure 6.7E**) or after 5-days of incubation ( $17.4 \pm 8.09$  pg/mL v.  $36.2 \pm 18.7$  pg/mL, HP v. RBP,  $p=0.30$ ) (**Figure 6.7F**). The raw data for figure 6.7 has been tabulated in table 6.9 for TNF- $\alpha$  cytokine production, and table 6.10 for IL-1 $\beta$  cytokine production.

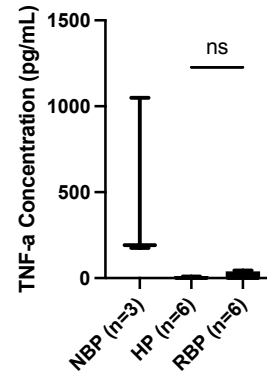
TNF-a Cytokine Production T1D



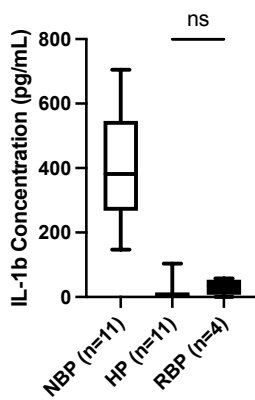
TNF-a Cytokine Production T3D



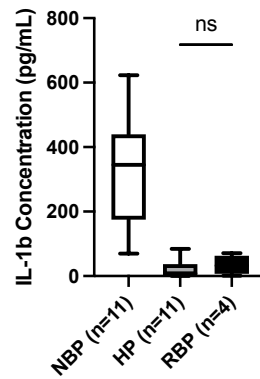
TNF-a Cytokine Production T5D



IL-1b Cytokine Production T1D



IL-1b Cytokine Production T3D



IL-1b Cytokine Production T5D

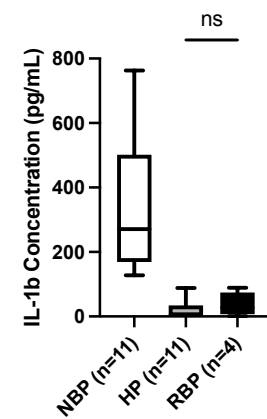


**Figure 6.7.** Autologous MSC recellularization (RBP) of native bovine pericardium reduces initial pro-inflammatory cytokine production equivalent to that generated by autologous human pericardium (HP). At 1, 3 and 5-days, there is no significant difference in TNF-a or IL-1b cytokine production between HP and RBP.

TNF-a Raw Data at T1D			TNF-a Raw Data at T3D			TNF-a Raw Data at T5D		
NBP (n=6)	HP (n=6)	RBP (n=6)	NBP (n=6)	HP (n=6)	RBP (n=6)	NBP (n=3)	HP (n=6)	RBP (n=6)
1462.8	0.0	67.9	656.5	0.0	0.0	192.1	0.0	0.0
843.3	0.0	100.3	849.2	0.0	55.3	1049.2	0.0	44.4
787.3	40.7	44.0	778.5	40.7	0.0	175.7	8.9	0.0
2098.4	0.0	56.3	787.3	139.6	0.0		6.8	0.0
2098.4	0.0	208.5	351.1	0.0	20.1		0.0	0.0
2098.4	9.4	465.5	465.5	0.0	70.1		0.0	37.0

**Table 6.9.** Raw data for TNF-a presented as concentrations in pg/mL for each sample at T1D, T3D and T5D.

IL-1b Raw Data at T1D			IL-1b Raw Data at T3D			IL-1b Raw Data at T5D		
NBP (n=11)	HP (n=11)	RBP (n=4)	NBP (n=11)	HP (n=11)	RBP (n=4)	NBP (n=11)	HP (n=11)	RBP (n=4)
440.2725	0.0460	43.1630	230.0415	0.9860	25.9012	189.1305	0.0	25.7845
267.3415	0.0	26.5455	69.736	6.7415	38.9560	209.1375	0.0	29.3870
288.196	1.5930	57.3500	299.692	0.0990	70.9080	168.672	1.3790	88.8900
179.1365	0.2675	0.4910	105.403	14.7585	0.8335	139.4965	11.0915	0.7455
342.5795	14.0865		439.8195	11.3450		401.7975	35.6600	
705.08	9.5840		555.13	5.5880		763.27	10.7275	
546.18	8.0640		433.76	8.5220		501.795	5.9180	
146.8025	0.0		174.723	0.0		127.376	0.0	
552.355	32.2		623.09	37.2755		510.075	34.3605	
381.565	4.85		344.945	36.9845		270.755	4.4130	
401.58	103.785		372.93	84.0200		354.885	88.2580	

**Table 6.10.** Raw data for IL-1b presented as concentrations in pg/mL for each sample at T1D, T3D and T5D.

Taken together, these data suggest that RBP does not stimulate any significant pro-inflammatory cytokine production, and is equivalent to autologous HP. The attenuation of immune activation observed in the RBP group is likely a result of the recellularized tissue not being recognized by the recipient immune system, suggesting the foreign bovine pericardium is being successfully masked from immune recognition.

## Discussion

We investigate whether autologous MSC recellularization of bovine pericardium can attenuate initial immune activation equivalent to autologous human pericardium in a human *in-*

*vitro* model. Additionally, we studied whether our decellularization and recellularization procedures preserve the ECM. Our results demonstrated that bovine pericardium is acutely immunogenic, stimulating an immune response similar to stimulation with PMA and ionomycin. Next, we confirmed that bovine pericardium can be decellularized and recellularized successfully without damaging the ECM. Finally, we determined that decellularization alone does not significantly reduce initial pro-inflammatory cytokine production, with residual alpha-gal epitope present, while recellularization with autologous MSCs reduces initial pro-inflammatory cytokine production equivalent to autologous levels. These data highlight the acute immunomodulatory effects of autologous MSC recellularized tissue on the recipient immune response, thus preventing recipient immune recognition of XTHVs and potentially leading to a reduction in SVD incidence.

We have previously observed that development of SVD is associated with immune cellular infiltrate correlated to the induction of a pro-inflammatory cytokine gradient around the XHTV, representing chronic immune rejection [194]. We and others have hypothesized that the onset of such chronic immune rejection begins acutely, with rapid induction of pro-inflammatory cytokine production in response to activation by the foreign, xenogenic tissue [38]. To test this hypothesis, we performed *in-vitro* stimulation of human whole blood with PMA/ionomycin and compared the amount of cytokine production to that elicited by only bovine pericardium. Our results confirm that bovine pericardium stimulates a robust *in-vitro* immune response, equivalent to known immune activators, PMA and ionomycin. Additionally, these data support the use of our human *in-vitro* model to further study the immunomodulatory effects of autologous MSC recellularization.

Since XTHVs develop SVD chronically, and bovine pericardium elicits a robust immune response acutely, we wanted to examine if modification of the bovine pericardium by decellularization alone would result in a reduction in initial pro-inflammatory cytokine production. Although previous studies have established various decellularization protocols, none have examined the effect of decellularized xenogenic tissue on human immune activation [94-97, 100, 113, 199, 204]. Li et al examined several decellularization protocols and suggested that decellularization resulted in a biocompatible scaffold, however, the investigators used a subcutaneous implantation method in rats hindering translation to humans [199]. Several other studies have investigated the use of discordant XTHV implantation utilizing a variety of animal models, but focusing on overall valve dynamics, with a limited assessment of the impact on recipient immune activation [94, 95, 97, 113].

Importantly, we found that even after decellularization, significant amounts of alpha-gal epitope were detected on the xenogenic tissue. This finding supports the notion that decellularized xenogenic scaffolds are inherently immunogenic and explains why we observed significant amounts of pro-inflammatory cytokine production in response to this tissue. In fact, a large immunoproteomic study of bovine pericardium identified 31 structural and functional matrix protein antigens, including alpha-gal [56]. The identification of the alpha-gal epitope on the ECM serves to reinforce the concept that absence of cellularity does not imply absence of antigenicity. This has been further highlighted by the catastrophic clinical failures of implanting a decellularized XTHV in pediatric patients, with a 75% early mortality, secondary to an acute and robust immune rejection of this tissue leading to rapid valvular degeneration [88]. Therefore, we sought to determine if autologous MSC recellularization of a decellularized XTHV would attenuate immune activation to levels equivalent to autologous tissue.

Our findings suggest that recellularizing a decellularized xenogenic matrix with autologous MSCs results in the same lack of pro-inflammatory cytokine production as that seen by autologous tissue. It has been well established that MSCs mediate their immunomodulatory effects by interacting with cells from both innate and adaptive immunity, leading to skewing the immune response towards an anti-inflammatory phenotype [202, 203]. These anti-inflammatory effects are in part mediated by inhibition of pro-inflammatory cytokine, TNF- $\alpha$  and IL-1 $\beta$ , secretion [202, 203]. Both of these cytokines are pro-inflammatory, generated very rapidly by activated macrophages in the initial phase of immune activation [38]. The generation of both TNF- $\alpha$  and IL-1 $\beta$  has also been established to occur *in vitro* by primary CD4<sup>+</sup> T-cells in response to an allogenic stimulant [203]. Importantly, the reduction of these cytokines occurs when co-cultured with MSCs, accompanied by a reduction in lymphocyte proliferation, is one of the potential mechanisms of MSC immunomodulation in this study [202]. In this study, we chose to use whole blood rather than specific isolated T- or B-cell populations. The rationale for this is two-fold. First, whole blood provides a more physiologic, translatable medium that better replicates the environment that the tissue types examined would encounter *in vivo*. Second, whole blood contains a variety of immune effectors, including polymorphonuclear cells, lymphocytes, circulating antibodies and complement proteins. Further study should isolate each of these components of the immune system to determine their individual contribution to the immune response generated in this study.

The reduction in immune activation seen in the recellularized tissue may be attributed to a combination of factors. First, as outlined above, MSCs possess inherent immunomodulatory capabilities that may be dampening the recipient immune response. Second, the mechanical effect of ‘masking’ the antigenic ECM may also be preventing the recipient immune system from

recognizing this tissue. Future study is necessary to elucidate the exact mechanisms of MSC immunomodulation. With regards to the first possible mechanism, namely the immunomodulation of the host immune response, our study does not provide any direct evidence that this is occurring. Future studies should investigate the effect of MSCs on immune cell proliferation, potentially by use of a proliferation assay. The measurement of anti-inflammatory cytokines (IL-4, IL-10) which can be released by MSCs may also provide some insight into the specific immunomodulatory mechanisms exerted by MSCs in this model. With regards to the second possible mechanism, namely the ‘masking’ of the antigenic ECM, our study does provide a little evidence this may be occurring. We observed that there was reduced alpha-gal antibody binding on the recellularized tissue. It is unlikely that the MSC itself is blocking the alpha-gal antibody from binding to its epitope, since there are no known examples of this occurring in the literature. Rather, it is possible that the MSC may be degrading the alpha-gal epitope directly or stimulating surrounding cells to degrade it [205]. One possible study that may help in distinguishing between these two possible mechanisms is the use of a transwell assay. Culturing the MSCs in this way will determine if the immunomodulatory effects seen are the result of soluble factors, or if there are specific cell-cell interactions occurring.

To date, an incredible amount of work has been done in conceptualizing and creating TEHVs [198]. These TEHVs are made with a variety of techniques, including decellularized xenografts, decellularized allografts, synthetic recellularized scaffolds, and xenogenic recellularized scaffolds [82-85, 92, 94, 95, 200]. Recellularization of these various scaffolds has been hypothesized to provide an immunoprivileged tissue; one that does not generate an immune response. The current study provides evidence that autologous MSC recellularization does in fact

attenuate generation of an acute immune response, without adversely affecting the biochemical composition of the ECM scaffold.

### **Study Limitations**

The tissue collected for isolation of MSCs and whole blood in this study all came from 14 healthy adults undergoing elective cardiac surgery, thus a small sample size may hinder the ability to interpret our results. The aim of this study was to demonstrate a reduction in acute immune activation with an endpoint of 5-days. Therefore, we cannot make any inference as to what long-term effects may be generated by autologous MSC recellularized tissue. The use of TNF- $\alpha$  and IL-1 $\beta$  as surrogate markers of immune activation also limits the interpretation of the results of this study. Alternative markers could include a more robust panel of pro-inflammatory cytokines and the use of a proliferation assay to assess specific immune cell responses to the antigenic stimulus. Cell viability was also not directly measured in this study; however, we did provide a control group of whole blood alone to account for any passive cytokine release from non-viable cells. Finally, we cannot definitively determine the exact mechanism by which the MSCs are exerting their immunomodulatory effects, only that such immunomodulation is occurring. Further studies are needed to define the long-term effects of this process, both *in-vitro* and *in-vivo*, and to elucidate the mechanism of immunomodulation by the autologous MSCs.

### **Conclusion**

Our results suggest that attenuation of immune activation in response to an autologous MSC recellularized bovine pericardium is likely a result of the recellularized tissue not being recognized by the recipient immune system, suggesting the foreign bovine pericardium is being successfully masked from immune recognition. Importantly, we have demonstrated it is possible to perform both decellularization and recellularization without incurring any significant

biochemical damage to the ECM scaffold. Preventing this initial immune activation with autologous MSC recellularization may be an effective approach to decrease the recipient immune response, thus preventing recipient immune recognition of XTHVs and potentially leading to a reduction in SVD incidence. These conclusions are largely speculative, given the nature of the limitations discussed in this study. Further work to establish mechanistically how this protected effect on cytokine release is occurring is needed.

**Chapter 7. Recellularization of Xenograft Heart Valves Reduces the  
Xenoreactive Immune Response in an *in vivo* Rat Model**

## Abstract

**Objectives:** Our aim was to address the role of autologous mesenchymal stem cell (MSC) recellularization of xenogenic valves on the activation of the xenoreactive immune response in an *in-vivo* rat model.

**Methods:** Explanted aortic valve constructs from female Hartley guinea pigs were procured and decellularized, followed by recellularization with syngeneic Sprague-Dawley rat MSCs. The recellularized aortic valve xenografts were then implanted into the infrarenal aorta of recipient female Sprague-Dawley rats. Grafts were implanted as either syngeneic grafts, non-decellularized (fresh), decellularized and recellularized xenografts. Rats were euthanized after 7- and 21-days, exsanguinated and the grafts explanted. Explanted grafts were analyzed using standard immunohistochemical staining techniques. Total serum immunoglobulin was quantified and histological analysis performed to assess the immune response.

**Results:** Overall survival to endpoint was lower in the decellularized xenograft group (67%; 4/6), compared to fresh (100%; 6/6) and recellularized grafts (100%; 6/6). Similarly grafts in the decellularized group were more likely to have completely thrombosed (50%; 2/4), compared to fresh (33%; 2/6) and recellularized grafts (0%; 0/6). Decellularized guinea pig xenografts, when implanted into rats *in-vivo*, result in equivalent total serum immunoglobulin production and equivalent graft cellular infiltrate when compared to fresh xenografts. Moreover, when decellularized guinea pig xenografts were recellularized with syngeneic rat MSCs there was a significant reduction in total serum immunoglobulin production and graft cellular infiltrate when compared to both fresh and decellularized xenografts. Importantly, recellularized guinea pig xenografts had significantly reduced total immunoglobulin production and graft cellular infiltrate when compared to syngeneic rat aortic valve controls.

Conclusions: Autologous MSC recellularization of xenogenic valves reduces the xenoreactive immune response in an *in-vivo* rat model and may be an effective approach to decrease the progression of xenograft valve dysfunction.

## Introduction

Valvular heart disease (VHD) is a common diagnosis with an approximate prevalence of 2.5% of the total population having moderate to severe VHD [184-188]. Xenograft tissue heart valves (XTHV) made from bovine pericardium are the most commonly implanted construct used for surgical valve replacements [165, 189-191]. The development of structural valve deterioration (SVD) of XTHVs is characterized by time-dependent onset, degeneration and/or hemodynamic dysfunction of the valve and in its most severe form requires reoperation [3]. Structural failure is strongly age dependent, making XTHVs suitable primarily for the elderly and less for children and young adults [192, 193]. Implantation of XTHVs is a form of xenotransplantation and is therefore subject to robust humoral and cellular immune system rejection, despite chemical crosslinking and anti-calcification treatments [194, 206]. Thus, we and others have hypothesized that the development of SVD is a result of a chronic, immune-mediated rejection to the foreign XTHV tissue [4-6, 33, 175, 194].

In an attempt to overcome the development of SVD, several modifications to XTHVs have been suggested, including decellularization and recellularization of these scaffolds [198]. Decellularized xenografts have demonstrated inconsistent outcomes in both animal and clinical studies, suffering from tissue degradation, calcification and limited cellular regeneration [88, 89, 207-212].

Subsequently, recellularization of decellularized xenografts has been proposed and investigated experimentally in both animal models and clinically in humans [82-85, 92, 94, 95, 200]. The use of syngeneic MSC to recellularize an acellular xenogenic scaffold is thought to skew the xenoreactive immune response towards an anti-inflammatory phenotype [202, 203]. Numerous experiments have been performed to examine XTHV transplantation in a rat model [29, 76, 213];

however, there is a paucity of data on what effect an autologous recellularized xenograft has on the immune response in the host.

The purpose of this study was to investigate the role of autologous MSC recellularization of xenogenic valves on the activation of the xenoreactive immune response in an *in-vivo* rat model. We hypothesized that recellularization of decellularized guinea pig aortic valve constructs with syngeneic rat MSCs would result in attenuation of immune activation, with equivalent graft cellular infiltrate and immunoglobulin production compared to that produced by syngeneic rat aortic valve constructs.

## **Methods**

### **Experimental Animals**

Inbred female Hartley guinea pigs (age 2-weeks) and Sprague-Dawley rats (weight, 275-300 grams) were purchased from Charles River (Quebec) and housed in the institutional animal care facility with food and water ad libitum for 1 week before experimentation in accordance with the guidelines of the Canadian Council of Animal Care.

### **Surgical Technique**

Aortic valve constructs were implanted into recipient animals according to a previously established infrarenal implantation model [29, 213] (**Figure 1**). Aortic valve constructs were removed from donor guinea pigs with a cuff of ventricular muscle and approximately 5mm of ascending aorta. The coronary arteries were suture ligated with 10-0 nylon suture. The aortic valve constructs were subsequently transplanted into the infrarenal abdominal aorta of recipient rats by using end-to-end anastomoses (10-0 nylon, Mani) during general anesthesia with isoflurane.

Grafts were implanted as either xenogenic (non-decellularized guinea pig-to-rat), decellularized guinea pig-to-rat, or recellularized guinea pig grafts with syngeneic rat MSCs (n=6-12/time/group). Implantation of syngeneic rat aortic valves (rat-to-rat) was used as a control for surgical inflammation (n=6-8/time). Xenogenic and syngeneic grafts were harvested from donor animals and implanted without delay into recipient animals. Decellularized and recellularized grafts were treated as described below before implantation.

The recipient animals were euthanized 7 and 21-days after transplantation for graft harvest. The aortic valve construct was dissected free and immersed in 10% formalin for histology and immunology. At the time of euthanization, rats were systemically heparinized with injection of 500U of heparin directly in the IVC, exsanguinated, and blood collected in 15mL tubes. The blood was then centrifuged for 10 min at 1200x g, the supernatant collected and frozen at -80°C until needed.

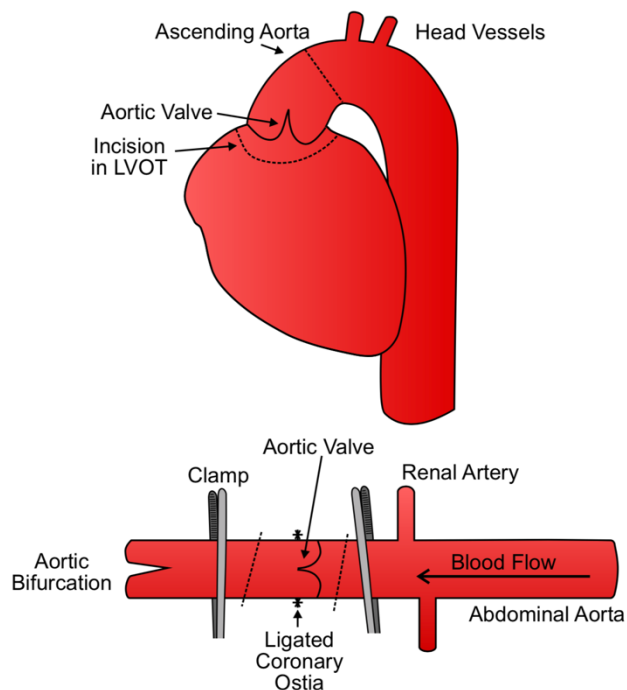


**Figure 7.1.** Schematic of aortic valve graft harvest and infrarenal implantation model.

## **MSC Isolation and Culturing**

Cadaveric syngeneic Sprague-Dawley rats were used to collect femoral bone marrow and subsequently isolate MSCs, as described previously [214]. The femoral bone marrow collected was directly plated onto T25 plastic cell culture flasks (Thermo Fisher Scientific, Massachusetts, USA). The cells were incubated at 37°C with 5% CO<sub>2</sub> in RPMI 1640 (Thermo Fisher Scientific, Massachusetts, USA) culture media completed with 10% fetal bovine serum, 0.2% ascorbic acid, and 0.2% primocin in order to only culture plastic adherent MSCs. The cells were washed with PBS and the media changed at 1 day after initial plating. The media was then changed every 3 days afterward and monitored regularly until the flask had reached 80% confluence. A small sample of isolated and cultured MSCs were utilized to confirm surface phenotyping. MSC phenotype was confirmed by staining negatively for CD34 on post-recellularization immunohistochemistry by the methods described below.

## **Decellularization and Recellularization**

Aortic valve constructs were harvested from donor animals and first washed with 25mL of phosphate-buffered saline (PBS) and then washed with 1% sodium dodecyl sulfate (SDS) (Bio-Rad Laboratories, California, USA) while oscillating at 40rpm at room temperature. The SDS was changed every hour for 4 changes in total. The fourth addition of SDS was left for 20 hours. The next day the SDS was removed and 25mL of Triton-X 100 (Thermo Fisher Scientific, Massachusetts, USA) was added while oscillating at 40rpm at room temperature. After 1 hour the Triton-X 100 was removed and replaced. This was repeated for a total of 4 changes, and after the last change was left for 20 hours. The next morning the Triton-X 100 was removed, and the tissue was rinsed with PBS and double distilled water (DDH<sub>2</sub>O) until bubbles no longer formed. The tissue was then washed with 1% sodium chloride for 1 hour while oscillating at 40rpm at

room temperature. The sodium chloride was removed, the tissue was again rinsed with PBS and DDH<sub>2</sub>O. After rinsing 25ml of DNAase and MgCl<sub>2</sub> was added and the tissue oscillated at 40rpm at 37°C. After aspirating, the tissues were rinsed twice with DDH<sub>2</sub>O, and 25ml of 1% PBS penicillin-streptomycin mixture was added, the tissue was left oscillating at 40rpm at 37°C for 30 minutes. Once decellularization was complete the tissue was stored in 1% Hank's balanced salt solution with primocin (InvivoGen, California, USA) in a 4°C fridge until use.

Recellularization began by incubating a decellularized guinea pig aortic valve construct in 10mL of RPMI 1640 culture media on a rotator at 37°C for 24h. The next day, approximately 1 million MSCs isolated as described above would be resuspended in 4mL of RPMI 1640 culture media. The tissue was then placed into the media in a 5mL centrifuge tube (MTC Bio, New Jersey, USA), including MSCs and was placed on a rotator at 37°C for 12h. The recellularized tissue was then implanted without delay into recipient animals.

Confirmation of successful decellularization and recellularization was completed by 4',6-diamidino-2-phenylindole (DAPI) staining. Tissue samples at each stage of processing including native, decellularized, and recellularized samples were stained with DAPI in order to identify the presence of original cells, the absence of those cells after decellularization, and presence of cells after recellularization. Further, quantitative biochemical analysis was also performed to determine the impact of the decellularization and recellularization process. DNA was quantified to confirm the decellularization process removed all genetic material and the recellularization process restored it. DNA was quantified as outline below.

Materials needed:

DNA digestion buffer (350uL/sample)

proteinase K stock (12uL/sample)

5M NaCl (67.5uL/sample)

100% isopropanol

70% EtOH

TE Buffer

Cut and weigh all tissues aiming for 20-30mg.

Add 350uL DNA digestion buffer, 12uL proteinase K (stock 20mg/mL stored in yellow box in -80, use directly from tubes) in a 1.5mL tube. Incubate at 56c overnight.

Chill samples on ice for 5 minutes. Add 67.5uL cold saturated 5M NaCl to salt out protein. mix by inversion and leave on ice for 5 minutes.

Spin at 14,000rpm at 4c for 10min.

Remove supernatant without disturbing pellet using a 200uL pipette and put in a new clean 1.5mL Eppendorf tube.

Add 150uL of cold isopropanol to the supernatant. gently invert the tube several times to precipitate out the DNA. Spin at 14,000rpm at 4c for 15min.

Remove supernatant and discard it keeping only the pellet.

Wash pellet by adding 250uL cold 70% EtOH. shake vigorously to dislodge pellet from bottom. spin at 14,000rpm at 4c for 15min.

Remove all supernatant and discard carefully with a pipette tip. Ensure all EtOH is gone but do not disturb the pellet. Dry for about 20 minutes, do not over dry.

Resuspend in 50uL TE buffer. take 1.5uL to nanodrop to run concentration.

Digestion Buffer-5mL 1M Tris pH 8.0

20mL 0.5M EDTA

2mL 5M NaCl

5mL 20% SDS

TE Buffer- 0.5mL Tris

100uL 0.5M EDTA

99.4mL ddH<sub>2</sub>O

Analyze using Nanodrop

Staining for overall morphology (hematoxylin and eosin) and mesenchymal cells (anti-vimentin) was performed by the methods described below.

### **Immunohistochemistry**

The implanted aortic valve construct was harvested for histology at the time of animal euthanasia at both endpoints of 7-days and 21-days. Samples were formalin fixed (10%), paraffin embedded (FFPE) and serially sectioned (5um) for histologic and immunohistochemical examination. Immunohistochemistry involved standard staining techniques with biotinylated secondary antibodies, a peroxidase avidin-biotin complex, and 3,3'-diaminobenzidine as the chromogen. Hematoxylin-eosin stains were prepared from the FFPE blocks using standard procedures for identification of granulocytes. Primary monoclonal antibodies for vimentin (P08671, R&D systems), CD34 (P28906, R&D systems) and T-cells (anti-CD3; clone 2GV6, Roche) were used.

### **Tissue Analysis**

Samples were examined with a light microscope, and images captured with an Aperio CS2 digital pathology slide scanner (Leica Biosystems). Cell density was obtained from sampling of the entire sample area from representative tissue cross-sections from each group. Cell counts were obtained from 5 high powered fields (HPFs), averaged per HPF, and the mean cell count per HPF recorded from each animal. All slides were quantified in a blinded fashion.

### **Rat IgG ELISAs**

Standard 96 well plates were used. The plates were coated with capture antibody (goat anti-rat IgG-Fc (A110-136A)) diluted to 1:100 in sodium bicarbonate solution. Each well was

coated with 100uL and left at room temperature for up to 24h. Each well was then washed with Tris Buffered Saline with Tween (TBST) 5 times then blocked with 200uL of blocking solution composed of TBS with 1% bovine serum albumin (BSA) at room temperature for 30 minutes. The wells were washed, and the samples added to the well in doublets for each sample. An IgG standard from Bethyl (Cat. No. E111-128) was used for this protocol with a concentration of 1000mg/mL. A serial dilution was performed until 6 standards were obtained. The 6 standards were added to the wells with the samples and all were incubated at room temperature for 1 hour. The wells were then washed and 100uL of HRP Conjugated Goat anti-Rat IgG-Fc Detection Antibody (A110-136P-27) was added to each of the well and was incubated for 1 hour at room temperature. The wells were then washed with TBST and 100uL of a 1 step TMB substrate (ThermoFisher Scientific, Cat. No. 34029) was then added to each well and incubated in the dark until color development approximately 10-15 minutes later. Once color has developed 100uL of 2N H<sub>2</sub>SO<sub>4</sub> was added to each well. The plate was then read at 450nm + 540nm for correction. The concentration of rat IgG in the samples was calculated from the standard curve.

### **Statistical Analysis**

Continuous data is expressed as mean  $\pm$  standard error of the mean. Two-sample t-testing was used to compare between groups when  $n > 5$ , while Wilcoxon test was used to compare between groups when  $n < 5$ . All tests were considered significant with a  $p < 0.05$ . All statistical analysis and figures were performed and generated using GraphPad Prism version 9.0.0.

## Results

### **Guinea pig aortic valve constructs can be successfully decellularized and recellularized with rat MSCs**

One method of developing an immunocompatible future heart valve construct necessitates modification of xenogenic scaffolds with decellularization followed by recellularization [198, 215]. Assessment of efficacy for both decellularization and recellularization is required to demonstrate successful removal of cellular material and subsequent restoration without gross structural damage to the tissue. We assessed our decellularization and recellularization procedures using immunofluorescence and histology.

Our decellularization and recellularization processes were assessed qualitatively using DAPI nuclear staining on non-decellularized guinea pig (NGP), decellularized guinea pig (DGP) and recellularized guinea pig (RGP) aortic valve constructs (**Figure 7.2A, 7.2B, and 7.2C**). As expected, the NGP contained a large number of cell nuclei (**Figure 7.2A**), which were completely eliminated after decellularization (**Figure 7.2B**). Following recellularization with rat MSCs, there was nearly equivalent nuclear material as the NGP (**Figure 7.2C**).

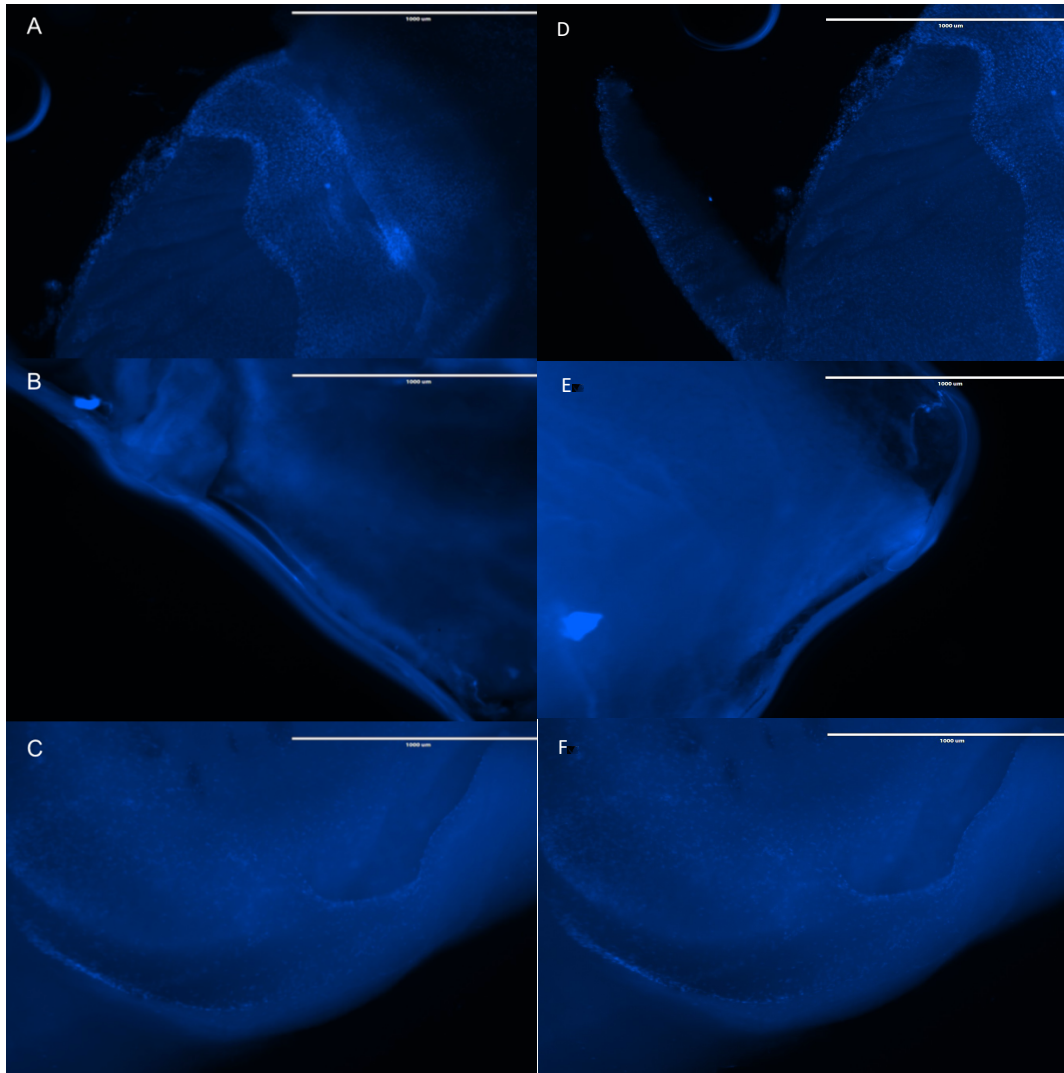


**Figure 7.2.** DAPI nuclear staining of two samples each of non-decellularized guinea pig (NGP, A&D), decellularized guinea pig (DGP, B&E) and recellularized guinea pig (RGP, C&F) aortic valve constructs.

Biochemical quantification of DNA in NGP, after decellularization (DGP), and after recellularization (RGP) was performed. DNA quantification confirms a significant reduction in genetic material following decellularization ( $25.6 \pm 4.5$  ng/uL v.  $5.6 \pm 0.8$  ng/uL, NGP v. DGP,  $p=0.002$ ), with a subsequent increase following recellularization ( $5.6 \pm 0.8$  ng/uL v.  $54.2 \pm 12.8$  ng/uL, DGP v. RGP,  $p=0.005$ ) to equivalent levels as NBP ( $25.6 \pm 4.5$  ng/uL v.

54.12±12.8 ng/uL, NGP v. RGP, p=0.07). These results are summarized in **Figure 7.3**. The raw tabulated data is presented in table 7.1.

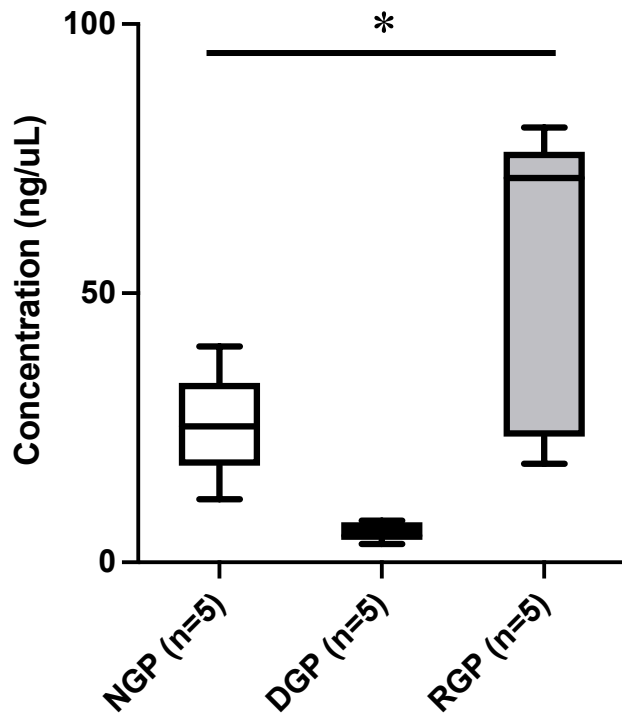


**Figure 7.3.** Biochemical quantification of DNA in NGP, after decellularization (DGP), and after recellularization (RGP).

DNA Raw Data		
NGP (n=5)	DGP (n=5)	RGP (n=5)
24.21	4.95	71.39
26.58	7.76	18.32
40.11	7.20	71.79
25.27	3.40	80.81
11.70	4.93	28.46

**Table 7.1.** Raw data for DNA presented as concentrations in ng/uL for each sample.

Gross histology was performed with H&E and vimentin staining. Syngeneic rat aortic valves are shown in **Figure 7.4A and B** confirming presence of cellular material and an intact ECM. Presence of cellular material and an intact ECM structure was observed in the NGP tissue prior to decellularization (**Figure 7.4C and D**). Following decellularization there is complete absence of cellular material, however the ECM structure is grossly preserved (**Figure 7.4E and F**). Recellularization with rat MSCs was performed and resulted in restoration of a confluent layer of MSCs lining the valvular tissue (**Figure 7.4G and H**). This layer of cells stained negatively for CD34, consistent with an MSC phenotype (**Supplementary Figure 7.1**) [201, 216]. A panel of higher magnification images for NGP, DGP and RGP tissue illustrating gross histology with H&E and vimentin staining is shown in **Supplementary Figure 7.2**.

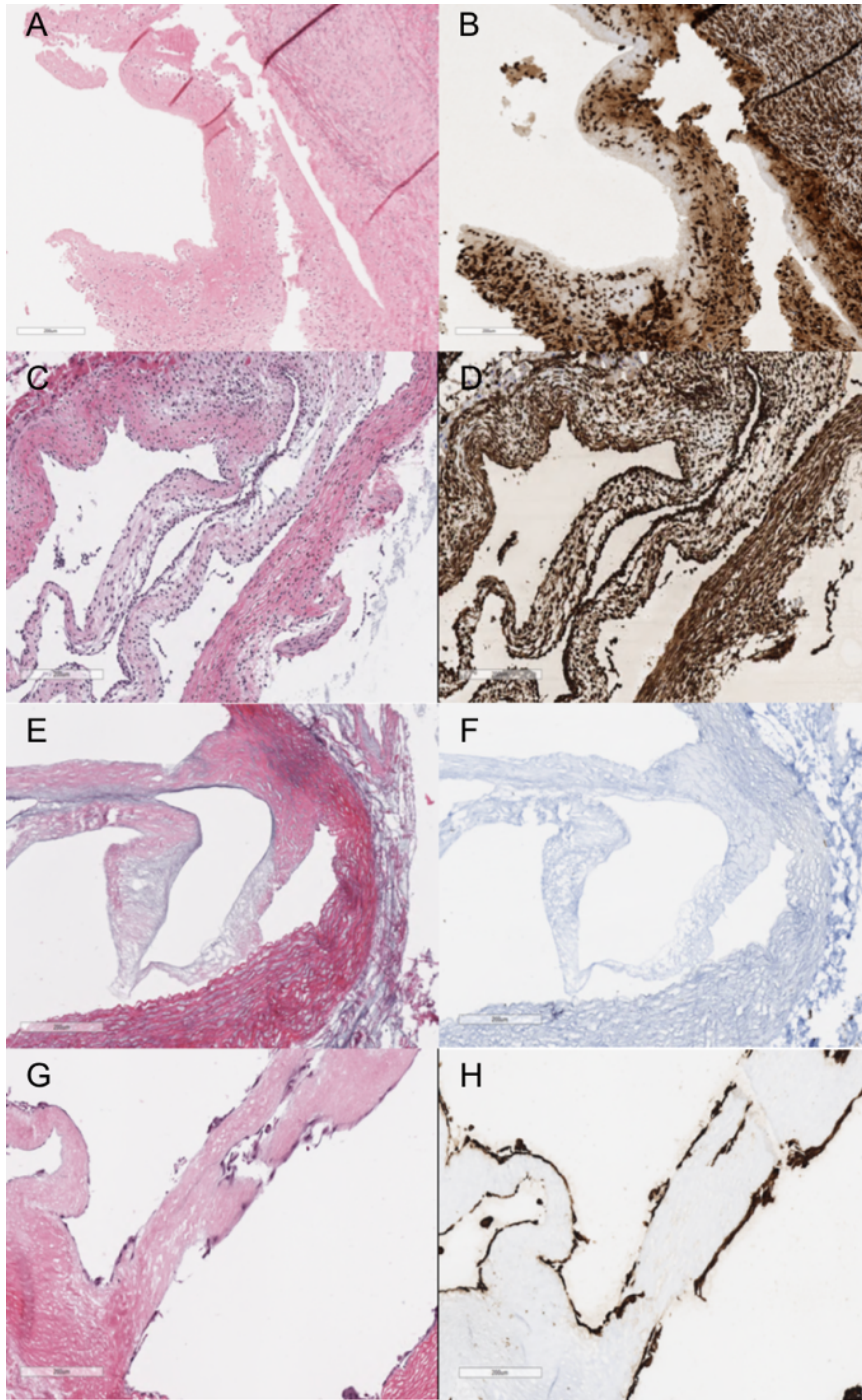
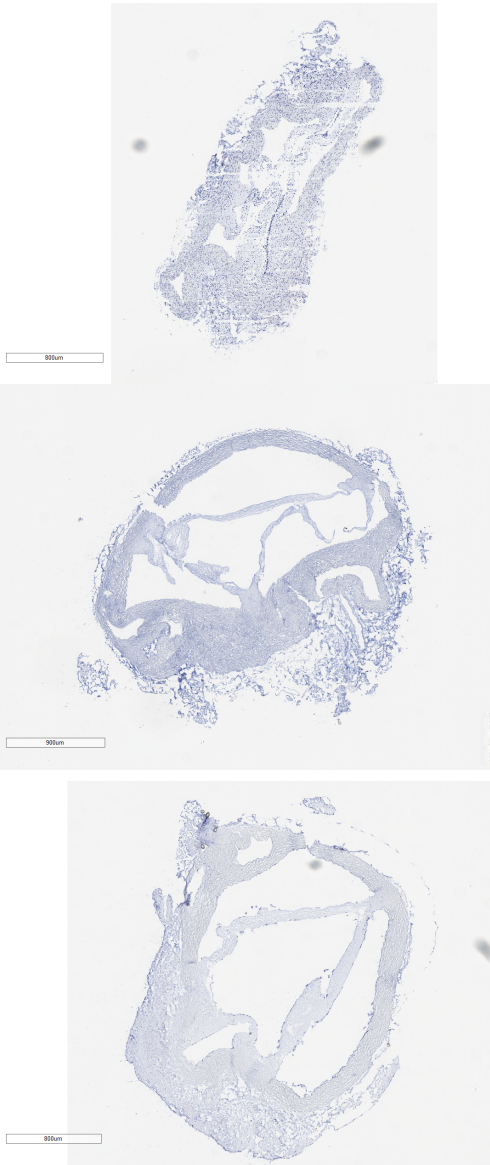
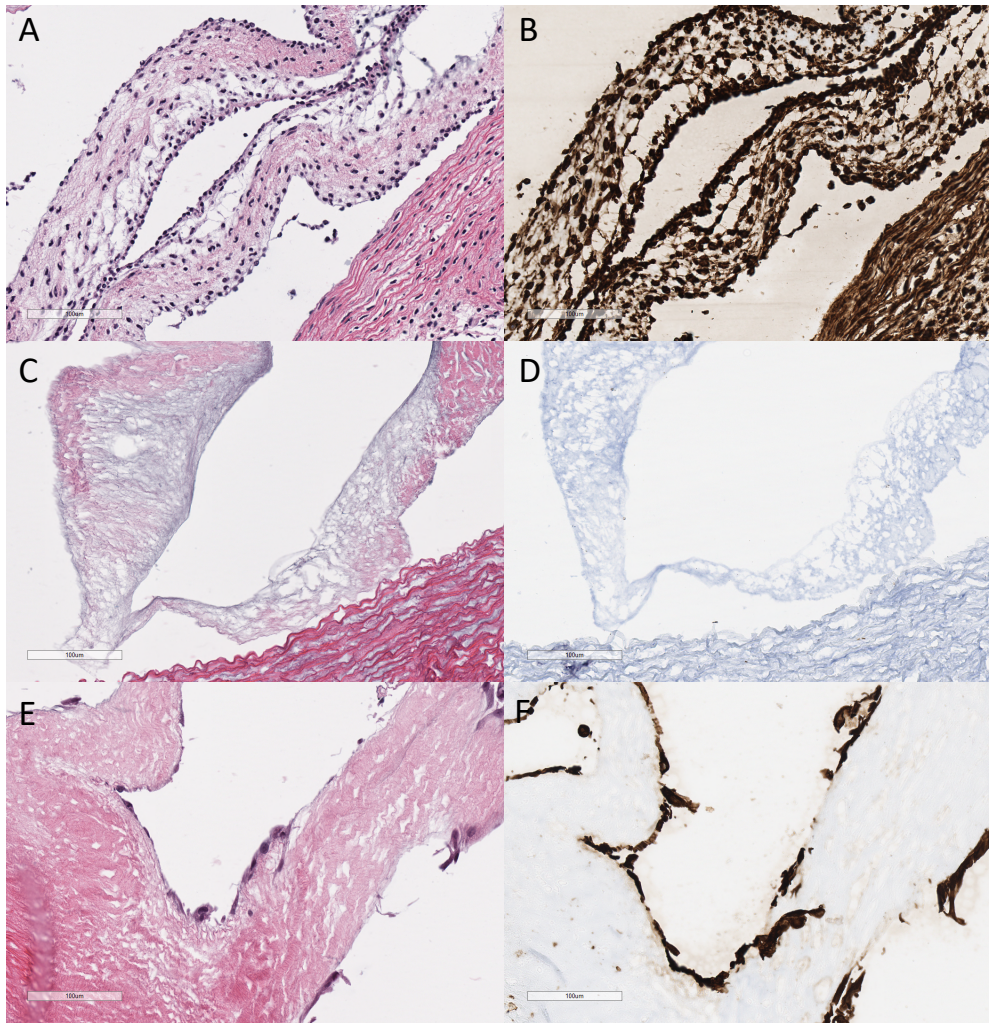


**Figure 7.4.** Gross histology was performed with H&E and vimentin staining. Syngeneic rat aortic valves are shown in A and B confirming presence of cellular material and an intact ECM. Presence of cellular material and an intact ECM structure was observed in the NGP tissue prior to decellularization (C and D). Following decellularization there is complete absence of cellular material, however the ECM structure is grossly preserved (E and F). Recellularization with rat MSCs was performed and resulted in restoration of a confluent layer of MSCs lining the valvular tissue (G and H).



**Supplementary Figure 7.1.** Gross histology demonstrating negative staining for CD34 of MSCs used in recellularization protocol.



**Supplementary Figure 7.2.** Gross histology was performed with H&E and vimentin staining. Presence of cellular material and an intact ECM structure was observed in the NGP tissue prior to decellularization (A and B). Following decellularization there is complete absence of cellular material, however the ECM structure is grossly preserved (C and D). Recellularization with rat MSCs was performed and resulted in restoration of a confluent layer of MSCs lining the valvular tissue (E and F).

Taken together, these data suggest complete decellularization is achievable without any gross structural damage to the ECM. Further, recellularization of the decellularized scaffold restores cellular material without adversely impacting the gross structure of the scaffold.

### **Recellularization of xenograft heart valves reduces the cellular immune response similar to syngeneic tissue**

To examine for the cellular immune response, the implanted aortic valve construct was harvested for histology at the time of animal euthanasia at the endpoints of 7-days and 21-days. **Figure 7.5A** summarizes the granulocyte cell infiltration observed in the explanted grafts at 7-days and 21-days. We observed a significant increase in granulocyte cell infiltration in the xenogenic grafts compared to the syngeneic grafts after 7-days ( $14.3 \pm 6.3$  cells/HPF v.  $2.1 \pm 0.6$  cells/HPF, xenogenic v. syngeneic,  $p=0.0008$ ). Further, we observed equivalent granulocyte cell infiltration in the xenogenic grafts compared to the decellularized grafts after 7-days ( $14.3 \pm 6.3$  cells/HPF v.  $7.9 \pm 4.8$  cells/HPF, xenogenic v. decellularized,  $p=0.08$ ). Finally, we observed equivalent granulocyte cell infiltration in the recellularized grafts compared to the syngeneic grafts after 7-days ( $2.4 \pm 0.8$  cells/HPF v.  $2.1 \pm 0.6$  cells/HPF, recellularized v. syngeneic,  $p=0.58$ ). After 21-days, similar trends were observed in the syngeneic ( $2.3 \pm 0.7$  cells/HPF) and recellularized ( $2.8 \pm 0.9$  cells/HPF) groups, while a trend towards lower absolute cell counts was observed in the xenogenic ( $6.4 \pm 2.1$  cells/HPF) and decellularized ( $3.9 \pm 1.7$  cells/HPF) groups. **Figure 7.5B** summarizes the CD3<sup>+</sup> T-cell infiltration observed in the explanted grafts at 7-days and 21-days. We observed a significant increase in CD3<sup>+</sup> T-cell infiltration in the xenogenic grafts compared to the syngeneic grafts after 7-days ( $3.9 \pm 1.7$  cells/HPF v.  $0.7 \pm 0.2$  cells/HPF, xenogenic v. syngeneic,  $p=0.001$ ). Further, we observed equivalent CD3<sup>+</sup> T-cell infiltration in the xenogenic grafts compared to the decellularized grafts after 7-days ( $3.9 \pm 1.7$  cells/HPF v.

2.7±1.6 cells/HPF, xenogenic v. decellularized, p=0.25). Finally, we observed equivalent CD3+ T-cell infiltration in the recellularized grafts compared to the syngeneic grafts after 7-days (0.6±0.2 cells/HPF v. 0.7±0.2 cells/HPF, recellularized v. syngeneic, p=0.50). After 21-days, similar trends were observed in the syngeneic (0.8±0.2 cells/HPF) and recellularized (0.7±0.2 cells/HPF) groups, while a trend towards lower absolute cell counts was observed in the xenogenic (2.8±1.2 cells/HPF) group and higher absolute cell counts in the decellularized (3.3±1.9 cells/HPF) group. The raw cell count data for **Figure 7.5** is displayed in table 7.2 for granulocytes and table 7.3 for T-cells. **Figure 7.6** illustrates representative gross histology for granulocytes with H&E staining and T-cells with anti-CD3 staining in syngeneic (**A** and **B**), NGP (**C** and **D**), DGP (**E** and **F**) and RGP (**G** and **H**) explanted tissues.

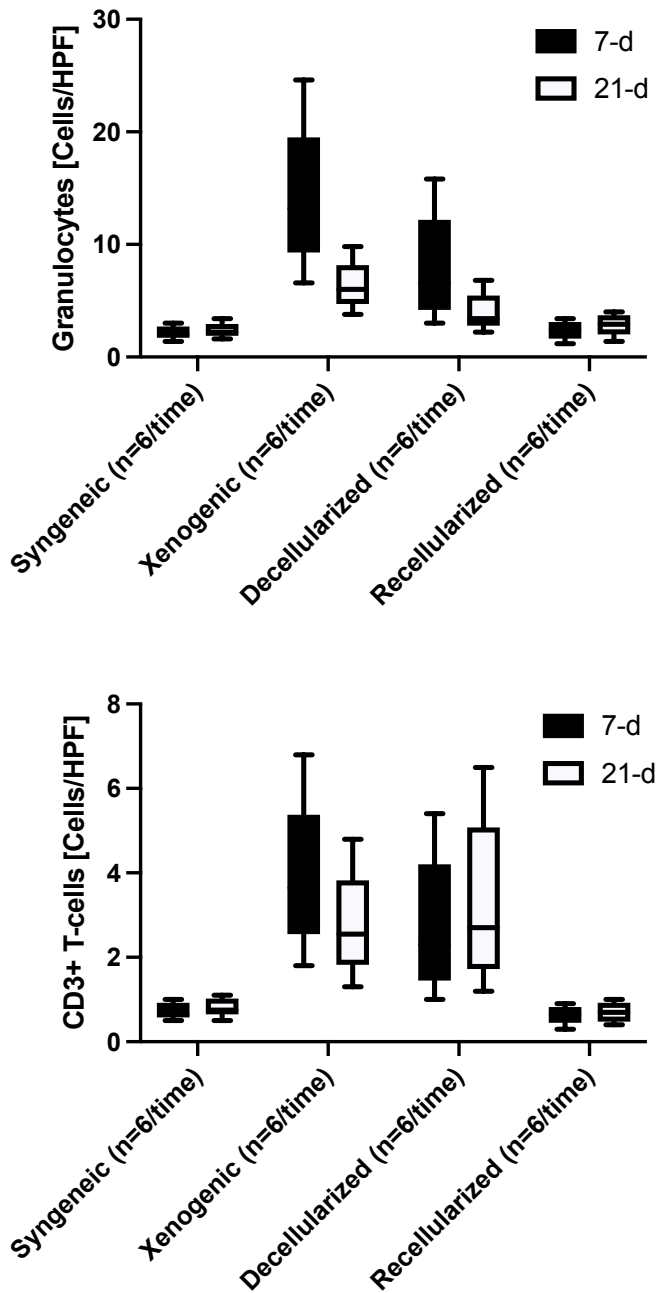


**Figure 7.5.** Panel A summarizes the granulocyte cell infiltration observed in the explanted grafts at 7-days and 21-days. Panel B summarizes the CD3+ T-cell infiltration observed in the explanted grafts at 7-days and 21-days

Granulocyte Infiltration at 7-days				Granulocyte Infiltration at 21-days			
Syngeneic (n=6)	Xenogenic (n=6)	Decel (n=6)	Recel (n=6)	Syngeneic (n=6)	Xenogenic (n=6)	Decel (n=6)	Recel (n=6)
2.6	10.2	5.4	3.4	2.8	5.0	3.0	4.0
1.8	6.6	3.0	2.6	2.0	3.8	2.2	3.2
1.4	13.4	7.8	3.0	1.6	6.0	3.8	3.6
1.8	17.8	11.0	1.8	2.0	7.6	5.0	2.2
2.2	24.6	15.8	1.2	2.4	9.8	6.8	1.4
3.0	13.0	4.6	2.2	3.4	6.0	3.0	2.6

**Table 7.2.** Raw granulocyte infiltration cell counts at 7-days and 21-days. Cell counts are presented as average per HPF for each sample examined.

T-cell Infiltration at 7-days				T-cell Infiltration at 21-days			
Syngeneic (n=6)	Xenogenic (n=6)	Decel (n=6)	Recel (n=6)	Syngeneic (n=6)	Xenogenic (n=6)	Decel (n=6)	Recel (n=6)
0.9	2.8	1.9	0.9	1.0	2.0	2.2	1.0
0.6	1.8	1.0	0.7	0.7	1.3	1.2	0.8
0.5	3.7	2.7	0.8	0.5	2.6	3.2	0.9
0.6	4.9	3.8	0.5	0.7	3.5	4.6	0.5
0.7	6.8	5.4	0.3	0.8	4.8	6.5	0.4
1.0	3.6	1.6	0.6	1.1	2.5	1.9	0.6

**Table 7.3.** Raw T-cell infiltration cell counts at 7-days and 21-days. Cell counts are presented as average per HPF for each sample examined.

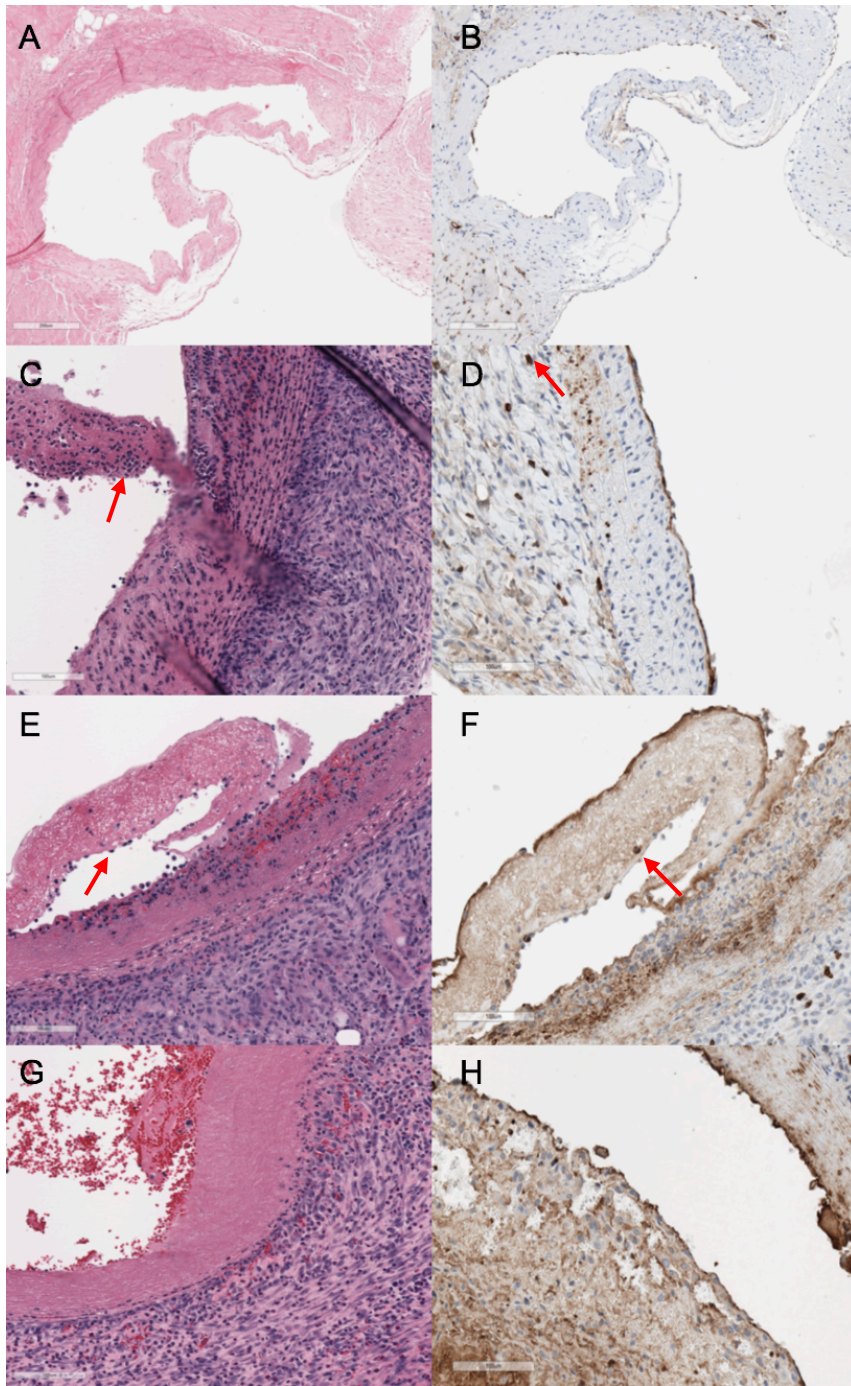


**Figure 7.6.** Representative gross histology for granulocytes with H&E staining and T-cells with anti-CD3 staining in syngeneic (A and B), NGP (C and D), DGP (E and F) and RGP (G and H) explanted tissues. Arrows highlight cells of interest, either granulocytes or T-cells.

Taken together, these data suggest that autologous MSC recellularization of xenograft heart valves reduces the cellular immune response to amounts similar to that produced in response to syngeneic tissue.

### **Recellularization of xenograft heart valves reduces the humoral immune response similar to syngeneic tissue**

To examine for the humoral immune response, the recipient rats were exsanguinated at the time of animal euthanasia at both endpoints of 7-days and 21-days and serum frozen for use in quantitative IgG ELISA analysis. **Figure 7.7A** summarizes the total serum immunoglobulin results observed after 7-days of implantation. We observed a significant increase in total serum immunoglobulin production in the xenogenic grafts compared to the syngeneic grafts after 7-days ( $111.1 \pm 15.7$  mg/mL v.  $52.7 \pm 5.6$  mg/mL, xenogenic v. syngeneic,  $p=0.006$ ). Further, we observed equivalent total serum immunoglobulin production in the xenogenic grafts compared to the decellularized grafts after 7-days ( $111.1 \pm 15.7$  mg/mL v.  $96.4 \pm 30.1$  mg/mL, xenogenic v. decellularized,  $p=0.65$ ). Finally, we observed equivalent total serum immunoglobulin production in the recellularized grafts compared to the syngeneic grafts after 7-days ( $40.8 \pm 7.6$  mg/mL v.  $52.7 \pm 5.6$  mg/mL, recellularized v. syngeneic,  $p=0.22$ ). **Figure 7.7B** summarizes the total serum immunoglobulin results observed after 21-days of implantation, revealing similar overall trends as seen after 7-days. We observed a significant increase in total serum immunoglobulin production in the xenogenic grafts compared to the syngeneic grafts after 21-days ( $89.3 \pm 3.8$  mg/mL v.  $71.6 \pm 4.8$  mg/mL, xenogenic v. syngeneic,  $p=0.008$ ). Further, we observed equivalent total serum immunoglobulin production in the xenogenic grafts compared to the decellularized grafts after 21-days ( $89.3 \pm 3.8$  mg/mL v.  $90.5 \pm 6.8$  mg/mL, xenogenic v. decellularized,  $p=0.86$ ). Finally, we observed reduced total serum immunoglobulin production in the recellularized grafts

compared to the syngeneic grafts after 21-days ( $29.5 \pm 15.0$  mg/mL v.  $71.6 \pm 4.8$  mg/mL, recellularized v. syngeneic,  $p=0.006$ ). The raw serum immunoglobulin concentrations are presented in table 7.4.

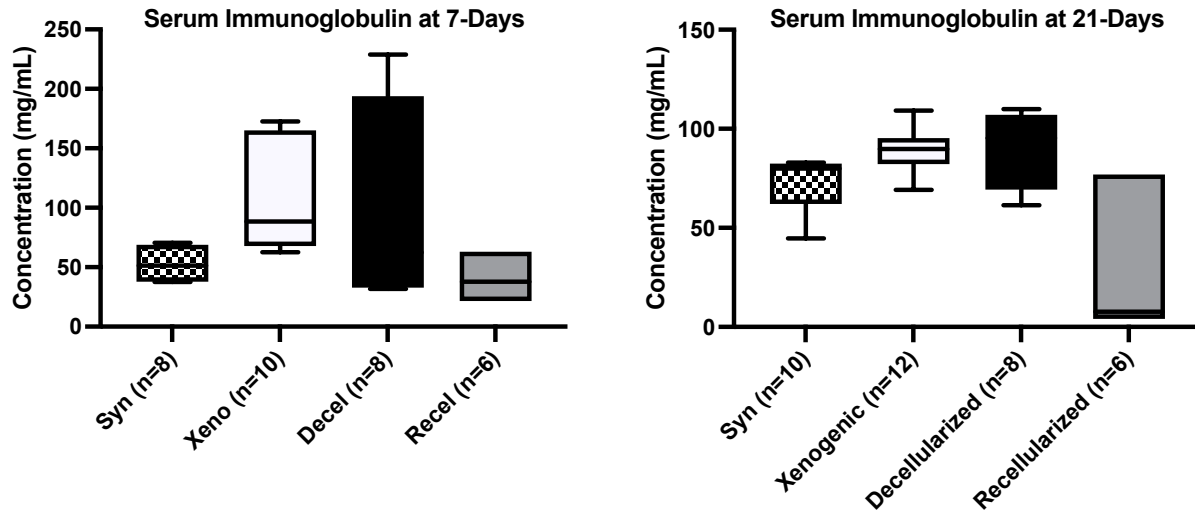


**Figure 7.7.** Panel A summarizes the total serum immunoglobulin results observed after 7-days of implantation. Panel B summarizes the total serum immunoglobulin results observed after 21-days of implantation, revealing similar overall trends as seen after 7-days.

Serum Immunoglobulin at 7-days				Serum Immunoglobulin at 21-days			
Syngeneic (n=8)	Xenogenic (n=10)	Decel (n=8)	Recel (n=6)	Syngeneic (n=10)	Xenogenic (n=12)	Decel (n=8)	Recel (n=6)
38.80	69.43	31.72	37.79	67.93	109.24	109.98	4.07
63.93	88.46	88.57	63.03	82.34	95.37	92.57	7.64
70.48	172.63	36.31	21.63	79.98	94.70	98.08	76.89
37.58	162.60	228.82	37.79	44.65	69.17	61.48	4.07
38.80	62.56	31.72	63.03	82.97	84.98	109.99	7.64
70.48	69.43	88.57	21.63	67.93	82.23	92.57	76.89
37.58	88.46	36.31		82.34	109.24	98.08	
	172.63	228.82		79.98	95.37	61.48	
	162.60			44.65	94.70		
	62.56			82.97	69.17		
					84.98		
					82.23		

**Table 7.4.** Raw serum immunoglobulin concentration at 7-days and 21-days. Concentrations are presented as mg/mL for each sample examined.

Taken together, these data suggest that autologous MSC recellularization of xenograft heart valves reduces the humoral immune response to amounts similar to that produced in response to syngeneic tissue.

### **Recellularization of xenograft heart valves improves graft patency and recipient survival compared to non-decellularized and decellularized xenograft**

In order to facilitate clinical translation of recellularized xenograft heart valves, assessment of graft patency and overall survival is required, thus we assessed these outcomes in our study. Several prior studies have established that vascular xenografts fail due to aneurysm formation and resulting thrombosis [217, 218]. Interestingly, increased rates of graft thrombosis and subsequent mortality have been observed in a similar rat *in-vivo* model [219]. Therefore, we hypothesized that recellularization of xenograft heart valves would lead to improved graft patency and animal survival at 21-days.

To test this hypothesis, we examined the explanted aortic valve construct at the time of animal euthanasia at 21-days for luminal patency (**Figure 7.8**). All animals survived to 7-days. Those animals that did not survive to 21-days were excluded. Overall survival to the 21-day endpoint was lower in the decellularized xenograft group (67%; 4/6), compared to non-decellularized (100%; 6/6) and recellularized grafts (100%; 6/6). Survival in the syngeneic group was similar to that observed in both the non-decellularized and recellularized groups (83%; 5/6). Similarly, grafts in the decellularized group were more likely to have completely thrombosed (50%; 2/4), compared to non-decellularized (33%; 2/6) and recellularized grafts (0%; 0/6). Thrombosis in the syngeneic group was similar to that observed in the recellularized group (0%; 0/5).

## Survival and Thrombosis of Implanted Graft at 21-days

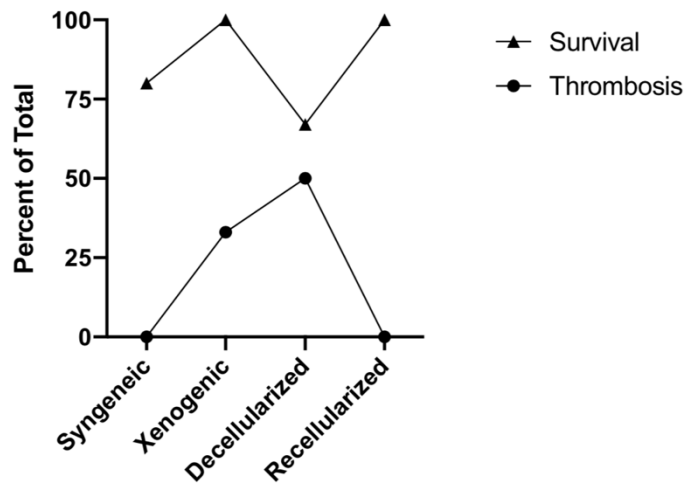


**Figure 7.8.** Overall survival and graft thrombosis at the 21-day endpoint.

Taken together, these data suggest a correlation between recellularization of xenograft heart valves with syngeneic MSCs and improved graft patency and improved recipient survival compared to non-decellularized and decellularized xenografts.

## Discussion

We investigate the role of autologous MSC recellularization of xenogenic valves on the activation of the xenoreactive immune response in an *in-vivo* rat model, hypothesizing that recellularization of decellularized guinea pig aortic valve constructs with syngeneic rat MSCs would result in attenuation of immune activation, with equivalent graft cellular infiltrate and immunoglobulin production compared to that produced by syngeneic rat aortic valve constructs. Our results demonstrated that guinea pig aortic valve constructs can be successfully decellularized and recellularized with rat MSCs. Next, we confirmed that recellularization of xenograft heart valves reduces the cellular and humoral immune response similar to syngeneic tissue, with a reduction in graft cellular infiltrate and total serum immunoglobulin production. Finally, we determined that recellularization of xenograft heart valves improves graft patency

and recipient survival compared to non-decellularized and decellularized xenograft. These data highlight the immunomodulatory effects of autologous MSC recellularized tissue on the recipient immune response, thus preventing recipient immune recognition of these aortic valve constructs.

Several prior studies have been performed using a similar aortic valve implantation rat model that have established its viability and usefulness in assessing the immune responses to transplanted tissues [29, 76, 213, 220]. Legare et al. performed allograft aortic valve implantation using an infrarenal aortic model, demonstrating that the allografts underwent T-cell mediated immune rejection leading to structural failure [213]. The onset of structural failure was rapid, beginning within 7-days, and progressively increasing over time. In another study by Meyer et al., decellularization of rat allograft aortic valves was performed followed by infrarenal aortic implantation [29]. The investigators found that allografts induced a significant increase in CD3+ T-cell infiltrate and a significant production of immunoglobulin. This robust immune response to the allografts was significantly reduced by decellularization. Building on this, Manji et al. analyzed the immune response to xenografts and decellularized xenografts using a guinea pig-to-rat aortic valve model [76]. The xenografts elicited a significant increase in immune cellular infiltrate and immunoglobulin production, compared to syngeneic valves, at 7 and 20-days and this immune response could be reduced with decellularization. These prior studies served to establish the feasibility of a xenograft transplant model with *in vivo* implantation in a rat and validate methods of assessing the immune responses to these tissues.

We sought to build on the previously performed experiments by performing autologous MSC recellularization of XTHVs and studying the impact on the immune response in the recipient animal. We focused on T-cell and granulocyte infiltration since these cells have been consistently demonstrated to correlate to development of valve structural failure [6, 194]. The

present analysis also focused on the humoral immune response, by quantifying total serum immunoglobulin production. Thus, the current study provides a more balanced assessment of the immune response to XTHVs than has been previously reported. Finally, in an attempt to provide more clinically translatable data, we measured overall survival rates and graft patency. The clinical utility of decellularized xenografts is limited, primarily due to severe immune rejection and thrombogenesis [29, 88, 207]. We have demonstrated that autologous MSC recellularization leads to not only a reduction in cellular and humoral immune response similar to syngeneic tissue, but also an improvement in graft patency. This is an important finding since it reinforces the concept that decellularized xenografts have limited clinical utility and that recellularization may provide an improvement on this strategy. The differences in survival observed in this study may be due to several factors not related to a direct effect of MSC recellularization. First, the sample sizes used were small and thus any differences should be interpreted with caution. Second, the surgical procedure itself carries a risk of mortality along with individual anatomic differences (presence of collateral arteries, size of rat, fat distribution, anesthetic time) that may result the differences in survival observed. Finally, one reason the decellularized xenografts had the highest mortality may be due to the fact that these grafts were mechanically compromised following the decellularization procedure, and not due to any inherent mortality risk from decellularized tissue itself.

Our findings suggest that recellularizing a decellularized xenogenic matrix with autologous MSCs results in the same lack of pro-inflammatory cytokine production as that seen by autologous tissue. It has been well established that MSCs mediate their immunomodulatory effects by interacting with cells from both innate and adaptive immunity, skewing the xenoreactive immune response towards an anti-inflammatory phenotype [202, 203]. The

reduction in immune activation seen in the recellularized tissue may be attributed to a combination of factors. First, as outlined above, MSCs possess inherent immunomodulatory capabilities that may be dampening the recipient immune response. Second, the mechanical effect of ‘masking’ the antigenic ECM may also be preventing the recipient immune system from recognizing this tissue. The mechanism of immune rejection in our model is likely a combination of hyperacute and acute rejection. This is a result of the fact that guinea pig to rat transplantation is considered discordant, meaning that pre-formed effectors are present in the serum of the recipient at the time of engraftment [219]. Our results support this notion with the development of significant immunoglobulin production within 7-days of implantation. Prior studies using animal models to assess the immune response to XTHVs have used concordant models, hindering the ability to apply these findings in humans where XTHV implantation is most commonly discordant [82-85, 92, 94, 95, 200].

### **Study Limitations**

The model used in this study is non-functional, meaning the transplanted aortic valve construct does not open and close with systole and diastole. This results in several limitations. First, thrombus formation in the sinus of Valsalva, but not within the entire graft lumen makes it possible that non-specific foreign-body inflammation may be occurring in our model in addition to a specifically generated immune response. However, the distribution of immune cellular infiltrate in a similar pattern to that seen in live cellular xenograft rejection coupled with the production of immunoglobulin supports a specific immune response. Second, the non-functional nature of our model limits the relevance of our model to clinical valve replacement. Our results should therefore be interpreted with caution and a functional model of xenograft valve replacement is necessary to allow for broader application of our findings. Since this valve model

is non-functional, and our endpoint was relatively short (7- and 21-days), we did not perform any *in vivo* functional imaging. We observed positive results in this study despite only having a small amount of MSC coverage on the surface of the recellularized xenograft. Optimization of the recellularization protocol is certainly an area of further investigation and one that can be improved based on the modest success observed in this study. Nonetheless, the incomplete coverage of the xenograft achieved here still resulted in the observation of a decrease in the amount of IgG production and a reduction in cell infiltration. This observation may hint towards the mechanism of MSC immunomodulation in this model. It is plausible that the MSCs are exerting some local, paracrine effects that independent of the amount of recellularization achieved. This finding warrants further investigation to determine the exact mechanisms and elucidate if they are dependent or independent of MSC adherence to the ECM. Another major limitation of this study is the lack of a glutaraldehyde fixed xenograft control. Since all xenograft prostheses implanted in humans are glutaraldehyde fixed, this limits the relevance of our study. We chose not to include a glutaraldehyde fixed xenograft control in the current study for several reasons. First, glutaraldehyde independently results in calcification of implanted tissues, thus this may have been an additional confounder when examining the immune response to xenograft tissue and the effect of autologous MSC recellularization. Thus, in order to account for this difference, a glutaraldehyde fixed control would be needed for all groups examined in this study, requiring a significantly increased number of animals. We felt that the examination of the effects of glutaraldehyde would be best examined by a dedicated study, rather than in combination with the novel investigation of the effects of MSC recellularization on the immune response. Finally, the effects of glutaraldehyde on MSCs are unknown, and again may have contributed to an additional confounding variable if included in the present study. Further studies are needed to

define the long-term effects of this process, both *in-vitro* and *in-vivo*, and to elucidate the mechanism of immunomodulation by the autologous MSCs.

## **Conclusion**

Our results suggest that attenuation of immune activation in response to an autologous MSC recellularized guinea pig aortic valve construct is likely a result of the recellularized tissue not being recognized by the recipient immune system, suggesting the foreign xenogenic aortic valve is being successfully masked from immune recognition. Preventing this initial immune activation with autologous MSC recellularization may be an effective approach to decrease the recipient immune response and improve graft patency, potentially leading to improved long-term durability.

**Chapter 8. Outcomes Following Bioprosthetic Valve Replacement in Prior  
Non-Cardiac Transplant Recipients**

*Clinical Transplantation*

2020

DOI: 10.1111/ctr.13720

## **Abstract**

We report on overall survival and valve-related outcomes after bioprosthetic valve replacement in prior transplant recipients. From January 2004 to December 2018, 20 consecutive patients (mean age 65.7-years, 90% male) with prior non-cardiac transplantation underwent bioprosthetic aortic (n=18) or combined aortic and mitral (n=2) valve replacement. Patients consisted of kidney (n=14), lung (n=2), liver (n=3) and bone-marrow (n=2) transplants with the most common indication for valve replacement being calcific degeneration (n=12). Outcomes were measured over a 12-year span, with a median follow-up duration of 3.9-years. Overall survival at 30-days was 100% and at median follow-up was 60%. Acute kidney injury occurred in 50% (n=10) with temporary dialysis required in 5% (n=1) and 15% (n=3) suffered respiratory failure. No patients experienced major bleeding, heart failure or sternal wound infection. No patients required redo valve replacement during the study period. Our results provide contemporary data demonstrating that patients with prior transplant can undergo bioprosthetic valve replacement with acceptable in-hospital mortality rates and long-term survival, with a low rate of major morbidity. Furthermore, bioprosthetic valve replacement is a viable option in this group of patients with no redo valve replacement and acceptable long-term hemodynamic valvular function.

## Introduction

Organ transplantation has become the gold standard in treatment for many end-stage pathologies. Furthermore, as long-term outcomes continue to improve due to changes in patient selection, surgical technique, immunosuppressive regimens, and a multitude of other clinical factors, the prevalence of transplant recipients within the general population continues to rise. In 2014, 1430 kidney transplants were performed in Canada, a significant increase of 29% compared to 2005, with >14,000 Canadians living with a kidney transplant[221]. As both longevity and prevalence continue to increase, so does the number of patients living with a transplanted organ who may develop cardiovascular pathology, specifically valvular disease.

Valvular heart disease (VHD) continues to affect millions of people worldwide, having a significant impact on survival and quality of life[10, 11]. The two most common valve replacement constructs in use are mechanical and bioprosthetic. Mechanical valves are more durable than bioprosthetic valves but require life-long anticoagulation contributing to the risk of bleeding and thromboembolic events[222]. Consequently, bioprosthetic valves are used in >80% of all aortic valve replacements[223]. Unfortunately, bioprosthetic valves tend to degenerate over time, termed structural valve deterioration (SVD). Long-term studies have demonstrated time-dependent increase in rates of SVD, with younger age at implant as a significant predictor of future development of SVD[224, 225]. Determining the cause of SVD, and subsequent therapeutic targets to mitigate its development, has proven to be a significant challenge. Several studies have hypothesized that SVD is a chronic, immune-mediated rejection process against the foreign xenogenic-derived bioprosthetic valve[6, 7, 213, 226]. This hypothesis was further strengthened when it was identified that calcific degeneration of bioprosthetic valves was decreased by concomitant steroid use, possibly related to its immunosuppressive effects[227].

A clear paucity of data exists regarding outcomes after bioprosthetic valve replacement in transplant recipients and we do not have reliable survival and complication profiles in patients undergoing bioprosthetic valve replacement who have had previous transplantation. Furthermore, patients with prior transplantation represent another population that require long-term immunosuppression. Whether this has any effect on the durability of bioprosthetic valves in this population is also unknown. Therefore, the purpose of the current study is to report on overall survival and valve-related outcomes after bioprosthetic valve replacement in prior transplant recipients.

## **Methods**

### **Data Source**

The Alberta Provincial Project for Outcome Assessment in Coronary Heart Disease (APPROACH) database, in addition to linkage to the discharge abstract database and other administrative ambulatory databases to detect events after discharged and at other hospitals, were used to obtain all data. The APPROACH database is a prospective data collection initiative that acquires detailed clinical information on all patients undergoing coronary angiography in Alberta, Canada.

### **Study Cohort**

Included in this study were patients with previous non-cardiac transplantation undergoing bioprosthetic aortic or combined aortic and mitral valve replacement surgery from January 1, 2004 to December 31, 2018 at the Mazankowski Alberta Heart Institute in Edmonton, Alberta, Canada. Patients undergoing emergency surgery, having a diagnosis of infective endocarditis and mechanical valve replacements were excluded from this cohort. Outcomes were measured over a 12-year period, with a median follow-up duration of 3.9-years.

## **Outcomes**

The primary outcome of this study was overall survival at 30-days and at median follow-up. Secondary outcomes include serious adverse events and valve-related events. Serious adverse events included in-hospital complications of acute kidney injury, dialysis, bleeding, heart failure, insertion of permanent pacemaker, ventricular fibrillation, respiratory failure, sternal wound infection, sepsis and intensive care unit and hospital length-of-stay. Acute kidney injury was defined according to the KDIGO definition of a rise in serum creatinine greater than 50% baseline within 7-days post-operatively. Major bleeding was defined as either mediastinal bleeding requiring a return to the operating room, or gastrointestinal bleeding requiring blood transfusion. Respiratory failure was defined as requiring reintubation, tracheostomy or inability to discontinue ventilatory support within 6-days of the index operation. Valve-related outcomes included average peak and mean gradient, incidence of prosthetic valve endocarditis, redo valve replacement and valve-related mortality. Comprehensive transthoracic echocardiograms (TTE) were performed in all patients at a median follow-up of 1.4-years. The transprosthetic gradients were calculated by using the modified Bernoulli equation. All outcomes were collected during admission for the index valve replacement procedure and after discharge, being identified based on admitting diagnosis for any readmission.

## **Statistical Analysis**

Continuous variables are expressed as mean  $\pm$  SD or as median (interquartile range) as appropriate. Categorical variables are expressed as frequency (percent). The cumulative survival curve was calculated on the basis of Kaplan-Meier method. The median follow-up time was estimated by Reverse Kaplan-Meier method. The long-term outcomes were evaluated at

the longest available follow-up. Statistical analysis was performed using the SPSS software version 24 (SPSS, Chicago, Illinois).

## **Results**

### **Study Population**

The study sample included 20 consecutive patients with prior non-cardiac transplantation who underwent bioprosthetic aortic (n=18) or combined aortic and mitral (n=2) valve replacement between January 1, 2004 and December 31, 2018. Baseline demographic data are summarized in Table 8.1. The mean age at time of implant was 65.7-years and majority of patients were male (90%). The most common indication for valve replacement was calcific degeneration in 60% (n=12). The mean time from transplantation to valve surgery was 12 years. 45% of patients were on chronic steroid therapy (n=9). Transplantation type included kidney (n=14), lung (n=2), liver (n=3), and bone-marrow (n=2). The majority of patients had left ventricular ejection fraction >50% pre-operatively (n=12). Operative characteristics of our cohort are summarized in Table 2. 85% of patients underwent full sternotomy (n=17) while 15% underwent hemi-sternotomy (n=3). There were no cases of transcatheter surgical approach in our patient cohort. Concomitant coronary artery bypass grafting (CABG) occurred in 55% (n=11), valve repair in 5% (n=1) and ascending aortic replacement in 5% (n=1). Valve implant type was composed of a variety of constructs, including stented in 75% (n=15), stentless in 10% (n=2) and sutureless valves in 15% (n=3). Blood product was administered in 5% of cases (n=1).

<b>Variables</b>	<b>Transplant recipients N=20</b>
<b>Baseline Characteristics</b>	
Age (Mean ± SD)	65.7 ± 9.8
Female	2(10%)
DM	7(35%)
CKD	11(55%)
Baseline Serum Creatinine	177 mmol/L
AFib	3(15%)
COPD	7(35%)
CVD	2(10%)
Chronic Steroid Therapy	9 (45%)
Time from Transplant (Mean ± SD)	12 years ± 9.31
<b>Valve Replaced</b>	
Aortic	18(90%)
Aortic + Mitral	2(10%)
<b>Initial Indication for Valve Replacement</b>	
Degenerative	3(15%)
Calcific Degeneration	12(60%)
Congenital	1 (5%)
Unspecified	3(15%)
<b>Transplanted organ</b>	
Kidney transplant	14 (70%)
Lung transplant	2 (10%)
Liver transplant*	3 (15%)
Bone marrow transplant	2 (10%)
<b>EF</b>	
<35%	1(5%)
35-50%	5(25%)
>50%	12(60%)
Not available	2(10%)

**Table 8.1.** Pre-Operative Characteristics

\*One patient with both kidney and liver transplantation

AFib: atrial fibrillation; CKD: chronic kidney disease; COPD: chronic obstructive pulmonary disease; CVD: cerebrovascular disease; DM: diabetes mellitus

<b>Variables</b>	<b>Transplant recipients N=20</b>
<b>Aortic cross clamp time (min.)</b>	95.7 ± 44.3
<b>Cardiopulmonary bypass time (min.)</b>	133.2 ± 64.3
<b>Blood product administration</b>	1 (5%)
<b>Surgical Approach</b>	
<b>Full sternotomy</b>	17 (85%)
<b>Mini sternotomy</b>	3 (15%)
<b>Transcatheter approach</b>	0
<b>Associated procedures</b>	
<b>CABG</b>	11(55%)
<b>Valve repair</b>	1(5%)
<b>Ascending aortic replacement</b>	1(5%)
<b>Implant device</b>	
<b>CE Perimount Magna Ease Pericardial Aortic-ThermaFix</b>	3(15%)
<b>CE Perimount Pericardial Aortic</b>	1(5%)
<b>CE/EL Peri-mount/cardial</b>	3(15%)
<b>CE/EL Pericardial Magna</b>	4(20%)
<b>Medtronic Freestyle-Root</b>	1(5%)
<b>SJM Trifecta</b>	3(15%)
<b>Sorin Group Freedom Solo Stentless Pericardial Valve</b>	1(5%)
<b>Sorin Group Mitroflow Aortic Pericardial Heart Valve</b>	1(5%)
<b>Sorin Group Perceval S</b>	3(15%)

**Table 8.2.** Intraoperative characteristics

### **Primary and Secondary Outcomes**

Overall survival at 30-days in our study cohort was 100%. At median follow-up for survival of 3.88-years, mortality was 40% (n=8) (Figure 1). Clinical outcomes are summarized in Table 3. Overall, acute kidney injury occurred in 50% (n=10), including 6 kidney transplant recipients, with temporary dialysis required in 5% (n=1). No patients experienced major bleeding, heart failure or sternal wound infection. One patient required insertion of a permanent pacemaker and 15% (n=3) suffered respiratory failure. Median ICU length-of-stay was 2.9-days (IQR 4.5) and median hospital length-of-stay was 17.6-days (IQR 26.0). At median follow-up,

the average peak gradient for aortic valves was 23.1-mmHg and the average mean gradient was 11.5-mmHg. Similarly, the average peak gradient for mitral valves was 18.0-mmHg and the average mean gradient was 6.5-mmHg. One patient developed prosthetic valve endocarditis. No patients required redo valve replacement for SVD during the study period. Of the 8 patients that died, 1 was a valve-related death secondary to prolonged ICU stay and eventual multisystem organ failure. In the remaining 7 patients that died, 4 died of transplanted organ failure, 2 of sepsis and 1 of ischemic bowel. All 4 patients that died of transplant graft failure were kidney transplant recipients. This included 2 patients with graft failure secondary to diabetic nephropathy, delayed graft rejection and failed renal transplant after 10 years due to reflux nephropathy and chronic pyelonephritis. In all cases, after multidisciplinary discussions involving the treating physicians, family and the patient, further treatment was not pursued.

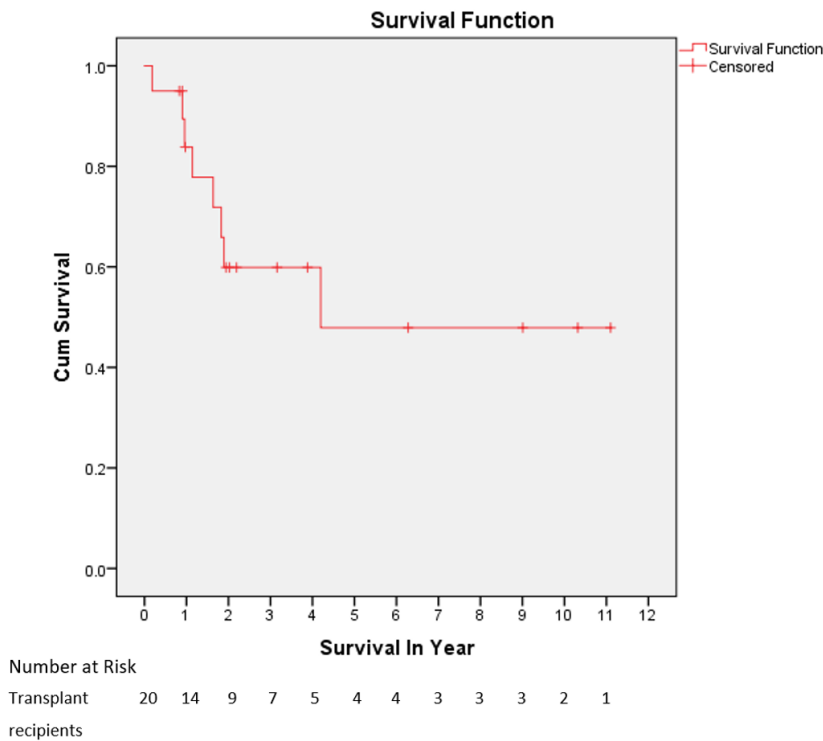


**Figure 8.1.** Kaplan-Meier curve for long-term survival

<b>Variables</b>	<b>Transplant recipients N=20</b>
<b>In-hospital complication</b>	
<b>AKI</b>	10 (50%)
<b>Dialysis</b>	1 (5%)
<b>Bleeding</b>	0
<b>Heart Failure</b>	0
<b>Insertion of Permanent Pacemaker</b>	1 (5%)
<b>Ventricular Fibrillation</b>	0
<b>Respiratory Failure</b>	3 (15%)
<b>Sternal Wound Infection</b>	0
<b>Sepsis</b>	1 (5%)
<b>ICU Length of Stay (days)</b>	
<b>Median (IQR)</b>	2.9 (4.5)
<b>Hospital Length of Stay (days)</b>	
<b>Median (IQR)</b>	17.6 (26.0)
<b>30-day Survival</b>	100% (n=20)
<b>2-year Survival</b>	66% (n=12)
<b>Valve-related Death</b>	1
<b>Valve-unrelated Death</b>	7

**Table 8.3.** Clinical outcomes

## **Discussion**

While previous studies have established outcomes after bioprosthetic valve replacement in several distinct patient populations[166], this paper aims to provide contemporary data on patients with prior transplantation. First, our results showed that while prior transplant recipients undergoing bioprosthetic valve replacement had 100% 30-day survival, 2-years survival of 60%, and close to 50% survival at long-term follow-up of 10-years. Second, our results showed that of all the deaths that occurred, only 1 was valve-related and the majority of patients are dying from transplant-related complications. Finally, our results showed that bioprosthetic valve function remained stable, with acceptable gradients and no patients required redo valve replacement for SVD during follow-up.

These results are consistent with those of the limited studies performed in the late 1990's examining outcomes after cardiac surgery in solid-organ transplant recipients[228, 229]. Mitruka

et al. reported on outcomes following cardiac operations in 64 prior solid-organ transplant recipients and found 30-day mortality of 3% and overall survival at 2-years of 86%[228]. Their cohort of patients included 24 patients undergoing valve replacement and they did not specifically analyze valve-related outcomes or valve function in follow-up. Similarly, Dresler et al. have reported their outcomes following open heart operations after renal transplant[229]. They reported on a total of 45 patients (31 undergoing coronary artery bypass grafting and 14 undergoing valve replacement) and found significant 30-day mortality of 8.8%. The main limitation continues to be the lack of contemporary data and analysis of valve-specific outcomes.

In the current study, we included both solid-organ (kidney, liver, lung) and bone-marrow transplant recipients to include all patients that received immunosuppressive therapy. We found an improved 30-day mortality of 0%, compared to the previous reports, which may reflect improvements in peri-operative and post-operative care over the last 20-years. Despite the low 30-day mortality, 2-year survival was reduced to 60%, in contrast to prior reports suggesting survival as high as 86%[228]. Despite that, survival approached 50% at long-term follow-up of 10-years. Our cohort of patients were significantly older at the time of valve replacement, with a mean age nearly 10-years older than prior reports. Furthermore, in our cohort, over half of patients had concomitant procedures and 30% (n=6) had a left ventricular ejection fraction <50%. These factors likely had a detrimental impact on midterm survival, however, represent a “real world” cohort of patients encountered by clinicians.

In our study, we included only patients that underwent a bioprosthetic valve replacement, in isolation or concomitantly. Deciding between a mechanical or bioprosthetic valve is challenging in this complex cohort of patients, where the balance between adding complexity with anticoagulation needs to be weighed against the risk of bioprosthetic valve dysfunction

secondary to SVD. We observed no redo valve replacement over midterm median follow-up of 1.9-years and 1 valve-related death 3-months post-operatively secondary to multisystem organ failure. Rates of redo valve replacement in large series of all-comers have been reported as high as 0.36%/patient-year[176]. Our data suggest that the rate of redo valve replacement, secondary to SVD, may be lower in transplant recipients undergoing immunosuppressive therapy. This result should be interpreted as hypothesis generating, however, given the small sample size and midterm follow-up.

The role of transcatheter aortic valve replacement (TAVR) and transcatheter mitral intervention continues to grow. In our cohort of patients, 85% (n=17) underwent a full sternotomy and 15% (n=3) underwent a hemi-sternotomy while no patients underwent TAVR or transcatheter mitral intervention. There are several reasons why this occurred in our patient cohort. Firstly, we have had limited accessibility to TAVR at our institution early in our registry, leading to all of our patients undergoing surgical AVR. Furthermore, over half of our patient cohort underwent a concomitant procedure such as coronary artery bypass grafting or multiple valve interventions. TAVR and transcatheter mitral interventions are excellent alternative choices to sternotomy, especially in patients who may present higher surgical risk such as transplant recipients.

### **Study Limitations**

This study is not without limitations. We performed a single-centre retrospective review of prospectively collected data. Weaknesses include the modest cohort size of 20 patients. These moderate numbers can be attributed to the select population of patients that have received prior transplantation, develop valvular heart disease and require valve replacement. Also contributing to the small cohort size is the fact that transplant patients are selected to have minimal valve

issues, so they are able to withstand a major operation. Therefore, any valve dysfunction must develop after transplantation. We included patients who received valve replacement between 2004 and 2018, however, median follow-up was limited to 3.9-years due to patient mortality, and the 13 out of 20 valve replacement surgeries occurring after 2014. The results of this study should be considered hypothesis-generating given the relatively short median follow-up time, however, still holds value given the rarity of a transplant recipient undergoing valve replacement and the decreased life expectancy in this complex patient population.

## **Conclusion**

In conclusion, transplant recipients represent a growing cohort of complex patients that clinicians will encounter, with an increasing number surviving post-transplant long enough to develop valvular dysfunction. Our results provide contemporary data demonstrating that patients with prior transplant can undergo bioprosthetic valve replacement with acceptable in-hospital mortality rates and long-term survival, without incurring major morbidity. Furthermore, bioprosthetic valve replacement is a viable option in this group of patients with no redo valve replacement and acceptable hemodynamic valvular function at midterm follow-up. While immunosuppressive therapy may have had an impact on the excellent bioprosthetic valve longevity demonstrated, further studies with a larger cohort of patients and longer follow-up is warranted to investigate this relationship further.

## Chapter 9: Thesis Summary

The clinical impact of valve replacement procedures using bioprosthetic xenogenic tissue heart valves (XTHVs) for the treatment of valvular heart disease (VHD) is limited by the development of subsequent structural failure of the prosthetic valve. Determining the cause of this structural failure and evaluating potential mitigating strategies is paramount to facilitate improved clinical outcomes for patients suffering from VHD that require valve replacement with a XTHV.

The purpose of this thesis was to explore the hypothesis that xenograft heart valve deterioration and subsequent prosthesis failure is due to a chronic, xenoreactive immune response. We further sought to explore the hypothesis that this xenoreactive immune response can be attenuated with creation of an autologous recellularized matrix or by administration of immunomodulatory medication, leading to improved valvular durability. To evaluate our hypotheses, we developed three main objectives: to establish the role of immunity in xenograft heart valve deterioration, to attenuate the immune response with autologous recellularized tissue, and to attenuate the immune response with immunomodulatory therapeutics.

This thesis established that xenograft heart valve deterioration is the result of chronic, immune-mediated rejection of this tissue. It is clear that these XTHVs elicit a robust immune response, characterized by infiltration of innate and adaptive immune cells, leading to the development of structural valve deterioration (SVD) and subsequent redo valve replacement. The data presented further demonstrates that the immune cell infiltrate is actively transcribing pro-inflammatory and chemotactic genes. This observation provides additional evidence supporting the notion that XTHVs are immunogenic and this immunogenicity is linked to eventual structural failure. Finally, the data presented suggest that SVD of XTHVs is correlated to the recruitment

of immune cellular infiltrate to the valve and a possible mechanism of this recruitment is the production and maintenance of a chemokine gradient. Further studies are needed to establish the mechanism of initiation of SVD, elucidate the interplay between the immune cells implicated in this analysis and determine if the gene transcripts identified are viable therapeutic targets.

This thesis also demonstrated the ability of autologous recellularization of acellular xenogenic matrices to attenuate the immune response implicated in the development of structural failure of XTHVs. We investigated whether autologous mesenchymal stem cell (MSC) recellularization of bovine pericardium can attenuate initial immune activation equivalent to autologous human pericardium in a human *in-vitro* model. The data presented demonstrates that recellularization of the xenogenic bovine pericardium matrix with autologous MSCs reduced initial pro-inflammatory cytokine production equivalent to autologous level, without inducing major structural damage to the extracellular matrix (ECM) of the scaffold. These findings were further demonstrated in a small animal *in-vivo* model of XTHV transplantation. Our results confirm that guinea pig aortic valve constructs recellularized with rat MSCs reduces the cellular and humoral immune response similar to syngeneic tissue, with a reduction in graft cellular infiltrate and total serum immunoglobulin production. These data highlight the acute immunomodulatory effects of autologous MSC recellularized tissue on the recipient immune response, thus preventing recipient immune recognition of XTHVs which may potentially lead to a reduction in SVD incidence. Further studies are needed to define the long-term effects of this process, both *in-vitro* and *in-vivo*, and to elucidate the mechanism of immunomodulation by the autologous MSCs.

Finally, this thesis demonstrated that patients that have undergone XTHV replacement and are receiving long-term immunosuppression have acceptable durability of their valvular

prosthesis. Over 12-years of follow-up, gradients across the implanted XTHV remained acceptable and no patient required redo valve replacement. This finding provides further support for the notion that SVD is an immune driven process that is directed towards foreign xenogenic tissue. While immunosuppressive therapy may have had an impact on the excellent bioprosthetic valve longevity demonstrated, further studies with a larger cohort of patients and longer follow-up is warranted to investigate this relationship further.

The ideal valvular prosthesis remains the Holy Grail of cardiac surgery. The ideal valve would be durable with a longevity approaching that of a native valve. Thrombogenicity would be nonexistent, and there would be no need for supplemental anticoagulation. In addition, the ideal replacement valve would have no inherent gradient, thus allowing unimpeded outflow. It also would be easily implanted and readily available. Finally, growth commensurate with that of the recipient would be possible. The concept of a tissue engineered heart valve (TEHV) attempts to create such ideal functional heart valve replacements with the ability to grow, repair and remodel. A recellularized xenogenic scaffold may provide the greatest likelihood of widespread clinical adoption, given the easy availability, inherent ECM and shelf stability.

Future research investigating the mechanisms of structural failure of XTHVs and long-term viability of autologous recellularized xenogenic tissue in large animal and human models is vital to ensure a broader application of TEHV in the future.

## References

1. Nkomo VT, Gardin JM, Skelton TN, Gottdiener JS, Scott CG, Enriquez-Sarano M. Burden of valvular heart diseases: A population-based study. *Lancet* 2006;368:1005-11.
2. Iung B, Vahanian A. Epidemiology of acquired valvular heart disease. *Can J Cardiol* 2014;30:962-70.
3. Dvir D, Bourguignon T, Otto CM, et al. Standardized definition of structural valve degeneration for surgical and transcatheter bioprosthetic aortic valves. *Circulation* 2018;137:388-99.
4. Dignan R, O'Brien M, Hogan P, et al. Aortic valve allograft structural deterioration is associated with a subset of antibodies to human leukocyte antigens. *J Heart Valve Dis* 2003;12:382-91.
5. O'Keefe KL, Cohle SD, McNamara JE, Hooker RL. Early catastrophic stentless valve failure secondary to possible immune reaction. *Ann Thorac Surg* 2011;91:1269-72.
6. Manji RA, Hara H, Cooper DKC. Characterization of the cellular infiltrate in bioprosthetic heart valves explanted from patients with structural valve deterioration. *Xenotransplantation* 2015;22:406-7.
7. Sellers SL, Turner CT, Sathananthan J, et al. Transcatheter aortic heart valves: Histological analysis providing insight to leaflet thickening and structural valve degeneration. *JACC Cardiovasc Imaging* 2018;12:135-45.

8. Butany J, Leask R. The failure modes of biological prosthetic heart valves. *J Long Term Eff Med Implants* 2001;11:115-35.
9. Shetty R, Pibarot P, Audet A, et al. Lipid-mediated inflammation and degeneration of bioprosthetic heart valves. *Eur J Clin Invest* 2009;39:471-80.
10. Iung B, Vahanian A. Epidemiology of valvular heart disease in the adult. *Nat Rev Cardiol* 2011;8:162-72.
11. Iung B, Baron G, Butchart EG, et al. A prospective survey of patients with valvular heart disease in europe: The euro heart survey on valvular heart disease. *Eur Heart J* 2003;24:1231-43.
12. Schoen FJ, Fernandez J, Gonzalez-Lavin L, Cernaianu A. Causes of failure and pathologic findings in surgically removed ionescu-shiley standard bovine pericardial heart valve bioprostheses: Emphasis on progressive structural deterioration. *Circulation* 1987;76:618-27.
13. Khan S. Long-term outcomes with mechanical and tissue valves. *J Heart Valve Dis* 2002;11 Suppl 1:8.
14. Eikelboom JW, Connolly SJ, Brueckmann M, et al. Dabigatran versus warfarin in patients with mechanical heart valves. *N Engl J Med* 2013;369:1206-14.
15. Christie GW. Anatomy of aortic heart valve leaflets: The influence of glutaraldehyde fixation on function. *Eur J Cardiothorac Surg* 1992;6 Suppl 1:S25,32; discussion S33.

16. Vyavahare N, Ogle M, Schoen FJ, et al. Mechanisms of bioprosthetic heart valve failure: Fatigue causes collagen denaturation and glycosaminoglycan loss. *J Biomed Mater Res* 1999;46:44-50.
17. Sacks MS, David Merryman W, Schmidt DE. On the biomechanics of heart valve function. *J Biomech* 2009;42:1804-24.
18. Grunkemeier GL, Jamieson WR, Miller DC, Starr A. Actuarial versus actual risk of porcine structural valve deterioration. *J Thorac Cardiovasc Surg* 1994;108:709-18.
19. Wong ML, Griffiths LG. Immunogenicity in xenogeneic scaffold generation: Antigen removal vs. decellularization. *Acta Biomater* 2014;10:1806-16.
20. Cissell DD, Hu JC, Griffiths LG, Athanasiou KA. Antigen removal for the production of biomechanically functional, xenogeneic tissue grafts. *J Biomech* 2014;47:1987-96.
21. Grauss RW, Hazekamp MG, van Vliet S, Gittenberger-de Groot AC, DeRuiter MC. Decellularization of rat aortic valve allografts reduces leaflet destruction and extracellular matrix remodeling. *J Thorac Cardiovasc Surg* 2003;126:2003-10.
22. Moroni F, Mirabella T. Decellularized matrices for cardiovascular tissue engineering. *Am J Stem Cells* 2014;3:1-20.
23. Schoen FJ, Levy RJ. Calcification of tissue heart valve substitutes: Progress toward understanding and prevention. *Ann Thorac Surg* 2005;79:1072-80.

24. Syedain ZH, Bradee AR, Kren S, Taylor DA, Tranquillo RT. Decellularized tissue-engineered heart valve leaflets with recellularization potential. *Tissue Eng Part A* 2013;19:759-69.
25. Ott HC, Matthiesen TS, Goh S, et al. Perfusion-decellularized matrix: Using nature's platform to engineer a bioartificial heart. *Nat Med* 2008;14:213-21.
26. Jordan JE, Williams JK, Lee S, Raghavan D, Atala A, Yoo JJ. Bioengineered self-seeding heart valves. *J Thorac Cardiovasc Surg* 2012;143:201-8.
27. Robertson MJ, Dries-Devlin JL, Kren SM, Burchfield JS, Taylor DA. Optimizing recellularization of whole decellularized heart extracellular matrix. *PLoS ONE* 2014;9:e90406.
28. Scarritt ME, Pashos NC, Bunnell BA. A review of cellularization strategies for tissue engineering of whole organs. *Front Bioeng Biotechnol* 2015;3:43.
29. Meyer SR, Nagendran J, Desai LS, et al. Decellularization reduces the immune response to aortic valve allografts in the rat. *J Thorac Cardiovasc Surg* 2005;130:469-76.
30. Grauss RW, Hazekamp MG, Oppenhuizen F, van Munsteren CJ, Gittenberger-de Groot AC, DeRuiter MC. Histological evaluation of decellularised porcine aortic valves: Matrix changes due to different decellularisation methods. *Eur J Cardiothorac Surg* 2005;27:566-71.
31. Jana S, Tefft BJ, Spoon DB, Simari RD. Corrigendum to "scaffolds for tissue engineering of cardiac valves" [*acta biomater.* 10 (2014) 2877-2893]. *Acta Biomater* 2015;27:305.

32. Seifert M, Bayrak A, Stolk M, et al. Xeno-immunogenicity of ice-free cryopreserved porcine leaflets. *J Surg Res* 2015;193:933-41.
33. Manji RA, Lee W, Cooper DKC. Xenograft bioprosthetic heart valves: Past, present and future. *Int J Surg* 2015;23:280-4.
34. Naso F, Gandaglia A, Iop L, Spina M, Gerosa G. Alpha-gal detectors in xenotransplantation research: A word of caution. *Xenotransplantation* 2012;19:215-20.
35. Galili U. The  $\alpha$ -gal epitope (Gal $\alpha$ 1-3Gal $\beta$ 1-4GlcNAc-R) in xenotransplantation. *Biochimie* 2001;83:557-63.
36. McMorrow IM, Comrack CA, Sachs DH, DerSimonian H. Heterogeneity of human anti-pig natural antibodies cross-reactive with the gal(alpha1,3)galactose epitope. *Transplantation* 1997;64:501-10.
37. Wood KJ, Goto R. Mechanisms of rejection: Current perspectives. *Transplantation* 2012;93:1-10.
38. Human P, Zilla P. Inflammatory and immune processes: The neglected villain of bioprosthetic degeneration?. *J Long Term Eff Med Implants* 2001;11:199-220.
39. Vadori M, Cozzi E. The immunological barriers to xenotransplantation. *Tissue Antigens* 2015;86:239-53.
40. As K, H Y, X C. Synthesis of N-glycolylneuraminic acid (Neu5Gc) and its glycosides. *Frontiers in immunology* 2019;10:2004.

41. Human P, Zilla P. Characterization of the immune response to valve bioprostheses and its role in primary tissue failure. *Ann Thorac Surg* 2001;71:385.
42. Barbarash L, Kudryavtsev I, Rutkovskaya N, Golovkin A. T cell response in patients with implanted biological and mechanical prosthetic heart valves. *Mediators Inflamm* 2016;2016:1937564.
43. Chen RH, Kadner A, Mitchell RN, Adams DH. Fresh porcine cardiac valves are not rejected in primates. *J Thorac Cardiovasc Surg* 2000;119:1216-20.
44. Böer U, Buettner FFR, Schridde A, et al. Antibody formation towards porcine tissue in patients implanted with crosslinked heart valves is directed to antigenic tissue proteins and  $\alpha$ Gal epitopes and is reduced in healthy vegetarian subjects. *Xenotransplantation* 2017;24:e12288.
45. Veinot JP, Prichett-Pejic W, Song J, et al. CD117-positive cells and mast cells in adult human cardiac valves--observations and implications for the creation of bioengineered grafts. *Cardiovasc Pathol* 2006;15:36-40.
46. Kim WG, Sung K, Seo JW. Time-related histopathologic analyses of immunologically untreated porcine valved conduits implanted in a porcine-to-goat model. *Artif Organs* 2007;31:105-13.
47. Ozkan S, Akay TH, Gultekin B, Sezgin A, Tokel K, Aslamaci S. Xenograft transplantation in congenital cardiac surgery at baskent university: Midterm results. *Transplant Proc* 2007;39:1250-4.

48. Huai G, Qi P, Yang H, Wang Y. Characteristics of  $\alpha$ -gal epitope, anti-gal antibody,  $\alpha$ 1,3 galactosyltransferase and its clinical exploitation (review). *Int J Mol Med* 2016;37:11-20.
49. Galili U. The  $\alpha$ -gal epitope (Gal $\alpha$ 1-3Gal $\beta$ 1-4GlcNAc-R) in xenotransplantation. *Biochimie* 2001;83:557-63.
50. Sharma A, Naziruddin B, Cui C, et al. Pig cells that lack the gene for alpha1-3 galactosyltransferase express low levels of the gal antigen. *Transplantation* 2003;75:430-6.
51. Farivar RS, Filsoufi F, Adams DH. Mechanisms of gal(alpha)1-3Gal(beta)1-4GlcNAc-R (alphaGal) expression on porcine valve endothelial cells. *J Thorac Cardiovasc Surg* 2003;125:306-14.
52. Konakci KZ, Bohle B, Blumer R, et al. Alpha-gal on bioprostheses: Xenograft immune response in cardiac surgery. *Eur J Clin Invest* 2005;35:17-23.
53. Kasimir M, Rieder E, Seebacher G, Wolner E, Weigel G, Simon P. Presence and elimination of the xenoantigen gal (alpha1, 3) gal in tissue-engineered heart valves. *Tissue Eng* 2005;11:1274-80.
54. Naso F, Gandaglia A, Bottio T, et al. First quantification of alpha-gal epitope in current glutaraldehyde-fixed heart valve bioprostheses. *Xenotransplantation* 2013;20:252-61.
55. Barone A, Benktander J, Teneberg S, Breimer ME. Characterization of acid and non-acid glycosphingolipids of porcine heart valve cusps as potential immune targets in biological heart valve grafts. *Xenotransplantation* 2014;21:510-22.

56. Griffiths LG, Choe LH, Reardon KF, Dow SW, Christopher Orton E. Immunoproteomic identification of bovine pericardium xenoantigens. *Biomaterials* 2008;29:3514-20.
57. Jm A, Dw G. Extracellular matrix-based biomaterial scaffolds and the host response. *Biomaterials* 2016;86:68-82.
58. Sf B, Tw G. Immune response to biologic scaffold materials. *Seminars in immunology* 2008;20:109-16.
59. L C, Dr M, F H, Jh E. Key players in the immune response to biomaterial scaffolds for regenerative medicine. *Advanced drug delivery reviews* 2017;114:184-92.
60. Gates KV, Dalglish AJ, Griffiths LG. Antigenicity of bovine pericardium determined by a novel immunoproteomic approach. *Sci Rep* 2017;7:2446.
61. R A, Em R, S LB, V P. Glycans in immune recognition and response. *Carbohydrate research* 2014;389:115-22.
62. Lee W, Long C, Ramsoondar J, et al. Human antibody recognition of xenogeneic antigens (NeuGc and gal) on porcine heart valves: Could genetically modified pig heart valves reduce structural valve deterioration?. *Xenotransplantation* 2016;23:370-80.
63. Reuven EM, Leviatan Ben-Arye S, Marshanski T, et al. Characterization of immunogenic Neu5Gc in bioprosthetic heart valves. *Xenotransplantation* 2016;23:381-92.
64. Lee W, Hara H, Cooper DKC, Manji RA. Expression of NeuGc on pig heart valves. *Xenotransplantation* 2015;22:153-4.

65. Salama A, Evanno G, Harb J, Soulillou J. Potential deleterious role of anti-Neu5Gc antibodies in xenotransplantation. *Xenotransplantation* 2015;22:85-94.
66. Kosuga T. The effect of allogeneic or xenogeneic immune responses and preservation techniques on transplanted aortic valve grafts. *Kurume Med J* 2000;47:13-23.
67. Nagasaka S, Taniguchi S, Nakayama Y, et al. Possibility of xenotransplantation with a cryopreserved porcine heart valve in a canine model. *Transplant Proc* 2000;32:2417-9.
68. Nagasaka S, Taniguchi S, Nakayama Y, et al. In vivo study of the effects of cryopreservation on heart valve xenotransplantation. *Cardiovasc Pathol* 2005;14:70-9.
69. Sung K, Kim WG, Seo JW. Immunologically untreated fresh xenograft implantation in a pig-to-goat model. *Artif Organs* 2008;32:810-5.
70. Park S, Kim W, Choi S, Kim Y. Removal of alpha-gal epitopes from porcine aortic valve and pericardium using recombinant human alpha galactosidase A. *J Korean Med Sci* 2009;24:1126-31.
71. Choi S, Jeong H, Lim H, Park S, Kim S, Kim YJ. Elimination of alpha-gal xenoreactive epitope: Alpha-galactosidase treatment of porcine heart valves. *J Heart Valve Dis* 2012;21:387-97.
72. H N, B P. The production of multi-transgenic pigs: Update and perspectives for xenotransplantation. *Transgenic research* 2016;25:361-74.

73. Byrne GW, Du Z, Stalboerger P, Kogelberg H, McGregor CGA. Cloning and expression of porcine  $\beta$ 1,4 N-acetylgalactosaminyl transferase encoding a new xenoreactive antigen. *Xenotransplantation* 2014;21:543-54.
74. Guldner NW, Bastian F, Weigel G, et al. Nanocoating with titanium reduces iC3b- and granulocyte-activating immune response against glutaraldehyde-fixed bovine pericardium: A new technique to improve biologic heart valve prosthesis durability?. *J Thorac Cardiovasc Surg* 2012;143:1152-9.
75. McGregor CGA, Carpentier A, Lila N, Logan JS, Byrne GW. Cardiac xenotransplantation technology provides materials for improved bioprosthetic heart valves. *J Thorac Cardiovasc Surg* 2011;141:269-75.
76. Manji RA, Zhu LF, Nijjar NK, et al. Glutaraldehyde-fixed bioprosthetic heart valve conduits calcify and fail from xenograft rejection. *Circulation* 2006;114:318-27.
77. Vesely I. Heart valve tissue engineering. *Circ Res* 2005;97:743-55.
78. Duncan AC, Boughner D, Vesely I. Dynamic glutaraldehyde fixation of a porcine aortic valve xenograft. I. effect of fixation conditions on the final tissue viscoelastic properties. *Biomaterials* 1996;17:1849-56.
79. Schenke-Layland K, Vasilevski O, Opitz F, et al. Impact of decellularization of xenogeneic tissue on extracellular matrix integrity for tissue engineering of heart valves. *J Struct Biol* 2003;143:201-8.

80. Goecke T, Theodoridis K, Tudorache I, et al. In vivo performance of freeze-dried decellularized pulmonary heart valve allo- and xenografts orthotopically implanted into juvenile sheep. *Acta Biomater* 2018;68:41-52.
81. Parravicini R, Cocconcelli F, Verona A, Parravicini V, Giuliani E, Barbieri A. Tuna cornea as biomaterial for cardiac applications. *Tex Heart Inst J* 2012;39:179-83.
82. Cebotari S, Mertsching H, Kallenbach K, et al. Construction of autologous human heart valves based on an acellular allograft matrix. *Circulation* 2002;106:I63-8.
83. Bader A, Schilling T, Teebken OE, et al. Tissue engineering of heart valves--human endothelial cell seeding of detergent acellularized porcine valves. *Eur J Cardiothorac Surg* 1998;14:279-84.
84. Bertipaglia B, Ortolani F, Petrelli L, et al. Cell characterization of porcine aortic valve and decellularized leaflets repopulated with aortic valve interstitial cells: The VESALIO project (vitalitate exornatum succedaneum aorticum labore ingenioso obtenibitur). *Ann Thorac Surg* 2003;75:1274-82.
85. Vincentelli A, Wautot F, Juthier F, et al. In vivo autologous recellularization of a tissue-engineered heart valve: Are bone marrow mesenchymal stem cells the best candidates?. *J Thorac Cardiovasc Surg* 2007;134:424-32.
86. Goldstein S, Clarke DR, Walsh SP, Black KS, O'Brien MF. Transpecies heart valve transplant: Advanced studies of a bioengineered xeno-autograft. *Ann Thorac Surg* 2000;70:1962-9.

87. Elkins RC, Goldstein S, Hewitt CW, et al. Recellularization of heart valve grafts by a process of adaptive remodeling. *Semin Thorac Cardiovasc Surg* 2001;13:87-92.
88. Simon P, Kasimir MT, Seebacher G, et al. Early failure of the tissue engineered porcine heart valve SYNERGRAFT in pediatric patients. *Eur J Cardiothorac Surg* 2003;23:1002,1006; discussion 1006.
89. Konertz W, Angeli E, Tarusinov G, et al. Right ventricular outflow tract reconstruction with decellularized porcine xenografts in patients with congenital heart disease. *J Heart Valve Dis* 2011;20:341-7.
90. Teebken O, Mertsching H, Haverich A. Modification of heart valve allografts and xenografts by means of tissue engineering. *Transplant Proc* 2002;34:2333.
91. Cebotari S, Lichtenberg A, Tudorache I, et al. Clinical application of tissue engineered human heart valves using autologous progenitor cells. *Circulation* 2006;114:132.
92. Koenig F, Lee J, Akra B, et al. Is transcatheter aortic valve implantation of living tissue-engineered valves feasible? an in vitro evaluation utilizing a decellularized and reseeded biohybrid valve. *Artif Organs* 2016;40:727-37.
93. Sutherland FWH, Perry TE, Yu Y, et al. From stem cells to viable autologous semilunar heart valve. *Circulation* 2005;111:2783-91.
94. Weber B, Scherman J, Emmert MY, et al. Injectable living marrow stromal cell-based autologous tissue engineered heart valves: First experiences with a one-step intervention in primates. *Eur Heart J* 2011;32:2830-40.

95. Motta SE, Fioretta ES, Dijkman PE, et al. Development of an off-the-shelf tissue-engineered sinus valve for transcatheter pulmonary valve replacement: A proof-of-concept study. *J Cardiovasc Transl Res* 2018;11:182-91.
96. Schmidt D, Achermann J, Odermatt B, et al. Prenatally fabricated autologous human living heart valves based on amniotic fluid derived progenitor cells as single cell source. *Circulation* 2007;116:64.
97. Schmidt D, Mol A, Breymann C, et al. Living autologous heart valves engineered from human prenatally harvested progenitors. *Circulation* 2006;114:125.
98. VeDepo MC, Detamore MS, Hopkins RA, Converse GL. Recellularization of decellularized heart valves: Progress toward the tissue-engineered heart valve:. *Journal of Tissue Engineering* 2017;8:e2041731417726327.
99. Dong X, Wei X, Yi W, et al. RGD-modified acellular bovine pericardium as a bioprosthetic scaffold for tissue engineering. *J Mater Sci Mater Med* 2009;20:2327-36.
100. Dijkman PE, Driessen-Mol A, Frese L, Hoerstrup SP, Baaijens FPT. Decellularized homologous tissue-engineered heart valves as off-the-shelf alternatives to xeno- and homografts. *Biomaterials* 2012;33:4545-54.
101. Hof A, Raschke S, Baier K, et al. Challenges in developing a reseeded, tissue-engineered aortic valve prosthesis. *Eur J Cardiothorac Surg* 2016;50:446-55.

102. Zhou J, PhD, Ye, Xiaofeng, MD, PhD, Wang Z, MD, et al. Development of decellularized aortic valvular conduit coated by Heparin–SDF-1 $\alpha$  multilayer. *Annals of Thoracic Surgery* 2015;99:612-8.
103. Ye X, Hu X, Wang H, Liu J, Zhao Q. Polyelectrolyte multilayer film on decellularized porcine aortic valve can reduce the adhesion of blood cells without affecting the growth of human circulating progenitor cells. *Acta Biomaterialia* 2012;8:1057-67.
104. Ye X, Wang H, Zhou J, et al. The effect of heparin-VEGF multilayer on the biocompatibility of decellularized aortic valve with platelet and endothelial progenitor cells. *PLOS ONE* 2013;8:e54622.
105. Huang W, Xiao D, Wang Y, et al. Fn14 promotes differentiation of human mesenchymal stem cells into heart valvular interstitial cells by phenotypic characterization. *J Cell Physiol* 2014;229:580-7.
106. Lichtenberg A, Cebotari S, Tudorache I, et al. Flow-dependent re-endothelialization of tissue-engineered heart valves. *J Heart Valve Dis* 2006;15:287-94.
107. Lichtenberg A, Tudorache I, Cebotari S, et al. In vitro re-endothelialization of detergent decellularized heart valves under simulated physiological dynamic conditions. *Biomaterials* 2006;27:4221-9.
108. Schenke-Layland K, Opitz F, Gross M, et al. Complete dynamic repopulation of decellularized heart valves by application of defined physical signals-an in vitro study. *Cardiovasc Res* 2003;60:497-509.

109. Converse GL, Buse EE, Neill KR, et al. Design and efficacy of a single-use bioreactor for heart valve tissue engineering. *J Biomed Mater Res Part B Appl Biomater* 2017;105:249-59.
110. Tudorache I, Calistru A, Baraki H, et al. Orthotopic replacement of aortic heart valves with tissue-engineered grafts. *Tissue Eng Part A* 2013;19:1686-94.
111. Kajbafzadeh A, Ahmadi Tafti SH, Mokhber-Dezfooli M, et al. Aortic valve conduit implantation in the descending thoracic aorta in a sheep model: The outcomes of pre-seeded scaffold. *Int J Surg* 2016;28:97-105.
112. Ghodsizad A, Bordel V, Wiedensohler H, et al. Magnetically guided recellularization of decellularized stented porcine pericardium-derived aortic valve for TAVI. *ASAIO J* 2014;60:582-6.
113. Kluin J, Talacua H, Smits, Anthal I. P. M., et al. In situ heart valve tissue engineering using a bioresorbable elastomeric implant - from material design to 12 months follow-up in sheep. *Biomaterials* 2017;125:101-17.
114. Bruder L, Spriestersbach H, Brakmann K, et al. Transcatheter decellularized tissue-engineered heart valve (dTEHV) grown on polyglycolic acid (PGA) scaffold coated with P4HB shows improved functionality over 52 weeks due to polyether-ether-ketone (PEEK) insert. *J Funct Biomater* 2018;9:64.
115. Dominici M, Le Blanc K, Mueller I, et al. Minimal criteria for defining multipotent mesenchymal stromal cells. the international society for cellular therapy position statement. *Cytotherapy* 2006;8:315-7.

116. Wang S, Qu X, Zhao RC. Clinical applications of mesenchymal stem cells. *J Hematol Oncol* 2012;5:19.
117. Murray IR, Péault B. Q&A: Mesenchymal stem cells — where do they come from and is it important?. *BMC Biol* 2015;13.
118. Blanc KL, Ringdén O. Immunomodulation by mesenchymal stem cells and clinical experience. *Journal of Internal Medicine* 2007;262:509-25.
119. Yi T, Song SU. Immunomodulatory properties of mesenchymal stem cells and their therapeutic applications. *Arch Pharm Res* 2012;35:213-21.
120. Le Blanc K, Rasmusson I, Sundberg B, et al. Treatment of severe acute graft-versus-host disease with third party haploidentical mesenchymal stem cells. *The Lancet* 2004;363:1439-41.
121. Chen S, Fang W, Ye F, et al. Effect on left ventricular function of intracoronary transplantation of autologous bone marrow mesenchymal stem cell in patients with acute myocardial infarction. *Am J Cardiol* 2004;94:92-5.
122. Zhang S, Ge J, Sun A, et al. Comparison of various kinds of bone marrow stem cells for the repair of infarcted myocardium: Single clonally purified non-hematopoietic mesenchymal stem cells serve as a superior source. *J Cell Biochem* 2006;99:1132-47.
123. Bruder SP, Kurth AA, Shea M, Hayes WC, Jaiswal N, Kadiyala S. Bone regeneration by implantation of purified, culture-expanded human mesenchymal stem cells. *Journal of Orthopaedic Research* 1998;16:155-62.

124. Gupta PK, Das AK, Chullikana A, Majumdar AS. Mesenchymal stem cells for cartilage repair in osteoarthritis. *Stem Cell Res Ther* 2012;3:25.
125. Rui Zhang, Jie Ma, Jing Han, Weijie Zhang, Jianbing Ma. Mesenchymal stem cell related therapies for cartilage lesions and osteoarthritis 2019;11:6275-89.
126. Tuan RS, Boland G, Tuli R. Adult mesenchymal stem cells and cell-based tissue engineering. *Arthritis Res Ther* 2003;5:32-45.
127. Keating A. Mesenchymal stromal cells: New directions. *Cell Stem Cell* 2012;10:709-16.
128. Friedenstein AJ, Chailakhjan RK, Lalykina KS. The development of fibroblast colonies in monolayer cultures of guinea-pig bone marrow and spleen cells. *Cell Tissue Kinet* 1970;3:393-403.
129. Friedenstein AJ, Chailakhyan RK, Latsinik NV, Panasyuk AF, Keiliss-Borok IV. Stromal cells responsible for transferring the microenvironment of the hemopoietic tissues. cloning in vitro and retransplantation in vivo. *Transplantation* 1974;17:331-40.
130. Friedenstein AJ, Gorskaja JF, Kulagina NN. Fibroblast precursors in normal and irradiated mouse hematopoietic organs. *Exp Hematol* 1976;4:267-74.
131. Pittenger MF, Mackay AM, Beck SC, et al. Multilineage potential of adult human mesenchymal stem cells. *Science* 1999;284:143-7.
132. Haynesworth SE, Goshima J, Goldberg VM, Caplan AI. Characterization of cells with osteogenic potential from human marrow. *Bone* 1992;13:81-8.

133. Miura M, Gronthos S, Zhao M, et al. SHED: Stem cells from human exfoliated deciduous teeth. *Proc Natl Acad Sci U S A* 2003;100:5807-12.
134. Zuk PA, Zhu M, Mizuno H, et al. Multilineage cells from human adipose tissue: Implications for cell-based therapies. *Tissue Eng* 2001;7:211-28.
135. Lee OK, Kuo TK, Chen W, Lee K, Hsieh S, Chen T. Isolation of multipotent mesenchymal stem cells from umbilical cord blood. *Blood* 2004;103:1669-75.
136. Gardner OFW, Alini M, Stoddart MJ. Mesenchymal stem cells derived from human bone marrow. *Methods Mol Biol* 2015;1340:41-52.
137. Ferrin I, Beloqui I, Zabaleta L, Salcedo JM, Trigueros C, Martin AG. Isolation, culture, and expansion of mesenchymal stem cells. *Methods Mol Biol* 2017;1590:177-90.
138. James AW, Zara JN, Zhang X, et al. Perivascular stem cells: A prospectively purified mesenchymal stem cell population for bone tissue engineering. *Stem Cells Transl Med* 2012;1:510-9.
139. Chahla J, M.D, Mannava, Sandeep, M.D., Ph.D, Cinque ME, B.S, Geeslin AG, M.D, Codina D, M.D, LaPrade, Robert F., M.D., Ph.D. Bone marrow aspirate concentrate harvesting and processing technique. *Arthroscopy Techniques* 2016;6:e441-5.
140. Asakura Y, Kinoshita M, Kasuya Y, Sakuma S, Ozaki M. Ultrasound-guided sternal bone marrow aspiration. *Blood Res* 2017;52:148-50.

141. Sivasubramaniyan K, Ilas DC, Harichandan A, et al. Bone Marrow–Harvesting technique influences functional heterogeneity of mesenchymal stem/stromal cells and cartilage regeneration. *Am J Sports Med* 2018;46:3521-31.
142. Davila E. Jamshidi needle biopsy of the sternal bone marrow. *Blood* 2009;114:4548-.
143. Trejo-Ayala RA, Luna-Pérez M, Gutiérrez-Romero M, Collazo-Jaloma J, Cedillo-Pérez MC, Ramos-Peñañiel CO. Bone marrow aspiration and biopsy. technique and considerations. *Revista Médica del Hospital General de México* 2015;78:196-201.
144. Arnáiz-García ME, González-Santos JM, Arnáiz-García AM, López-Rodríguez J, Arnáiz J. Acute type A aortic dissection after sternal bone marrow puncture. *The Annals of Thoracic Surgery* 2017;104:e455.
145. Santavy P, Troubil M, Lonsky V. Pericardial tamponade: A rare complication of sternal bone marrow biopsy. *Hematology reports* 2013;5:e13.
146. Gendron N, Zia Chahabi S, Poenou G, et al. Pain assessment and factors influencing pain during bone marrow aspiration: A prospective study. *PLoS One* 2019;14.
147. Bozso S, Kang J, Adam B, et al. Canadian society of cardiac surgeons (CSCS) CSCS260 poster: CSCS poster session II monday, october 25, 2010. *Canadian Journal of Cardiology* 2010;26:101D-4D.
148. Bozso SJ, Kang JJ, Adam B, et al. The role of autologous mesenchymal stem cell recellularization in rescuing the xenoreactive immune response. *The Journal of Heart and Lung Transplantation* 2020;39:S361.

149. Skowroński J, Skowroński R, Rutka M. Large cartilage lesions of the knee treated with bone marrow concentrate and collagen membrane--results. *Ortop Traumatol Rehabil* 2013;15:69-76.
150. Skowroński J, Rutka M. Osteochondral lesions of the knee reconstructed with mesenchymal stem cells - results. *Ortop Traumatol Rehabil* 2013;15:195-204.
151. Kim J, Lee GW, Jung GH, et al. Clinical outcome of autologous bone marrow aspirates concentrate (BMAC) injection in degenerative arthritis of the knee. *Eur J Orthop Surg Traumatol* 2014;24:1505-11.
152. Elgaz S, Kuçi Z, Kuçi S, Bönig H, Bader P. Clinical use of mesenchymal stromal cells in the treatment of acute graft-versus-host disease. *Transfusion Medicine and Hemotherapy* 2019;46:27-34.
153. Kim N, Cho S. Clinical applications of mesenchymal stem cells. *The Korean Journal of Internal Medicine* 2013;28:387-402.
154. Singh A, Singh A, Sen D. Mesenchymal stem cells in cardiac regeneration: A detailed progress report of the last 6 years (2010–2015). *Stem Cell Res Ther* 2016;7.
155. Golpanian S, Wolf A, Hatzistergos KE, Hare JM. Rebuilding the damaged heart: Mesenchymal stem cells, cell-based therapy, and engineered heart tissue. *Physiol Rev* 2016;96:1127-68.
156. Castro-Manreza ME, Montesinos JJ. Immunoregulation by mesenchymal stem cells: Biological aspects and clinical applications. *J Immunol Res* 2015;2015.

157. Nimura A, Muneta T, Koga H, et al. Increased proliferation of human synovial mesenchymal stem cells with autologous human serum: Comparisons with bone marrow mesenchymal stem cells and with fetal bovine serum. *Arthritis & Rheumatism* 2008;58:501-10.
158. Spees JL, Gregory CA, Singh H, et al. Internalized antigens must be removed to prepare hypoimmunogenic mesenchymal stem cells for cell and gene therapy. *Mol Ther* 2004;9:747-56.
159. Kuznetsov SA, Mankani MH, Robey PG. Effect of serum on human bone marrow stromal cells: Ex vivo expansion and in vivo bone formation. *Transplantation* 2000;70:1780-7.
160. Improved Expansion of MSC Without Loss of Differentiation Potential. Available at: <https://www.rnssystem.com/resources/posters/improved-expansion-msc-without-loss-differentiation-potential>. Accessed Jun 6, 2020.
161. Kobayashi T, Watanabe H, Yanagawa T, et al. Motility and growth of human bone-marrow mesenchymal stem cells during ex vivo expansion in autologous serum. *J Bone Joint Surg Br* 2005;87:1426-33.
162. Shahdadfar A, Frønsdal K, Haug T, Reinholt FP, Brinchmann JE. In vitro expansion of human mesenchymal stem cells: Choice of serum is a determinant of cell proliferation, differentiation, gene expression, and transcriptome stability. *Stem Cells* 2005;23:1357-66.
163. Stute N, Holtz K, Bubenheim M, Lange C, Blake F, Zander AR. Autologous serum for isolation and expansion of human mesenchymal stem cells for clinical use. *Exp Hematol* 2004;32:1212-25.

164. Yamamoto N, Isobe M, Negishi A, et al. Effects of autologous serum on osteoblastic differentiation in human bone marrow cells. *J Med Dent Sci* 2003;50:63-9.
165. Kaneko T, Aranki S, Javed Q, et al. Mechanical versus bioprosthetic mitral valve replacement in patients
166. Johnston DR, Soltesz EG, Vakil N, et al. Long-term durability of bioprosthetic aortic valves: Implications from 12,569 implants. *Ann Thorac Surg* 2015;99:1239-47.
167. Chen RH, Kadner A, Mitchell RN, Adams DH. Fresh porcine cardiac valves are not rejected in primates. *J Thorac Cardiovasc Surg* 2000;119:1216-20.
168. Bromley SK, Peterson DA, Gunn MD, Dustin ML. Cutting edge: Hierarchy of chemokine receptor and TCR signals regulating T cell migration and proliferation. *J Immunol* 2000;165:15-9.
169. Siddiqui I, Erreni M, van Brakel M, Debets R, Allavena P. Enhanced recruitment of genetically modified CX3CR1-positive human T cells into fractalkine/CX3CL1 expressing tumors: Importance of the chemokine gradient. *J Immunother Cancer* 2016;4:21.
170. Nagarsheth N, Wicha MS, Zou W. Chemokines in the cancer microenvironment and their relevance in cancer immunotherapy. *Nat Rev Immunol* 2017;17:559-72.
171. Adam BA, Smith RN, Rosales IA, et al. Chronic antibody-mediated rejection in nonhuman primate renal allografts: Validation of human histological and molecular phenotypes. *Am J Transplant* 2017;17:2841-50.

172. Adam B, Afzali B, Dominy KM, et al. Multiplexed color-coded probe-based gene expression assessment for clinical molecular diagnostics in formalin-fixed paraffin-embedded human renal allograft tissue. *Clin Transplant* 2016;30:295-305.
173. Butany J, Leong SW, Cunningham KS, D'Cruz G, Carmichael K, Yau TM. A 10-year comparison of explanted Hancock-II and Carpentier-Edwards supraannular bioprostheses. *Cardiovasc Pathol* 2007;16:4-13.
174. Palomino DCT, Marti LC. Chemokines and immunity. *Einstein (Sao Paulo)* 2015;13:469-73.
175. Bozso SJ, Kang JJH, Al-Adra D, et al. Outcomes following bioprosthetic valve replacement in prior non-cardiac transplant recipients. *Clin Transplant* 2019;33:e13720.
176. Lund O, Nielsen SL, Arildsen H, Ilkjaer LB, Pilegaard HK. Standard aortic St. Jude valve at 18 years: Performance profile and determinants of outcome. *Ann Thorac Surg* 2000;69:1459-65.
177. Grunkemeier GL, Furnary AP, Wu Y, Wang L, Starr A. Durability of pericardial versus porcine bioprosthetic heart valves. *J Thorac Cardiovasc Surg* 2012;144:1381-6.
178. Nalluri N, Atti V, Munir AB, et al. Valve-in-valve transcatheter aortic valve implantation (ViV-TAVI) versus redo-surgical aortic valve replacement (redo-SAVR): A systematic review and meta-analysis. *J Interv Cardiol* 2018;31:661-71.
179. Kühne L, Jung B, Poth H, et al. Renal allograft rejection, lymphocyte infiltration, and de novo donor-specific antibodies in a novel model of non-adherence to immunosuppressive therapy. *BMC Immunol* 2017;18.

180. Girlanda R, Kleiner DE, Duan Z, et al. Monocyte infiltration and kidney allograft dysfunction during acute rejection. *Am J Transplant* 2008;8:600.
181. Ozkan S, Akay TH, Gultekin B, Sezgin A, Tokel K, Aslamaci S. Xenograft transplantation in congenital cardiac surgery at baskent university: Midterm results. *Transplant Proc* 2007;39:1250-4.
182. Erkhem-Ochir B, Tatsuishi W, Yokobori T, et al. Inflammatory and immune checkpoint markers are associated with the severity of aortic stenosis. *JTCVS Open* 2021;5:1-12.
183. Nguyen DC, Joyner CJ, Sanz I, Lee FE. Factors affecting early antibody secreting cell maturation into long-lived plasma cells. *Front Immunol* 2019;10:2138.
184. Iung B, Baron G, Butchart EG, et al. A prospective survey of patients with valvular heart disease in europe: The euro heart survey on valvular heart disease. *Eur Heart J* 2003;24:1231-43.
185. Nkomo VT, Gardin JM, Skelton TN, Gottdiener JS, Scott CG, Enriquez-Sarano M. Burden of valvular heart diseases: A population-based study. *Lancet* 2006;368:1005-11.
186. Iung B, Vahanian A. Epidemiology of valvular heart disease in the adult. *Nat Rev Cardiol* 2011;8:162-72.
187. Iung B, Vahanian A. Epidemiology of acquired valvular heart disease. *Can J Cardiol* 2014;30:962-70.
188. Manji RA, Eksler B, Menkis AH, Cooper DKC. Bioprosthetic heart valves of the future. *Xenotransplantation* 2014;21:1-10.

189. Bozso SJ, White A, Kang JJH, et al. Long-term outcomes following mechanical or bioprosthetic aortic valve replacement in young women. *CJC Open* 2020;2:514-21.
190. White A, Bozso SJ, Lakey O, et al. Rapid deployment valves versus conventional tissue valves for aortic valve replacement. *J Thorac Cardiovasc Surg* 2020:S0022-4.
191. Forgie K, Bozso SJ, Hong Y, et al. The effects of body mass index on outcomes for patients undergoing surgical aortic valve replacement. *BMC Cardiovasc Disord* 2020;20:255.
192. Saleeb SF, Newburger JW, Geva T, et al. Accelerated degeneration of a bovine pericardial bioprosthetic aortic valve in children and young adults. *Circulation* 2014;130:51-60.
193. Johnston DR, Soltesz EG, Vakil N, et al. Long-term durability of bioprosthetic aortic valves: Implications from 12,569 implants. *Ann Thorac Surg* 2015;99:1239-47.
194. Bozso SJ, Kang JJH, Basu R, et al. Structural valve deterioration is linked to increased immune infiltrate and chemokine expression. *J of Cardiovasc Trans Res* 2020:1-10.
195. Yi T, Song SU. Immunomodulatory properties of mesenchymal stem cells and their therapeutic applications. *Arch Pharm Res* 2012;35:213-21.
196. Le Blanc K, Ringdén O. Immunomodulation by mesenchymal stem cells and clinical experience. *J Intern Med* 2007;262:509-25.
197. Belouski SS, Wilkinson J, Thomas J, et al. Utility of lyophilized PMA and ionomycin to stimulate lymphocytes in whole blood for immunological assays. *Cytometry B Clin Cytom* 2010;78:59-64.

198. Bozso SJ, Kang JJH, Mathew A, et al. Comparing scaffold design and recellularization techniques for development of tissue engineered heart valves. *Regenerative Engineering and Translational Medicine* 2020.
199. N L, Y L, D G, C X, X L, Z X. Efficient decellularization for bovine pericardium with extracellular matrix preservation and good biocompatibility. *Interactive cardiovascular and thoracic surgery* 2018;26:768-76.
200. Theodoridis K, Tudorache I, Cebotari S, et al. \* Six-year-old sheep as a clinically relevant large animal model for aortic valve replacement using tissue-engineered grafts based on decellularized allogenic matrix. *Tissue Eng Part C Methods* 2017;23:953-63.
201. Dominici M, Le Blanc K, Mueller I, et al. Minimal criteria for defining multipotent mesenchymal stromal cells. the international society for cellular therapy position statement. *Cytotherapy* 2006;8:315-7.
202. Aggarwal S, Pittenger MF. Human mesenchymal stem cells modulate allogeneic immune cell responses. *Blood* 2005;105:1815-22.
203. Batten P, Sarathchandra P, Antoniw JW, et al. Human mesenchymal stem cells induce T cell anergy and downregulate T cell allo-responses via the TH2 pathway: Relevance to tissue engineering human heart valves. *Tissue Eng* 2006;12:2263-73.
204. Weber B, Emmert MY, Behr L, et al. Prenatally engineered autologous amniotic fluid stem cell-based heart valves in the fetal circulation. *Biomaterials* 2012;33:4031-43.

205. Ristivojević MK, Grundström J, Tran TaT, et al. A-gal on the protein surface affects uptake and degradation in immature monocyte derived dendritic cells. *Sci Rep* 2018;8:12684.
206. Bozso SJ, El-Andari R, Al-Adra D, et al. A review of the immune response stimulated by xenogenic tissue heart valves. *Scand J Immunol* 2020:e13018.
207. Voges I, Bräsen JH, Entenmann A, et al. Adverse results of a decellularized tissue-engineered pulmonary valve in humans assessed with magnetic resonance imaging. *Eur J Cardiothorac Surg* 2013;44:272.
208. Erdbrügger W, Konertz W, Dohmen PM, et al. Decellularized xenogenic heart valves reveal remodeling and growth potential in vivo. *Tissue Eng* 2006;12:2059-68.
209. Dodge-Khatami A, Hallhagen S, Limacher K, Söderberg B, Jenni R. Minimally invasive insertion of an equine stented pulmonary valve with a built-in sinus portion in a sheep model. *Catheter Cardiovasc Interv* 2012;79:654-8.
210. Paniagua Gutierrez JR, Berry H, Korossis S, et al. Regenerative potential of low-concentration SDS-decellularized porcine aortic valved conduits in vivo. *Tissue Eng Part A* 2015;21:332-42.
211. Leyh RG, Wilhelmi M, Rebe P, et al. In vivo repopulation of xenogeneic and allogeneic acellular valve matrix conduits in the pulmonary circulation. *Ann Thorac Surg* 2003;75:1457,1463; discussion 1463.

212. Takagi K, Fukunaga S, Nishi A, et al. In vivo recellularization of plain decellularized xenografts with specific cell characterization in the systemic circulation: Histological and immunohistochemical study. *Artif Organs* 2006;30:233-41.
213. Legare JF, Lee TD, Creaser K, Ross DB. T lymphocytes mediate leaflet destruction and allograft aortic valve failure in rats. *Ann Thorac Surg* 2000;70:1238-45.
214. Zhang L, Chan C. Isolation and enrichment of rat mesenchymal stem cells (MSCs) and separation of single-colony derived MSCs. *J Vis Exp* 2010:1852.
215. Fioretta ES, Dijkman PE, Emmert MY, Hoerstrup SP. The future of heart valve replacement: Recent developments and translational challenges for heart valve tissue engineering. *J Tissue Eng Regen Med* 2018;12:e323-35.
216. Pittenger MF, Mackay AM, Beck SC, et al. Multilineage potential of adult human mesenchymal stem cells. *Science* 1999;284:143-7.
217. Isik FF, McDonald TO, Ferguson M, Yamanaka E, Gordon D. Transplant arteriosclerosis in a rat aortic model. *Am J Pathol* 1992;141:1139-49.
218. Plissonnier D, Nochy D, Poncet P, et al. Sequential immunological targeting of chronic experimental arterial allograft. *Transplantation* 1995;60:414-24.
219. Allaire E, Mandet C, Bruneval P, Bensenane S, Becquemin JP, Michel JB. Cell and extracellular matrix rejection in arterial concordant and discordant xenografts in the rat. *Transplantation* 1996;62:794-803.

220. Légaré JF, Nanton MA, Bryan P, Lee TD, Ross DB. Aortic valve graft implantation in rats: A new functional model. *J Thorac Cardiovasc Surg* 2000;120:679-85.
221. Canadian Organ Replacement Register 2017. Available at: <https://www.cihi.ca/en/corr-annual-statistics-2017>.
222. Havers-Borgersen E, Butt JH, Vinding NE, et al. Time in therapeutic range and risk of thromboembolism and bleeding in patients with a mechanical heart valve prosthesis. *J Thorac Cardiovasc Surg* 2019:S0022-9.
223. Brown JM, O'Brien SM, Wu C, Sikora JAH, Griffith BP, Gammie JS. Isolated aortic valve replacement in north america comprising 108,687 patients in 10 years: Changes in risks, valve types, and outcomes in the society of thoracic surgeons national database. *J Thorac Cardiovasc Surg* 2009;137:82-90.
224. Rodriguez-Gabella T, Voisine P, Dagenais F, et al. Long-term outcomes following surgical aortic bioprosthesis implantation. *J Am Coll Cardiol* 2018;71:1401-12.
225. Rahimtoola SH. Choice of prosthetic heart valve in adults an update. *J Am Coll Cardiol* 2010;55:2413-26.
226. Stein PD, Wang CH, Riddle JM, Magilligan DJ. Leukocytes, platelets, and surface microstructure of spontaneously degenerated porcine bioprosthetic valves. *J Card Surg* 1988;3:253-61.
227. Eishi K, Ishibashi-Ueda H, Nakano K, et al. Calcific degeneration of bioprosthetic aortic valves in patients receiving steroid therapy. *J Heart Valve Dis* 1996;5:668-72.

228. Mitruka SN, Griffith BP, Kormos RL, et al. Cardiac operations in solid-organ transplant recipients. *Ann Thorac Surg* 1997;64:1270-8.

229. Dresler C, Uthoff K, Wahlers T, et al. Open heart operations after renal transplantation. *Ann Thorac Surg* 1997;63:143-6.